Lappeenrannan teknillinen yliopisto
Lappeenranta University of Technology

Veli-Matti Lihavainen

A NOVEL APPROACH FOR ASSESSING THE FATIGUE STRENGTH OF ULTRASONIC IMPACT TREATED WELDED STRUCTURES

Thesis for the degree of Doctor of Science (Technology) to be presented with due permission for public examination and criticism in the Auditorium 1382 at Lappeenranta University of Technology, Lappeenranta, Finland on the 21th of November, 2006, at noon.

Acta Universitatis Lappeenrantaensis 252

Supervisor	Professor Gary Marquis Department of Mechanical Engineering Lappeenranta University of Technology Finland
Reviewers	Professor Per Haagensen Department of Structural Engineering Norwegian University of Science and Technology Norway
	Associate Professor Niklas Järvstråt Department of Technology, Mathematics and Computer Science University West Sweden
Opponents	Professor Per Haagensen Department of Structural Engineering Norwegian University of Science and Technology Norway
	Dr. Aslak Siljander Chief Research Scientist VTT Industrial Systems Finland

ISBN 952-214-304-9, ISBN 952-214-305-7 (pdf)
ISSN 1456-4491
Lappeenrannan teknillinen yliopisto
Digipaino 2006

ABSTRACT

Veli-Matti Lihavainen

A NOVEL APPROACH FOR ASSESSING THE FATIGUE STRENGTH OF ULTRASONIC IMPACT TREATED WELDED STRUCTURES

Lappeenranta 2006
77 pages, 2 appendices
Acta Universitatis Lappeenrantaensis 252
Diss. Lappeenranta University of Technology
ISBN 952-214-304-9, ISBN 952-214-305-7 (pdf), ISSN 1456-4491

It is commonly observed that complex fabricated structures subject to fatigue loading fail at the welded joints. Some problems can be corrected by proper detail design but fatigue performance can also be improved using post-weld improvement methods. In general, improvement methods can be divided into two main groups: weld geometry modification methods and residual stress modification methods. The former remove weld toe defects and/or reduce the stress concentration while the latter introduce compressive stress fields in the area where fatigue cracks are likely to initiate. Ultrasonic impact treatment (UIT) is a novel post-weld treatment method that influences both the residual stress distribution and improves the local geometry of the weld.

The structural fatigue strength of non-load carrying attachments in the as-welded condition has been experimentally compared to the structural fatigue strength of ultrasonic impact treated welds. Longitudinal attachment specimens made of two thicknesses of steel S355 J0 have been tested for determining the efficiency of ultrasonic impact treatment. Treated welds were found to have about 50% greater structural fatigue strength, when the slope of the S-N–curve is three. High mean stress fatigue testing based on the Ohta-method decreased the degree of weld improvement only 19%. This indicated that the method could be also applied for large fabricated structures operating under high reactive residual stresses equilibrated within the volume of the structure. The thickness of specimens has no significant effect to the structural fatigue strength. The fatigue class difference between 5 mm and 8 mm specimen was only 8%.

It was hypothesized that the UIT method added a significant crack initiation period to the total fatigue life of the welded joints. Crack initiation life was estimated by a local strain approach. Material parameters were defined using a modified Uniform Material Law developed in Germany. Finite element analysis and X-ray diffraction were used to define, respectively, the stress concentration and mean stress. The theoretical fatigue life was found to have good accuracy comparing to experimental fatigue tests. The predictive behaviour of the local strain approach combined with the uniform material law was excellent for the joint types and conditions studied in this work.

Keywords: Fatigue of welded structures, ultrasonic impact treatment, uniform material law, post-weld improvement methods
UDC 621.789 : 539.422.24 : 624.014.2 : 534.321.9

ACKNOWLEDGEMENTS

This research that comprises this thesis was carried out in the Department of Mechanical Engineering at Lappeenranta University of Technology.

Most of the experimental and analytical work has been carried out in two research projects "The fatigue strength of welded joints improved by ultrasonic impact treatment" funded by Finnish Funding Agency for Technology and Innovation (TEKES), VTT industrial systems, Andritz Oy, Loglift Oy, Metso Minerals Oy, Rautaruukki Oyj and Sandvik Tamrock Oy. The second project was "Improving the fatigue performance of welded stainless steels" funded primarily by the European Coal and Steel Community. Funding for finalizing the manuscript was provided by the Research Foundation of Lappeenranta University of Technology. Prof Arto Verho is thanked for his role in nominating this work for a foundation grant.

Technical assistance with the UIT device was provided by Dr. Efim Statnikov from Applied Ultrasonics, Alabama, USA and Mr. Vladislav Korostel from the Northern Scientific and Technical Centre, Severodvinsk, Russian Federation.

I wish to express my gratitude to Professor Gary Marquis for stimulating my interest in this subject and for his help during all stages of this work.

I would also like to thank my previous professors, Erkki Niemi and Teuvo Partanen and my family, co-workers and friends.

Lappeenranta 31.10.2006

Veli-Matti Lihavainen

NOMENCLATURE

Symbols and abbreviations

C_{fm}	Fracture mechanics crack growth rate coefficient
C_i	Fatigue capacity of specimen i
$C_{50\%}$	Mean fatigue capacity
$C_{95\%}$	Characteristic fatigue capacity
E	Modulus of elasticity
FAT	Fatigue strength at $2x10^6$ cycles
$FAT_{50\%}$	Mean fatigue strength
$FAT_{95\%}$	Characteristic fatigue class
FEA	Finite element analysis
FEM	Finite element method
HB	Brinell -hardness
$K^{/}$	Cyclic hardening coefficient
K_s	Hot spot stress concentration factor
K_t	Elastic stress concentration factor
$M_k(a,c)$	Stress magnification factor
N, N_f	Number of fatigue cycles
N_{ini}	Initiation fatigue life
N_D	Fatigue endurance
N_t	Transition fatigue life
N_i	Number of cycles at the level i
N_{ini}	Initiation fatigue life
N_{pro}	Propagation fatigue life
N_{tot}	Total number of cycles
Q(a,c)	Crack shape factor
R	Minimum stress / maximum stress
$R_{e,}$ f_y	Yield strength
R_m	Ultimate tensile strength
RA	Percentage reduction of area
S_a	Nominal stress amplitude
S_{ar}	Nominal stress amplitude corrected by mean stress
S_m	Nominal mean stress
S_{res}	Residual stress
UIT	Ultrasonic impact treatment
UML	Uniform material law
a	Crack depth
a_0	Initial depth of crack
a_f	Final depth of crack
b	Fatigue strength exponent
c	Fatigue ductility exponent
c(a)	Half width of crack
m	Slope of the S-N-curve, material constant of fracture mechanics
n	Number of test specimens in a test series
$n^{/}$	Cyclic strain hardening exponent

s	Standard deviation of a test series
t	Thickness of test specimen

Greek symbols

$\Delta\varepsilon$	Strain range
$\Delta\varepsilon_e$	Elastic strain range
$\Delta\varepsilon_p$	Plastic strain range
$\Delta\varepsilon^*$	Elastic strain range at 10^4 cycles
$\Delta\sigma$	Stress range
$\Delta\sigma_{eq}$	Equivalent stress range
$\Delta\sigma_{hs}$	Hot spot stress range
$\Delta\sigma_i$	Stress range at the level i
$\Delta\sigma_{nom}$, ΔS	Nominal stress range
ε_a	Strain amplitude
ε_D	Fatigue strain limit
ε_f	True fracture strain
ε'_f	Fatigue ductility coefficient
σ_a	Notch stress amplitude
σ_B	Ultimate tensile strength
σ_D	Fatigue stress limit
σ_f	True fracture stress
σ'_f	Fatigue strength coefficient
σ_{max}	Maximum stress
σ_{min}	Minimum stress

CONTENTS

1 INTRODUCTION

1.1 Background

Preventing premature fatigue failure is a dominant objective in the design of many load-carrying structures used in the mechanical engineering and process industries. Construction and agricultural equipment, bridges, ships, cranes and rotating equipment are just a few examples of heavily fatigue loaded complex welded structures. During cyclic loading, the weakest points in fabricated structures are normally the welded joints themselves. Welds represent regions of global stress concentration, very high local stress concentration, and normally possess high tensile residual stress. Additionally, welding processes often introduce small weld toe defect such as undercuts or cold laps that serve as starter cracks during cyclic loading. For these reasons, fatigue cracks in welded structures are normally observed to initiate and begin cycle-by-cycle growth very early in the service life of a structure (Maddox 1991, Lihavainen 2003).

It has been experimentally observed that most of the fatigue life for welded joints is consumed in crack propagation. This is commonly assumed during analysis. For steels, fatigue crack propagation properties are not significantly influenced by either yield or ultimate strength. In the as-welded condition, therefore, material strength has no significant effect on the measured fatigue strength. The rate of crack propagation in welded structures can be reduced by reducing the high tensile residual stress and to a lesser degree by improving the local stress concentration in a joint. Another effective means of improving the fatigue resistance of welded joints is to increase the normally very short crack initiation period. The use of the term crack initiation through this thesis is primarily pragmatic. Researchers, aided by high magnification microscopes, have shown that the so-called crack initiation period is actually a period of crack growth on a microstructural scale (Suresh 1998). Throughout this thesis the term crack propagation period is considered to be that region of fatigue life where linear elastic fracture mechanics, LEFM, can be applied and crack initiation is the number of cycles needed to form a crack of that size. The precise crack size dividing these two regimes is not easy to define, but crack sizes 0.1 – 1.0 mm are frequently used.

Methods for increasing the fatigue strength of welded structures are generally divided to two main categories:

(1) methods that modify the stress distribution near the weld to reduce tensile residual stresses or even produce beneficial compressive residual stress, and

(2) methods that modify the local geometry of the weld toe to eliminate the initial defects and decrease the local stress concentration.

Many weld improvement methods include elements of both categories. Methods in the second category may introduce a significant crack initiation period.

Ultrasonic impact treatment, UIT, is a novel post weld treatment method originally developed in the former Soviet Union for use in shipbuilding and submarine construction. When properly applied, the method is able to provide a more gradual weld metal to base metal transition reducing the local stress concentration. The area being treated is highly plastically deformed which has the effect of both work hardening the material and introducing favourable compressive residual stresses. UIT can be used to improve fatigue strength and

form a so-called “white-layer” possessing high corrosion fatigue resistance (Statnikov 1997A).

The goal of this work has been to present some new experimental data illustrating the significant fatigue strength improvement obtained using UIT and to investigate one method for explaining this degree of fatigue improvement. The novel method for predicting degree of fatigue improvement assumes that UIT is able to induce a significant period of crack initiation which can be assessed using statically measurable quantities, e.g. residual stress state, hardness and UIT groove geometry.

The fatigue strength improvement is based on the assumption that total life is the sum of crack initiation and crack propagation lives. Because the ultrasonic impact treatment effectively removes any initial crack-like flaw caused by the welding process, the local strain approach is used for computing the crack initiation portion of fatigue life (Bannantine et al. 1990, Dowling 1999). Fatigue strength and fatigue ductility coefficients along with the associated exponents, which are needed for the local strain approach, can sometimes be found from published literature (Boller and Seeger 1987), but for many materials these quantities are unavailable and must be estimated. In a case of ultrasonic impact treatment, the material is highly cold formed and thus the required coefficients and exponents are not available. In this study, coefficients and exponents at the weld toe are estimated based on the concept of the uniform material law, UML, developed by Bäumel and Seeger (1990).

Predicted total fatigue lives, i.e., the sum of crack initiation lives and crack propagation lives, have been compared to experimental fatigue lives. Experimental data was obtained on fatigue tests performed at the Lappeenranta University of Technology. Test specimens with longitudinal non-load-carrying attachment were fabricated from S355J0 structural steel with plate thickness of 5 or 8 mm. Constant amplitude fatigue testing was executed with axial tension. The purpose of fatigue testing was to define the as-welded and the UIT improved fatigue strength for the welded non-load carrying longitudinal attachments. Other objectives were to evaluate the effect of thickness between 5 and 8 mm specimens and the effect of mean stress. For some tests beach marking techniques were used to help experimentally establish the portion of total fatigue life involved in crack initiation.

The crack propagation part of fatigue life has been calculated using LEFM. Finite element analysis was used to assess the expected stress distribution through the thickness of the specimen in the crack growth direction. Stress magnifications factors, M_k factors, were computed using the weight function method. Fracture mechanic predictions were based on the range of stress intensity factor and Paris crack growth law.

1.2 Overview of the thesis

Following this introductory chapter, Chapter 2 of this thesis gives a brief survey of typical methods for post-weld fatigue improvement. Short descriptions of some of the most common methods are presented. Chapter 2 has been divided according to main categories of weld geometry improvement and residual stress methods and their subcategories. At the end of Chapter 2, one comparison between effectiveness and brief data on costs of various methods

has been referenced. This general description is followed in Chapter 3 by a discussion of the ultrasonic impact treatment equipment, its uses and benefits. Some data of previous studies have been surveyed.

Chapter 4 presents details of the analysis methods used in this study. Because fatigue tests of welded joints always have some random variation, the statistical method used to interpret the fatigue test results is briefly presented. Estimating the fatigue strength coefficient, ductility coefficient, fatigue strength exponent and fatigue ductility exponent is an important element of this thesis. So, a brief description of eight published methods for estimating these coefficients and exponents are summarized. These eight methods are: the uniform material law, four-point correlation method, universal slopes method, Mitchell's method, modified four-point correlation method, a modified universal slopes method, the hardness method and a method involving statistical evaluation.

Chapter 5 presents details of the specific experimental work. In the current study, the fatigue strength of specimens with non-load carrying longitudinal attachment has been determined experimentally. Fabrication procedures for test specimens are presented along with the parameters for base material, welding and ultrasonic impact treatment. Details of the axial tension fatigue tests and calculation of geometric (hot spot) stress ranges are presented. The procedure of beach marking is also introduced.

In Chapter 6, the two-stage life prediction is divided to initiation and propagation periods. This chapter presents details of the local strain approach for fatigue analysis that has been applied in an attempt to help understand the degree of fatigue strength improvement observed for UIT treated welds based on previous experience with base material fatigue. It is assumed that the fatigue strength improvement is due primarily to the introduction of a significant crack initiation period that can be modelled using a local model of the weld toe.

The finite element method was used to model the weld and estimate the stress concentration factor at the weld toe. A sensitivity analysis of K_t has been prepared for determining the relationship between stress concentration and the local geometry of weld. Residual stress and hardness measurements are needed for defining the state of mean stress and ultimate strength, respectively. Calculation of propagation period has been made according to fracture mechanics approach. Stress gradient through the crack propagation path is based on finite element method and the fatigue life has been estimated using weight function and Paris´ crack growth law.

In Chapter 7 the experimental results are presented and discussed. Fatigue strength in the as-welded condition is compared with fatigue strength of ultrasonic impact treated specimens. Two specimen thicknesses, 5 mm and 8 mm, and two R-values have been used for studying the thickness and the mean stress effect. Both nominal and hot spot S-N –curves have been presented with the statistical analysis of the fatigue test data. Comparison is made between the observed degree of improvement and that predicted from local strain approach. Conclusions and recommendations for further work are presented in Chapter 8.

1.3 Aim and scope of the thesis

The primary aim of this thesis has been to develop and present a method for assessing the expected degree of fatigue strength improvement for welded structures following post weld treatment using UIT. The local strain approach, a method originally developed for low cycle fatigue assessment of base materials, has been modified and integrated with FE analysis and non-destructive residual stress measurement to form a method suitable for UIT treated welds. Some new fatigue data on UIT treated welds is also presented. The main difficulty in achieving this was to find a method that could be used to deduce the material parameters needed in local strain based fatigue analysis. Values were not available from the literature and methods usually require that the ultimate strength of the material is known. UIT treatment, however, severely cold works the weld metal base metal transition region so that base material strength values would be too low. A modified version of the so-called uniform material law was used. The second difficulty was the consideration of high compressive residual stress induced by UIT.

The title of the thesis and the work presented in the thesis deals specifically with UIT treated welds. However, from a mechanistic point-of-view, the method would be expected to also work for a variety of peening-type improvement techniques including , e.g., needle peening, hammer peening, ultrasonic peening. These methods produced different local notch geometries, residual stress states and degrees of cold working which in theory could be taken into account using this method.

2 POST WELD IMPROVEMENT METHODS

Design guidance documents for fatigue of welded structures normally rely on the nominal stress approach in which different joint types are assigned characteristic fatigue strength values based on laboratory testing of a large number of typical joints. Each fatigue strength curve is identified by the characteristic fatigue strength which corresponds to the 95% survival probability stress range of the detail at 2 million cycles to failure. This value is often termed the fatigue class or FAT (Hobbacher 2006). Joint details are grouped into fatigue classes that have similar fatigue strength. For example, IIW (Hobbacher 2006) defines 13 fatigue classes and BSI (BS 5400 1980) defines 8 fatigue classes.

Post weld improvement is frequently specified during the repair of existing structures and only more recently for new structures. The first priority when improving the fatigue resistance of welded structures is to design the structure so that welds are placed in regions of lower stress whenever possible. Once this is achieved, the expected fatigue strength of a dynamically loaded structure can often be further improved by upgrading from a welded detail with lower strength to a geometry having higher fatigue strength. Once these basic steps have been accomplished, post weld improvement methods that reduce the stress concentration at the weld toe, remove weld imperfections and/or introduce local compressive stresses at the weld can be implemented to further improve fatigue strength. The use of post weld improvement methods to simply cover up a bad welding process or weak design should be avoided.

As previously mentioned in Chapter 1 of this thesis, weld improvement methods can generally be divided into two main categories: weld geometry improvement methods and residual stress alteration methods. Methods in the first group remove weld toe defects and/or reduce the stress concentration. The weld geometry improvement methods are sub-divided into grinding, re-melting and special welding techniques. Methods in the latter group introduce reduce the high tensile residual stresses at the weld toe and may introduce a compressive stress field in the area of crack initiation and propagation. Residual stress methods include mechanical and thermal stress relief methods. Kirkhope et al. (1999) have categorized a variety of the available improvement technologies as shown in Fig. 2.1. According to this figure the ultrasonic impact treatment is under the general category of residual stress methods.

Historically, weld improvement methods have been implemented primarily in conjunction with the repair welding of damaged structures. There has been strong interest in the research community to quantify the benefits of different improvement techniques and specify procedures that represent good improvement procedure practice. Interest has been to prepare guidelines that apply equally to both repair welding situations and new constructions. Working Group 2 of Commission XIII of the International Institute of Welding (IIW) has been active in this task since it was founded in 1989. In 1991 the group established an inter-laboratory comparison exercise, or round robin, test program both to consider the post weld improvement methods themselves and also to harmonize the expected degree of improvement.

The main objectives of the program were to:

- establish design S-N curves for several commonly used methods
- establish reproducibility of the methods
- compare effectiveness of methods

The as-welded condition and four weld toe improvement methods: burr grinding, TIG-dressing, needle peening and hammer peening, were included in the testing program. Eight laboratories took part in testing program. Integrated results, statistical analysis and the comparison between results have been presented by Haagensen (1997). The improvement procedures and the S-N curves have been included in the IIW document "IIW Recommendations on Post Weld Improvement of Steel and Aluminium Structures" (Haagensen and Maddox 2006). Because it is only a relatively new method within the international research community, UIT was not included in this original study. But it is planned that UIT along with other newer techniques would be included in subsequent IIW studies. Some basic aspects of these and other more traditional weld improvement methods are given in the next sections and a more detailed explanation of the UIT method is given in the following chapter.

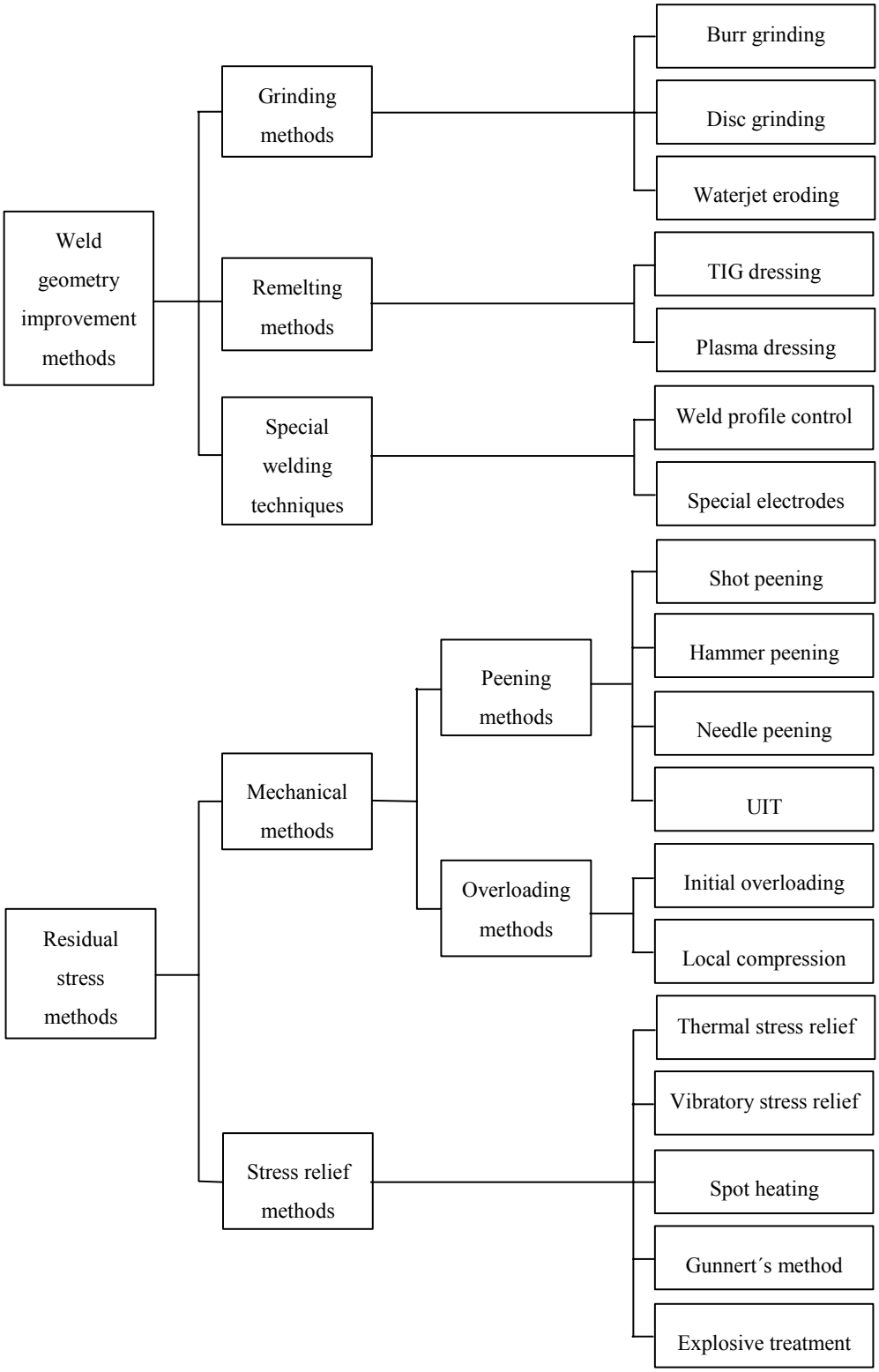

Figure 2.1 Classification of post weld improvement methods (Kirkhope et al. 1999).

2.1 Weld geometry improvements methods

2.1.1 Grinding methods

Grinding methods are implemented in order to reduce the stress concentration at the weld toe and remove weld toe defects. The main grinding methods are burr grinding, disc grinding and water jet eroding. Burr and disc grinding can be used to obtain a favourable shape, which reduces the local stress concentration at the weld toe. The harmful defects at the toe can also be reduced. For all types of grinding it is extremely important that material is removed to a depth of 0,5 to1,0 mm. This is needed to remove defects like intrusions, cold laps and sharp undercuts, see Fig. 2.2.

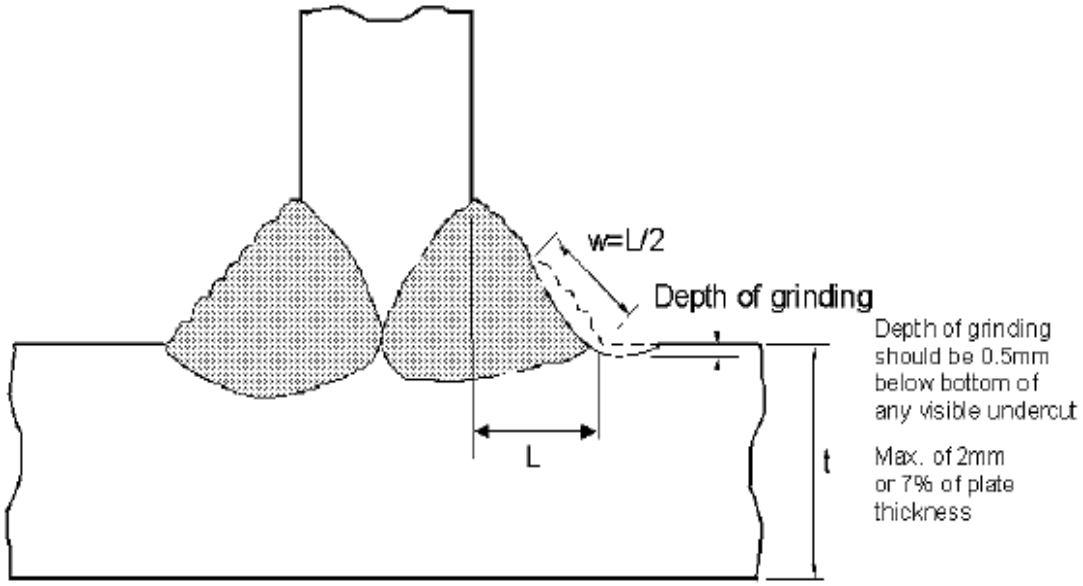

Figure 2.2 Depth and width of the groove after burr grinding (Haagensen and Maddox 2006).

Water jet eroding is one application of the so-called abrasive water jet technologies that have rapidly gained acceptance by many fabricators. Other main applications include: cutting, groove preparation, gouging and piercing. The technology is based on pressurized water passing through an orifice to form a coherent high velocity jet. In one method, the water is mixed with a dry abrasive while other methods employ abrasive water slurry. The abrasives are introduced separately into the mixing chamber.

The abrasive water jet technique is effective for the enhancement of the fatigue life of welded structures, especially for fillet welds. The main parameters of abrasive water jet technology are: pressure, travel speed, angle of impact, nozzle diameter and stand-off distance between nozzle and treated surface, see Fig. 2.3. Harris (1994) has summarized the following conclusions with regard to water jet eroding:

1. Erosion of the toe in fillet welded steel specimens improved their fatigue strengths. The improvement was significant for applied stress ranges below 200 N/mm^2.
2. The improvement in fatigue life was comparable to that obtained by local grinding, plasma dressing and shot peening, particularly in the high cycle regime.
3. The weld toe erosion rates of 20 - 45 m/hr were significantly greater than those achieved by conventional weld toe dressing methods.

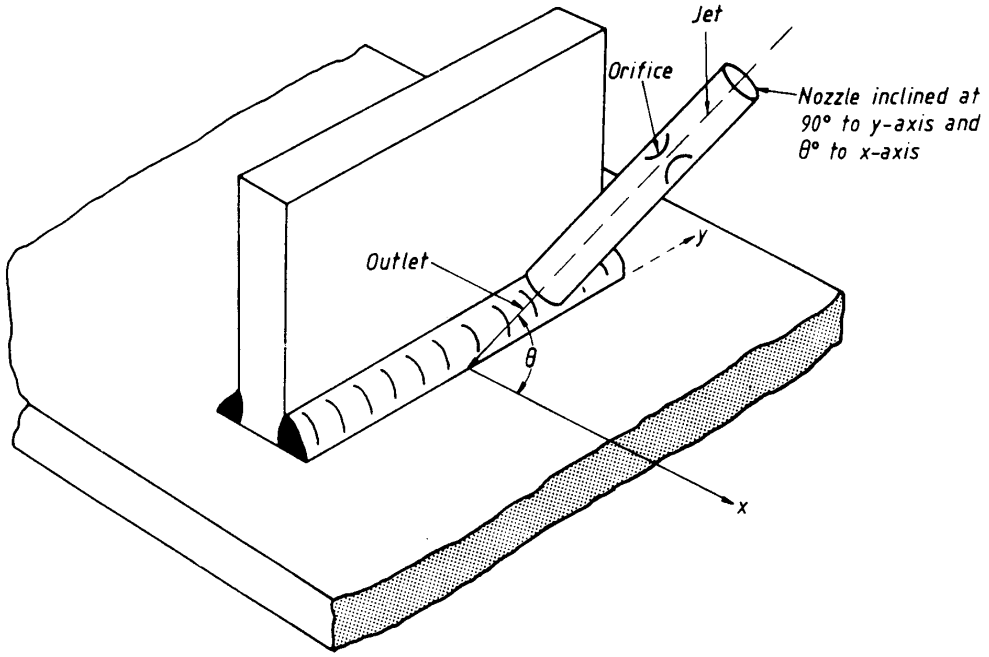

Figure 2.3 Schematic representation of weld toe dressing with an abrasive water jet(Harris 1994)

2.1.2 Re-melting methods

In these methods the weld toe area is re-melted to remove weld flaws at weld toe and reduce the local stress concentration effect by forming a smooth transition between the plate and the weld face (Haagensen and Maddox 2006). When properly applied, re-melting substantially increases the fatigue strength of a welded joint.

TIG dressing can be performed with standard TIG welding equipment. The heat input should exceed 1,0 kJ/mm to obtain a good weld profile and low hardness in the heat-affected zone. Argon is the most commonly used shielding gas, but helium could be a better choice to obtain greater depth of penetration and a higher heat input (Haagensen 1985). Positioning of the torch is one of the main TIG dressing parameters. Normally the best result is obtained when the arc centre is located 0,5 – 1,5 mm from the weld toe. Fig. 2.4 illustrates the torch position and the desired final profile from TIG dressing.

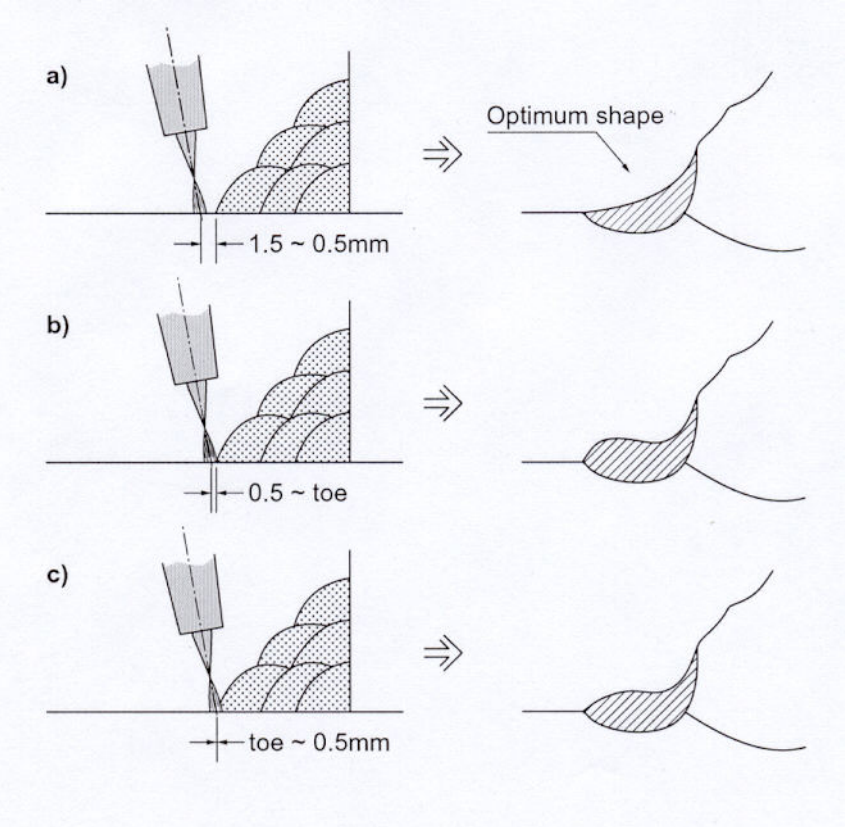

Figure 2.4 Position of torch and resulting profiles (Kado 1975)

Plasma dressing is similar to TIG dressing. The main difference is that the heat input is about twice that used in TIG dressing. Higher heat input produces a larger re-melt zone and can result in a better transition between the weld material and the base plate. The larger pool makes the plasma dressing less sensitive to electrode position relative to the weld toe (Kirkhope et al. 1999).

2.1.3 Special welding techniques

In multi-pass welding, weld profile control can be implemented to achieve favourable global weld geometry and to obtain a smooth transition at the weld toe. The beneficial weld geometry decreases the stress concentration factor at the weld toe.

In some cases special electrodes that provide a more smooth transition profile at the weld toe are used in the final pass. By achieving a large weld toe radius, the stress concentration factor is reduced and fatigue strength increased. The best improvement in fatigue performance has been obtained with high strength steels.

2.1.4 Arc brazing methods

Arc brazing methods are sometimes comprised in weld geometry improvement methods. They are not included in classification of Kirkhope et al. and are not included in Fig. 2.1. The following methods can be considered as arc-brazing methods: MIG- and MAG-brazing, plasma brazing and TIG–brazing. The principle of these methods is similar, but the difference is the way in which the filler material is melted. The fatigue strength improvement of arc-brazing methods is similar to that obtained using special welding electrodes. Sometimes, MIG- and MAG –brazing can be used as primary joining methods to obtain good fatigue strength. When these methods are applied as fatigue improvement techniques, they are used to make a final pass along the toe of conventionally welded joint. The weld toe is partially melted during the brazing. The parameters obtaining suitable heat input have to be chosen properly. Because of the melting point of the filler material is lower than that of steel, there is no significant melting in the base material at the weld toe and no crack-like flaws are theoretically generated. If the brazing is successfully performed, a smooth joint between base and filler material is produced and the low stress concentration factor is induced (Lepistö and Marquis 2004).

In the study of Lepistö and Marquis (2004), MIG-brazing has been investigated as a potential fatigue strength improvement method. The fatigue strength of MIG-brazed cruciform and T-joints were determined using tensile fatigue tests. The results indicated that hot spot -fatigue strength of MIG-brazed transverse non-load carrying welds were 70–80% higher than design curves of corresponding welded joint.

2.2 Residual stress methods

2.2.1 Mechanical methods

Mechanical peening methods are cold working techniques, which eliminate the tensile residual stresses caused by the welding process at the weld toe and induce useful compressive residual stresses. Mechanical methods also modify the geometry of the weld toe by forming a groove between parent and weld material and decrease the role of initial welding defects at the weld toe.

In many production environments shot peening is sometimes used. This method is similar to sand blasting, however, instead of sand, small diameter cast iron balls or small pieces of steel wire are fed into a high velocity air stream. The air stream is directed against the surface of the material. Shot peening causes yielding of the material surface layer thus building up compressive residual stresses that can be as high as 70–80% of the yield strength. The effectiveness of shot peening is controlled by two parameters: Almen intensity and coverage (Kirkhope et al.1999, Haagensen 1985).

Hammer peening is executed manually using a pneumatic or electrical hammer operating at about 20-100 impacts/s. A hardened steel tool with rounded 6–18 mm radius hemispherical tips is applied to the weld toe line. A typical hammer peening arrangement is shown in Fig. 2.5. The surface is plastically deformed and high compressive residual stresses are introduced. Hammer peening normally results in higher degrees of improvement in fatigue strength than shot or needle peening (Kirkhope et al. 1999).

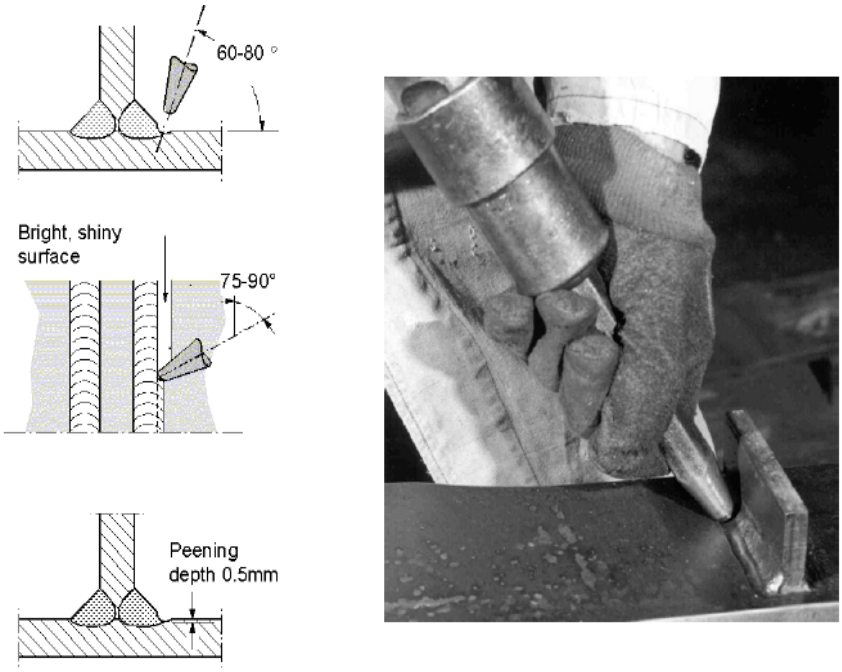

Figure 2.5 Hammer peening operation (Haagensen and Maddox 2006)

The effectiveness of hammer peening depends on the number of passes and the duration of the operation. If hammer peening is performed too rapidly, the depth of the deformed area may be insufficient to surround all defects with a field of compressive residual strain. Generally speaking, an indentation depth of 0,5 mm is a good compromise between treatment time and effectiveness (Haagensen and Maddox 2006).

Needle peening is similar to hammer peening except that the solid steel tool is replaced by a bundle of steel wires with rounded ends. The diameter of wires is approximately 2 mm (Kirkhope et al. 1999).

Ultrasonic impact treatment, UIT, has been shown to be an effective method for increasing the fatigue strength of a welded structure. The method produces an increase in fatigue strength of 50 to 200% which can be translated into a fatigue life improvement of 5 to 10 times. The exact degree of improvement depends on material properties, joint type and parameters of cyclic loading (Statnikov 1996). The UIT device and similar equipment are sometimes referred to in literature under the category of ultrasonic peening. The UIT procedure and equipment used in this study are more fully described in Chapter 3.

Initial overloading of a component is known to alter the residual stress state at the local notches of the structure. When a structure containing a stress concentration is loaded so that local yielding occurs in the regions of high stress concentration and the load is then removed, residual stresses in the structure will be reduced. A structure with no residual stresses due to manufacture will have compressive residual stresses at unloading and a structure with initially tensile residual stresses will have these reduced or even compressive residual stresses will be left if the load and stress concentration conditions are sufficient.

The important consideration is that the sign of the residual stress will be opposite to the sign of the overload. To create the compressive residual stress it is necessary to apply a tensile initial overload (Gurney 1979). In most practical design situations this alternative is difficult to implement, but it can be used, for example, in welded pressure vessels.

The principle of using local compression to produce local compressive plastic strains in portions of a structure can be implemented in other ways. Experimental work has been done using circular cross-section dies to generate compressive residual stresses. This is illustrated in Fig. 2.6. When the load is applied to the dies, the plate yields plastically and introduces radial compressive stresses in the material beneath the dies. With suitable loading, a state of general yielding can be induced between the dies so that they indent the surface and "squeeze" material out radially. When the load is removed the indentation and the compressed region remain. Some experimental work on fillet weld joints has been carried out with steel and aluminium alloy specimens. Fatigue strength increase of about 100% at two million cycles under pulsating tension loading has been observed for both materials. In these tests the residual indentation left at the surface of the material was 0,18 mm deep. The diameters of the dies were 19 mm and 44 mm (Gurney 1979).

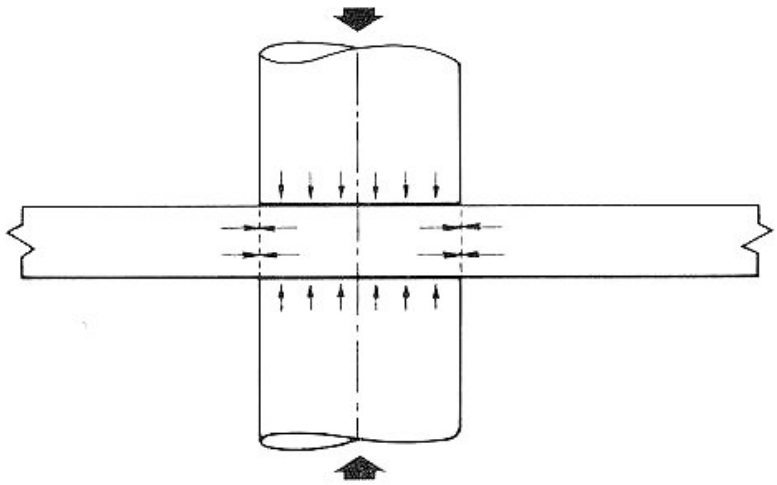

Figure 2.6 The principle of local compression treatment (Gurney 1979)

2.2.2 Stress relief methods

Thermal stress relief, also called post-weld heat treatment (PWHT), removes harmful welding residual stresses from the welded joint. A common post-weld heat treatment for steels is to heat the joint to a sufficiently high temperature, maintain this temperature for some time depending on the plate thickness and then allow slow cooling. PWHT can successfully reduce tensile residual stresses (Kirkhope et al. 1999).

Vibratory stress relief (VSR) is a method in which a vibrator is solidly coupled to the welded component and resonant vibration is induced. The induced strains and residual strains caused by welding will produce local plasticity in high stress areas. The VSR procedure requires that the resonant frequency peak for the vibrator/specimen system is first defined. The second phase is the stress relief step and involves excitation of the component at approximately 70 % of the resonance frequency for 20 minutes. The resonance frequency is the measured again and if the resonance frequency has been changed, the procedure must be repeated (James 1997).

Spot heating improves fatigue strength by producing residual stress distribution, which is self-balancing over the width of the cross-section. The structure is heated locally, usually with a gas torch, to produce yielding by means of thermal stresses. The residual stresses are formed by a mechanism similar to that which produces residual stresses during welding. The local spot heated area becomes an area of residual tensile stress and, because the internal stress distribution must be self-balancing, compressive residual stresses will exist some distance from the heated spot (Kirkhope et al.1999).

The positioning of treated spots must be located so that the line joining the centre of the heated spot and the notch is normal to the direction of the applied stress. In other words, the expected path of the fatigue crack should not pass through the centre of the spot. If the crack reaches the centre of spot, crack propagation would accelerate due to the tensile residual stresses. This is of course contrary to the objective of impeding crack growth (Gurney 1979). Proper placement of the spot heating is shown in Fig. 2.7 for one and two sided gusset specimens.

There are two difficulties in use of spot heating: the first is to decide precisely where the heat should be applied and second is to deduce the temperature that should be reached so as to obtain the maximum benefit. To avoid these difficulties, another method for improving fatigue strength has been suggested by Gunnert. In this method the real notch, rather than area adjacent to it, is heated. After heating to a temperature that causes plastic deformation, but is below the material transformation temperature, the surface is rapidly quenched by water spray. The surface cools rapidly while the underlying material cools more slowly so that, compression stresses are created in the previously cooled surface layers (Gurney 1979).

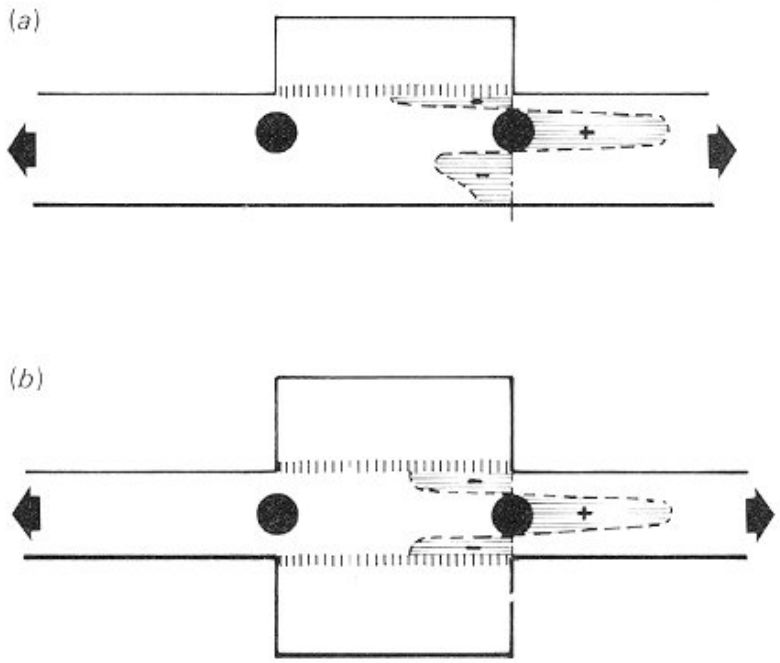

Figure 2.7 The positioning of heated spots. (a) Specimen with single gusset. (b) Specimen with two gussets (Gurney 1979)

Explosive treatment is a technology for relieving the detrimental residual stresses. In this method the working tool is explosive charges of certain shapes and masses, which are placed on the surface of the weld (Kirkhope 1999). One application of explosive treatment is so-called local explosive treatment. The application is based on a relatively small quantity of explosive material in form of cord or stripe. The explosive is placed on both sides of the heat-affected zone of the weld. The detonation front moves along the weld causing a series of shock wave, which reduce and redistribute welding residual stresses (TO-13 2003). A relatively new method related to explosion treatment involves a short duration high intensity laser pulse applied to a metallic surface. This laser peening techniques involves laser pulses lasting 10 - 30 nanoseconds but with intensities up to 15 GW/cm^2. The resulting planar shockwave travels through the work piece and plastically deforms a layer of material producing compressive residual stresses (Hill et al. 2003).

There are several difficulties to compare the fatigue data of some post weld treatment method, especially if the nominal stress approach has been used. For example, the fatigue results are dependent on the joint type, plate thickness, material, welding and treatment parameters and loading type. Huther et al. (1994) have collected a large amount of fatigue data, based on nominal stress, for comparing the effectiveness of post weld improvement methods.

The research of Huther et al. (1994) has been concerned with four types of specimen: butt welds, cruciform, T and longitudinal non-load carrying fillet welds. Test have been prepared in air –condition, R varied between 0 and 0,1. Plate thickness was less than 25 mm. Specimens were improved by one of the following techniques: hammer peening, grinding, TIG –dressing and shot peening. Results have been categorized to three classes dependent on the yield strength of the parent material.

As seen from the Table 2.1, a large amount of data has been collected for comparing the improvement efficiency. The slope of the S-N –curve, m, varies from 4 to 10. Hammer peening seems to have the highest slope and usually the highest fatigue strength.

Table 2.1 Statistical data of improvement techniques of welded joints (Huther et al. 1994).

f_y	Joint	Technique	n	m	$FAT_{50\%}$	$FAT_{95\%}$
< 400	butt joint	hammer peening	30	10	222	195
		TIG –dressing	60	7	291	202
	cruciform	hammer peening	19	10	244	211
		TIG –dressing	48	6	233	152
		shot peening	66	9	196	150
	T –joint	grinding	18	7	138	78
		TIG dressing	25	4	164	127
	longitudinal	grinding	45	5	164	115
		hammer peening	11	8	226	210
		shot peening	26	5	123	97
400 < < 600	butt joint	TIG –dressing	156	7	280	215
	cruciform	grinding	25	7	195	164
		TIG –dressing	154	6	273	182
	T –joint	TIG –dressing	74	4	213	143
		shot peening	30	9	278	222
> 600	butt joint	shot peening	99	9	326	242
	cruciform	shot peening	33	9	232	163
	longitudinal	shot peening	18	5	148	122

One of the main reasons for choosing the most adequate post weld improvement method is costs of treatment. According to Kosteas (2006), the peening methods are rather inexpensive. Evaluations from literature referring to manufacturing and application of improvement methods for welded small specimens show the cost relation presented in Table 2.2. It must be pointed that in real structures the number and extent of areas to be treated would normally be small in relation to the entire length of weld in the structure and, accordingly, the cost of the improvement methods will probably be different than in these examples with small specimens.

Table 2.2 Comparison of costs of improvement methods (Kosteas 2006).

Method	Comparative costs
Hammer peening	1
Disc grinding	2 – 4
Burr grinding	4,5
Burr grinding + polishing	12
Burr grinding + polishing + grinding depth measurement	110
TIG –dressing	3 – 4,5
Spot heating	2
Needle peening	0,5

From these results it appears that inspection and measurement of the treated groove increases the cost of treatment significantly. The costs of peening methods are distinctly lower compared to other post weld improvement methods. For comparison, welding costs, without cutting, handling and fitting, are approximately equivalent to TIG –dressing (Kosteas 2006).

2.2.3 Low transformation temperature welding consumables

One application that can be assumed to belong to the residual stress methods is low transformation temperature wire developed by National Research Institute for Metals in Japan and Kawasaki Steel Co. The primary idea of this method is to induce compressive residual stress at the weld toe. Because of that the stress ratio, R, decreases and the fatigue strength at the weld toe grows.

Particularly in Japan, the method of low transformation temperature welding wire has been a new and innovative research area. In this method, the weld filler metal alloy is chosen such that the transformation from austenite to martensite begins at a relatively low temperature. The goal is that the combination of thermal contraction due to cooling combined with transformation volume expansion should lead to a net volume increase. The expansion of the weld metal of 10 % Cr and 10 % Ni wire in the final period of cooling induces compressive residual stress at the weld toe. The effect of compressive residual stress increases the fatigue life (Ohta et al. 2000A, Ohta et al. 2000B). In multi-pass welds only the final pass is made with the relatively expensive special alloy filler wire.

Fig. 2.8 illustrates the low temperature martensitic transformation temperature and measured elongation of the new filler wire. The martensitic transformation temperature is lowered to about 200ºC as compared to 500ºC for traditional weld wire.

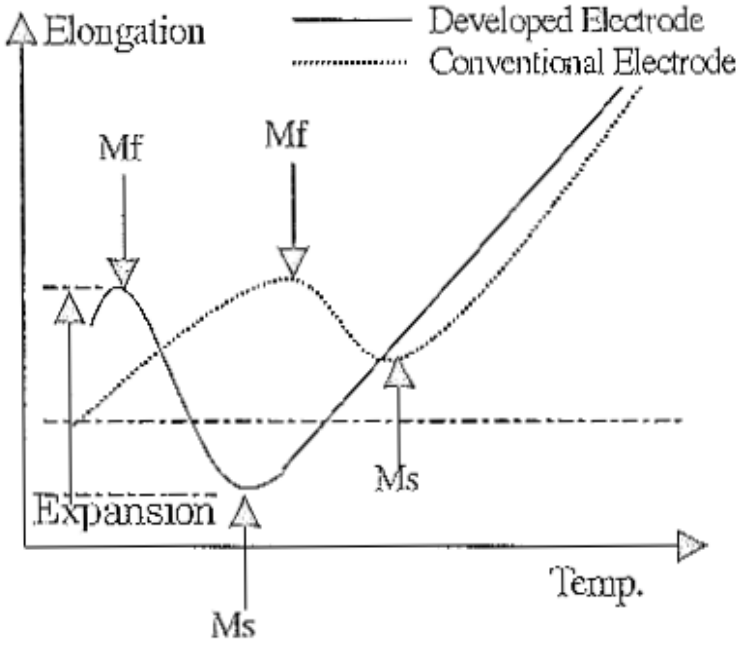

Figure 2.8 Relationship between strain and temperature during cooling (Ohta et al. 2000A)

3 ULTRASONIC IMPACT TREATMENT

3.1 Equipment and mechanism

Ultrasonic impact treatment, UIT is a novel treatment method originally developed in the former Soviet Union for use in shipbuilding and submarine construction. When properly applied, the method is able to improve and provide a more gradual weld metal to base metal transition reducing the local stress concentration. The area being treated is highly plastically deformed which has the effect of both work hardening the material and introducing favourable compressive residual stresses. UIT can be used to improve fatigue strength and form a so-called "white-layer" possessing high corrosion fatigue resistance (Statnikov 1997A).

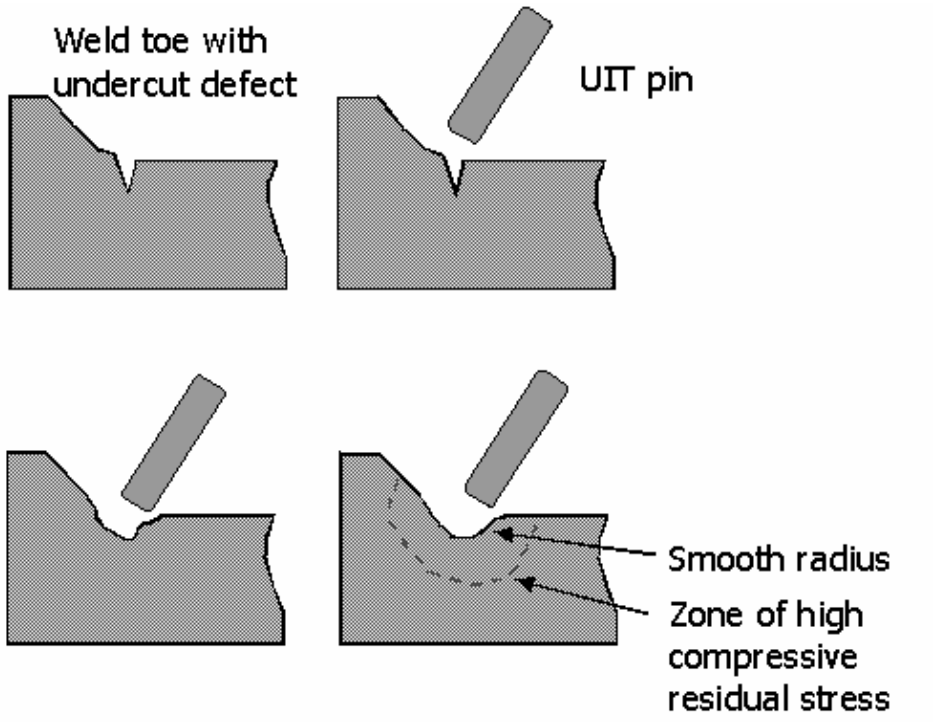

Figure 3.1 Main benefits of ultrasonic impact treatment

Fig. 3.1 illustrates the three main benefits of UIT with respect to those features of welds that most severly limit their fatigue strength. The method demolishes the undercut defect caused by welding. The stress concentration at the weld toe is decreased because of the smoother base metal to weld metal transition radius. UIT also forms a zone of high compressive residual stress.

Techniques like hammer and needle peening operate at relatively low frequencies, typically in the range of 50 to 100 Hz. In these cases the effectiveness of the treatment depends on the pressure on the tool against the treated surface with the result that the tool vibrations are transmitted directly to the hands of the operator. The required force of the impacting tool against the work piece is > 200 N. The peening tool moves in an unsteady manner and demands considerable effort from the operator to keep the tool aligned on the weld toe line

during treatment. This leads to some concerns about quality control. Additionally, the high levels of vibration and noise make these peening methods uncomfortable.

In contrast, the UIT method operates at a very high carrier frequency, approximately 27 kHz for the device used in this study, and the impact frequency of the moving pins against the work piece is in the range 150 - 300 Hz. Specifications of the UIT equipment used at Lappeenranta University of Technology are given in Table 3.1. The UIT method is less sensitive to the pressure of the tool against the work piece and the noise and vibration are much lower (Fisher 2002). The required force of the UIT tool against the work piece is approximately 30 N. The ease of use of the UIT equipment can result in considerable benefits in terms of quality of the treatment compared with conventional methods since the operator uses less effort in keeping the tool aligned with weld toe being treated. The efficiency of UIT -technology has been presented by several international research groups specializing in fatigue of welded structures (Statnikov 2000, Haagensen 1998).

In Fig. 2.1, ultrasonic impact treatment was generally categorized as a post treatment method that improves the residual stress state of the weld. In fact, UIT influences both the residual stress distribution and improves the local geometry of the weld. Because of the local work hardening, UIT creates residual stresses that are higher than yield stress of the base metal and plastic deformation to a the depth of 1500 μm has been observed. A smooth transition between the weld and base metal is formed and initial weld defects are removed. Other major features of ultrasonic impact treatment have been given by Statnikov (1997B):
(1) high quality of treated surfaces
(2) possibility for operation in diverse space positions and narrow places
(3) high stability of treatment quality
(4) relatively small weight of the instrument
(5) electric safety, low noise and vibration

While originally applied as a means of treating submarine hulls for extreme conditions, today the UIT technology has been applied to aerospace, automotive, rail transportation and large structures exposed to fatigue loading (Haagensen 1998).

Table 3.1 Specification of the 27 kHz ultrasonic impact treatment equipment (Statnikov 1999)

Operating frequency [kHz]	27
Design	For manual treatment
Consumed power [VA]	600-1200
Excitation voltage [V]	60-110
Bias current [A]	10-15
Oscillating amplitude [μm]	35-40
Treatment speed in manual mode [m/min]	0,3-1,5
Dimensions of manual tool [mm]	455*85*80
Manual tool weight [kg]	3,5
Cooling	Liquid
Replaceable tool head	Straight, angle
Intender (=needle) diameter [mm]	2-5
Hardness of intender work face [HRC]	62-64

The UIT tool and control units at LUT are shown in Fig. 3.2. A photograph of the UIT tool in use and the smooth transition obtained in the treated weld toe region is shown in Fig. 3.3. Depending on the specific application, a variety of needle sizes and configurations are available. Several examples are shown in Fig. 3.4.

Figure 3.2 27 kHz ultrasonic impact treatment equipment

Figure 3.3 Ultrasonic impact treatment of a weld toe in progress

Figure 3.4 Several examples of needle sizes and configurations for the UIT device

UIT imparts a high velocity impact to the component being treated to form an area of high plastic deformation and energy transfer. The UIT equipment introduces high-power ultrasonic oscillation and stress waves into the structure being treated through the relatively small indenter contact area. The features of UIT that influence the quality of the treatment are the energy of a single impulse, the impact repetition rate and the duration of contact between the indenter and the treated surface. The phase of uninterrupted oscillation in the "indenter-surface-transducer" system during each single impact defines the nature of treatment and is the most important aspect of treatment. The duration of a single contact ranges from several hundred microseconds to a few milliseconds depending on the resonant frequency of the ultrasonic transducer (Statnikov 2005).

Table 3.2 Physical zones of UIT effect on material properties (Statnikov 1997A)

Zone	Technical effect
"White layer"	Wear-resistance, corrosion resistance
Plastic deformation	Cyclic endurance, compensation of deformation, corrosion fatigue strength
Impulse relaxation	Reduction in residual welding stress and strain of up to 70% of the initial state
Ultrasonic relaxation	Reduction in residual welding stress and strain of up to 50% of the initial state

Figure 3.5 illustrates the so-called physical action zones through a material cross-section induced by UIT treatment. A thin layer on the surface of the cross section, "white layer", represents an area of very fine microstructure with good wear and corrosion resistance. The maximum depth of the region of plastic deformation is 1,5 mm. The impulse area and ultrasonic relaxation zone are reported to be 3 - 5 mm and 10 - 12 mm, respectively (Statnikov 1997A).

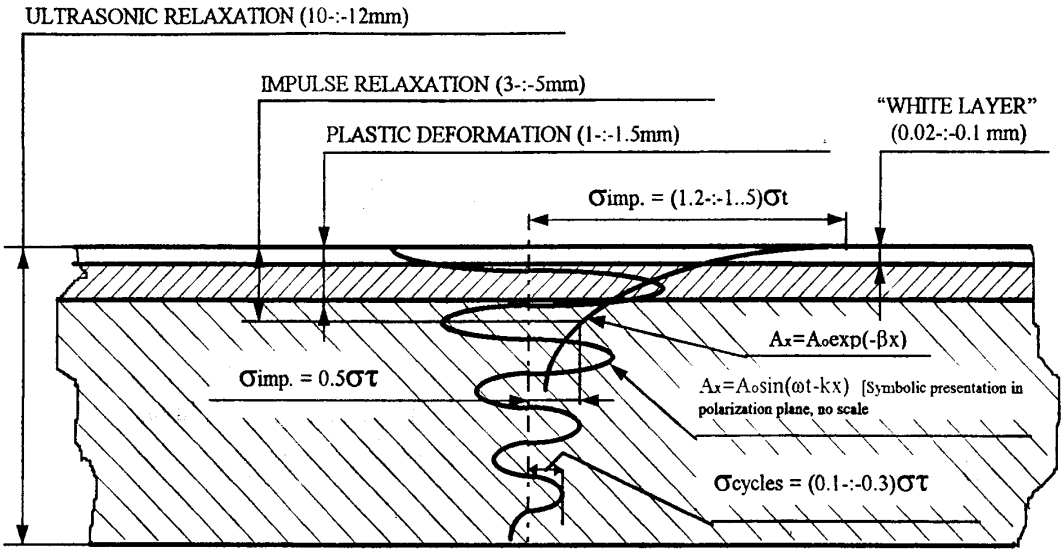

Figure 3.5 Zones of physical action on a welded joint (Statnikov 1997A)

3.2 Fatigue data related to UIT

Experimental data for UIT treated welds are presented frequently, for example, within documents presented in Commission XIII of IIW. The data here is by no means exhaustive, but can be considered as representative.

3.2.1 Longitudinal attachments

The study of Haagensen et al. (1998) summarizes fatigue test series on welded high strength Weldox 700 steel specimens and aluminium welds. Conditions of tested specimens were as-welded, ultrasonic impact treatment, TIG dressing and a combination of TIG –dressing and ultrasonic impact treatment. Two aluminium materials were tested in as-welded and ultrasonic impact treated state. The fatigue strength of non-load carrying specimens with longitudinal attachments were determined at stress ratio R = 0,1.

Table 3.3 Fatigue strength results based on nominal stress range (Haagensen et al. 1998).

	t [mm]	Slope m	$C_{50\%}$	Deviation	$FAT_{50\%}$	Difference [%]
High strength steel - Weldox 700						
AW	6	3,02	$1{,}39 \cdot 10^{12}$	-	86	-
UIT	6	6,54	$1{,}66 \cdot 10^{21}$	0,452	190	121
TIG	6	3,05	$5{,}93 \cdot 10^{12}$	0,397	132	53
TIG+UIT	6	5,14	$1{,}45 \cdot 10^{18}$	0,133	202	135
Aluminium - AlMg4.5Mn						
AW	8	4,48	$1{,}59 \cdot 10^{13}$	0,387	35	-
UIT	8	4,48	$3{,}26 \cdot 10^{14}$	0,345	68	94

The ultrasonic impact treatment gives 121 and 94 per cent higher mean fatigue strength compared to welds in the as-welded condition. The SN slope of ultrasonic impact treated series of high strength steel is distinctly higher that that of the as-welded series.

3.2.2 Large scale structure

The majority of fatigue tests reported in literature have been executed with relative small specimens or coupons. For small specimens the residual stress state during the fatigue test may be significantly different from than existing in large complex structures. In such cases the fatigue strength found with small specimens is probably too high. In a study carried out at the Lehigh University, USA, some large scale beam sections have been tested for determining the fatigue strength of UIT treated large structures (Sougata et al. 2003, Fisher et al. 2002).

Eighteen rolled wide flange beams having minimum yield stresses of 366 - 435 MPa were tested under this research program. The thickness of flanges and cover plates were 28 and 25 mm, respectively. Three cover plate end weld details were investigated. Transverse stiffeners covering half the web height and the full web height were welded to the compression and tension flanges and to the web, see Fig. 3.6. Ultrasonic impact treatment was carried out using 3 mm diameter pins. The number of passes for treatment was 3 - 5.

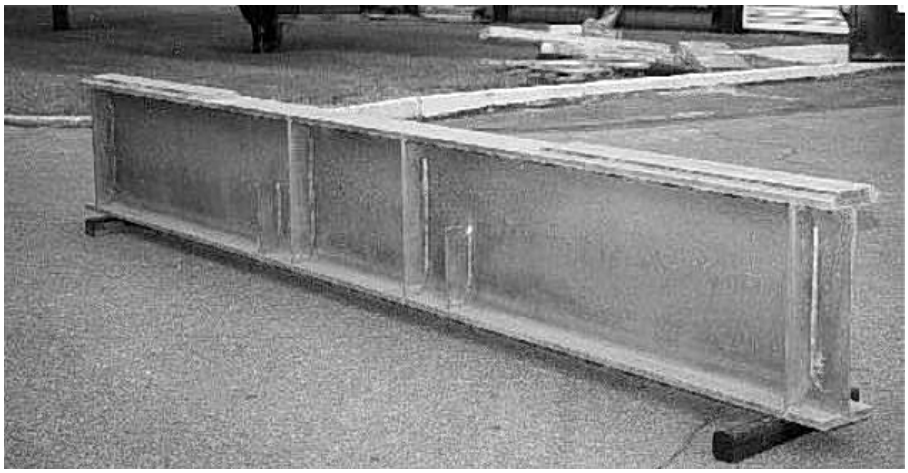

Figure 3.6 Rolled wide flange beam section with the transverse stiffeners and cover plates.

The AASHTO (American Association of State Highway and Transportation Officials) fatigue design guideline classifies the details of welded beam sections using six curves.

Table 3.4 AASHTO fatigue design curves for welded beams (Keating and Fisher 1986)

Category	Detail
A	rolled beams
B	longitudinal welds, flange splices
C	stiffeners, short attachments (< 50 mm)
D	attachments (< 100 mm)
E	cover plates
E´	thick cover plates, long attachments

The results of large beam test program showed that use of ultrasonic impact treatment increases fatigue strength of thick cover plate weld details from E´ to category C. The category C transverse stiffener details on tension flange and web can achieve category B (Fisher et al. 2002).

3.2.3 Fatigue strength of high strength steel

Similarly, Venkateshwaran (2005) from LUT reported some experimental results for UIT treated high strength steel welds using variable amplitude loading. The fatigue strength was significant with respect to specimens in the as-welded condition, but failure of the longitudinal specimens initiated from the root side for all post weld treated specimens. Fig. 3.7 shows the test specimens and Fig. 3.8 shows the fatigue test data. Further tests in this program are in progress.

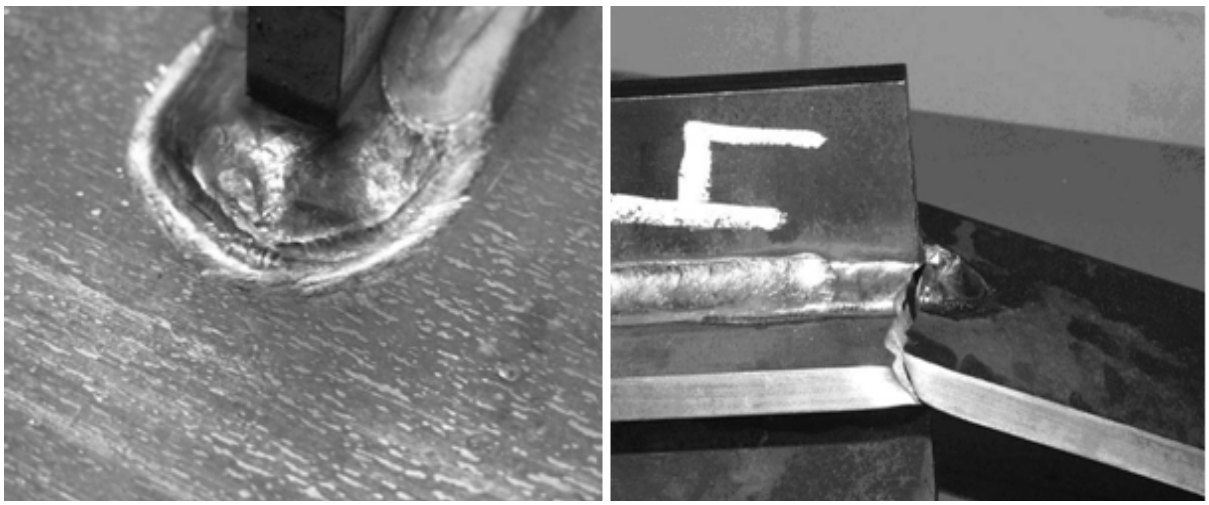

Figure 3.7 UIT treated longitudinal attachments from 700 MPa steel a) the UIT treated weld toe and b) the specimen failure from a weld root defect (Venkateshwaran 2005).

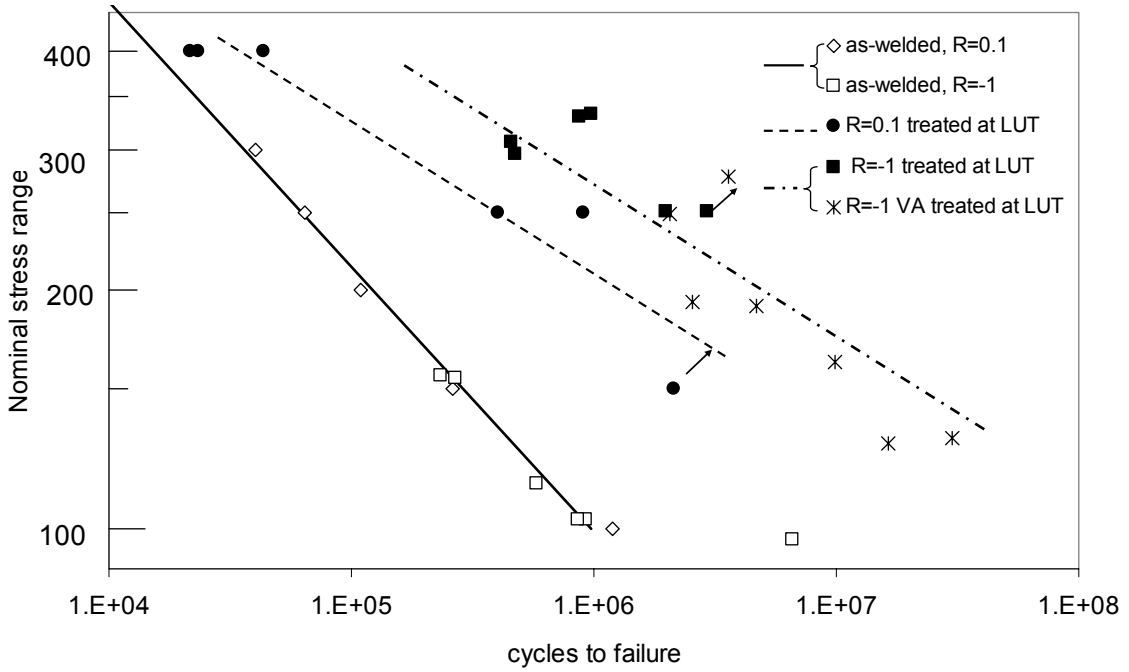

Figure 3.8 UIT treated longitudinal attachments from 700 MPa steel (Venkateshwaran 2005).

3.2.4 Ultrasonic peening

Ultrasonic impact treatment is a patented technology and trade name. However, other ultrasonic based improvement technologies also exist (Huo et al. 2001, Huo et al. 2002, Kudryavtsev et al. 2005, Kudryavtsev and Kleiman 2005). The other technologies often are described as ultrasonic peening, UP. These devices employ the same basic solution as is used in the UIT tool. The major distinction between tools is that UIT utilizes a high-power magnetostrictive ultrasonic transducer, e.g., 1200 W, while UP devices use a piezoelectric transducer of less power, 400 – 800 W. One commercially available UP device is shown in Fig. 3.9. The duration of UP impulse does not exceed 10 microseconds when UIT is accompanied by impulse excitation of impacts at least 500 microseconds (Statnikov et al. 2005).

Figure 3.9 A UP device manufactured by Integrity Testing Laboratory (Kudryavtsev and Kleiman 2005).

In the study of Huo et al. (2001), experimental results showed that fatigue strength can be dramatically increased by ultrasonic peening. To define the effectiveness of ultrasonic peening, fatigue tests were performed on butt and cruciform joints of structural steel, R_e =260 MPa, both in the as-welded and UP conditions. Butt joints were tested using R=0,1 and R=0 loading. Cruciform joints were subjected to four point bending with R=0,25. Thicknesses of the specimen were 8 mm. The relative improvements in fatigue mean class due to UP at 2 million cycles was 57% for butt joints and 64 % for cruciform welds.

Many constant amplitude fatigue tests have been proved that fatigue strength of welded joints increases after UP. However, there is a need to check the benefit of UP for structures subjected to variable amplitude loading. Huo et al. (2002) have used the test specimens of 8 mm thick plates with non-load carrying longitudinal attachments for clarifying the efficiency of UP under block amplitude loading. The programmed sequence of block loading consisted of three levels of stress ranges (252, 225 and 207 MPa).

Under constant amplitude loading, UP increased the fatigue strength 84% and under block loading the corresponding benefit were 80% in fatigue strength (Huo et al. 2002).

4 ANALYSIS METHODS

4.1 Statistical Analysis of the test data

Data has been evaluated according to statistical methods for fatigue testing developed within the International Institute of Welding. These have been outlined by Hobbacher (1994). The term fatigue class, FAT, indicates the characteristic stress range in MPa, which gives a fatigue life of two million cycles at 95 % survival probability. In equation (4.5), the fatigue class FAT has been presented as $FAT_{95\%}$. The statistical analysis of test series has been calculated according to equations 4.1 - 4.5.

First, the fatigue capacity of each test specimen, i, in a sample is calculated using the equation

$$\Delta\sigma_i^m \cdot N_i = C_i = FAT_i^m \cdot 2000000 \tag{4.1}$$

where *m* is the slope of the S-N curve and is here assumed to be 3. N_i, C_i and $\Delta\sigma_i$ are the number of cycles to failure, fatigue capacity, and applied stress range for specimen, i.

The mean value of fatigue capacity is computed by

$$\log C_{50\%} = \frac{\sum \log C_i}{n} \tag{4.2}$$

where *n* is the number of test specimens in the sample. The standard deviation, s, of the fatigue capacity of the sample is then

$$s = \sqrt{\frac{\sum (\log C_i - \log C_{50\%})^2}{n-1}} \tag{4.3}$$

The characteristic value of fatigue capacity, $C_{95\%}$, is

$$\log C_{95\%} = \log C_{50\%} - s \cdot (1{,}64 + \frac{1{,}15}{\sqrt{n}}) \tag{4.4}$$

The characteristic fatigue class is

$$FAT_{95\%} = \sqrt[m]{\frac{C_{95\%}}{2000000}} \tag{4.5}$$

Whenever possible, comparisons of fatigue strength between treated and as-welded specimens, or between different test conditions are made based on $FAT_{95\%}$ since this value reflects both the measured fatigue strength and the observed scatter in the results.

4.2 Methods for estimating fatigue properties for local strain analysis

The relationship between strain amplitude and fatigue life under uniaxial loading can be expressed by Basquin-Coffin-Manson equation (Bannantine et al 1990, Dowling 1999):

$$\varepsilon_a = \left(\frac{\sigma_f^{/}}{E}\right)\cdot\left(2\cdot N_f\right)^b + \varepsilon_f^{/}\cdot\left(2\cdot N_f\right)^c \qquad (4.6)$$

This equation is illustrated in Fig 4.1. Application of the Basquin-Coffin-Manson equation requires material parameters ($\sigma_f^{/}$, b, $\varepsilon_f^{/}$, c) that must be defined by relatively expensive strain controlled fatigue testing. The lack available material parameters has somewhat limit the use of Eq. (4.6) in design. Over the last decades, many researchers have tried to develop relations between material parameters and monotonic tensile properties of engineering materials. If reliable relations with reasonable accuracy can be established, they can provide fast solutions to calculate the material parameters for local strain analysis (Kim et al. 2002). Eight of these proposed relationships are presented in subsequent sections. Park and Song (1995), Kim et al. (2002) and Meggiolaro and Castro (2004) have provided helpful summaries of many of the approximation methods.

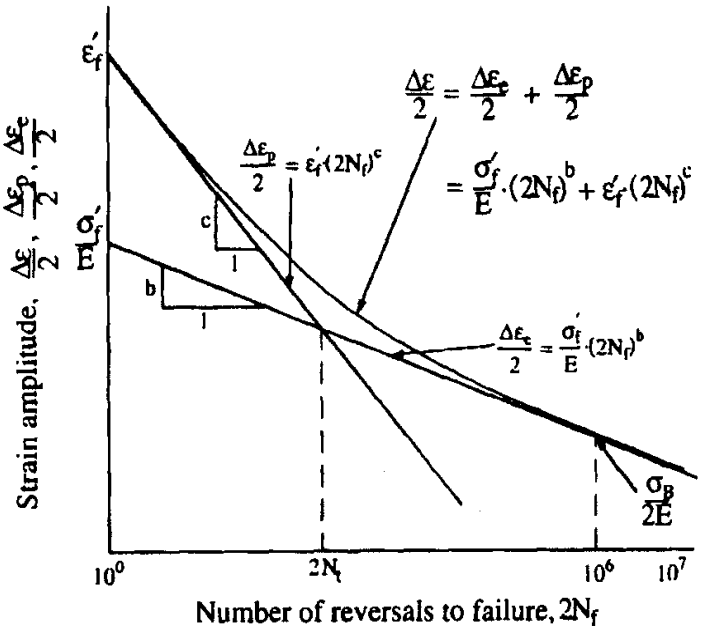

Figure 4.1 Elastic, plastic and total strain (Park and Song 1995).

4.2.1 Four-point correlation method

Manson (1965) first suggested that the monotonic tensile properties could be used for estimating the strain-life curve using a four-point correlation method. The four points include two points on elastic strain-life and two points on the plastic strain-life curve as shown in Fig 4.2. These four points are obtained by solving Eqs (4.7a – 4.7e). It should be noted that these equations require only static values R_m, ε_f and E as material inputs.

$$\sigma_f^{/} = \frac{E}{2} \cdot 10^{b \cdot \log(2) + \log\left[\frac{2.5 \cdot R_m \cdot (1+\varepsilon_f)}{E}\right]} \tag{4.7a}$$

$$b = \frac{\log\left[\frac{2.5 \cdot (1+\varepsilon_f)}{0.9}\right]}{\log\left[\frac{1}{4 \cdot 10^5}\right]} \tag{4.7b}$$

$$\varepsilon_f^{/} = \frac{1}{2} \cdot 10^{c \cdot \log\left(\frac{1}{20}\right) + \log\left(\frac{1}{4} \cdot \varepsilon_f^{3/4}\right)} \tag{4.7c}$$

$$c = \frac{1}{3} \cdot \log\left[\frac{0.0132 - \Delta\varepsilon^*}{1.91}\right] - \frac{1}{3} \cdot \log\left(\frac{1}{4} \cdot \varepsilon_f^{3/4}\right) \tag{4.7d}$$

where $\Delta\varepsilon^*$ is the elastic strain range at 10^4 cycles and is estimated by

$$\Delta\varepsilon^* = 10^{b \cdot \log\left(4 \cdot 10^4\right) + \log\left[\frac{2.5 \cdot R_m \cdot (1+\varepsilon_f)}{E}\right]} \tag{4.7e}$$

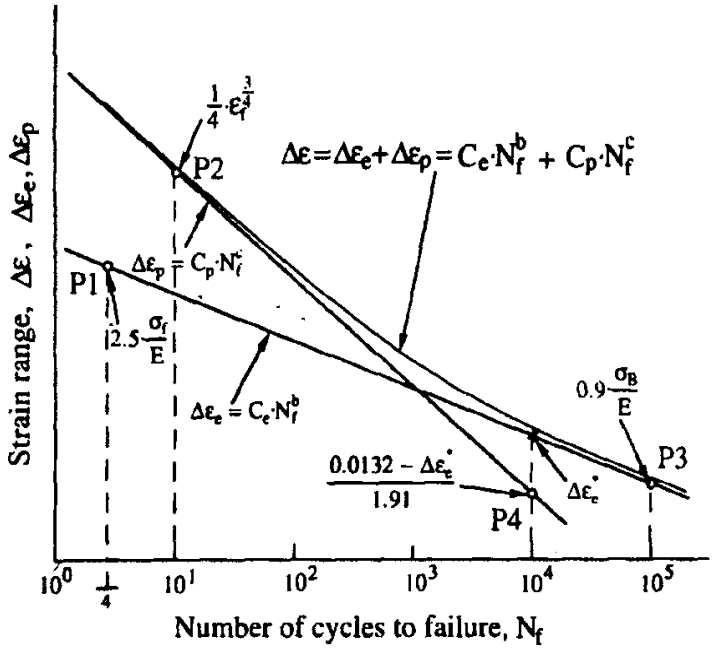

Figure 4.2 Four-point correlation method (Park and Song 1995).

The four-point correlation method defines estimates of the elastic and plastic strain ranges $\Delta\varepsilon_e$ and $\Delta\varepsilon_p$ at four different lives N = ¼, 10, 10^4 and 10^5.

4.2.2 Universal slopes method

An alternative method, also proposed by Manson (1965), assumes that the slopes of the elastic strain-life and plastic strain-life curves do not vary with materials. The fatigue properties based on the universal slopes method are given by:

$$\sigma_f^{/} = 1.9018 \cdot R_m \tag{4.8a}$$

$$b = -0.12 \tag{4.8b}$$

$$\varepsilon_f^{/} = 0.7579 \cdot \varepsilon_f^{0.6} \tag{4.8c}$$

$$c = -0.6 \tag{4.8d}$$

4.2.3 Mitchell's method

Mitchell (1979) suggested using the following equations for steels with hardness below 500 HB.

$$\sigma_f^{/} = R_m + 345(MPa) \tag{4.9a}$$

$$b = -\frac{1}{6} \cdot \log\left[\frac{2 \cdot (R_m + 345)}{R_m}\right] \tag{4.9b}$$

$$\varepsilon_f^{/} = \varepsilon_f = \ln\left[\frac{100}{100 - RA}\right] \tag{4.9c}$$

$$c = -0.6 \tag{4.9d}$$

Where RA is the percentage reduction of the area. Mitchell also recommended constructing the plastic line using an empirical presentation of the hardness and transition fatigue life $2 \cdot N_t$. The transition fatigue life is the number of reversals at which the elastic and plastic strain-life lines cross, see Fig. 4.1. Because the hardness-transition life data are not usually available, a constant value of c = -0.6 for most materials can be used as the slope of the plastic line.

4.2.4 Modified four-point correlation method

A modified four-point correlation method that uses four locations of strain range-life cycle diagram for estimating the coefficients and exponents needed in local strain approach has been proposed by Ong (1993). The resulting equations are given as:

$$\sigma_f^{/} = R_m \cdot \left(1 + \varepsilon_f\right) \tag{4.10a}$$

$$b = \frac{1}{6} \cdot \left\{ \log\left[0.16 \cdot \left(\frac{R_m}{E} \right)^{0.81} \right] - \log\left(\frac{R_m}{E} \right) \right\} \tag{4.10b}$$

$$\varepsilon_f^{/} = \varepsilon_f \tag{4.10c}$$

$$c = \frac{1}{4} \cdot \log\left(\frac{0.00737 - \frac{\Delta\varepsilon_e^*}{2}}{2.074} \right) - \log \varepsilon_f \tag{4.10d}$$

where $\Delta\varepsilon_e^*$ is the elastic strain range at 10^4 cycles and is presented by the expression

$$\frac{\Delta\varepsilon_e^*}{2} = \frac{\sigma_f}{E} \cdot \left[10^{\frac{2}{3} \cdot \left\{ \log\left[0.16 \cdot \left(\frac{R_m}{E} \right)^{0.81} \right] - \log\left(\frac{\sigma_f}{E} \right) \right\}} \right] \tag{4.10e}$$

where the true fracture stress $\sigma_f = \sigma_f^{/}$.

4.2.5 Modified universal slopes method

The universal slopes method was later modified by Muralidharan and Manson (1988). This method provides lower slopes, b and c, for the elastic and plastic lines than the original method. The term including ultimate tensile strength and modulus of elasticity is increased to the coefficient of the plastic line.

$$\sigma_f^{/} = E \cdot 0.623 \cdot \left(\frac{R_m}{E} \right)^{0.832} \tag{4.11a}$$

$$b = -0.09 \tag{4.11b}$$

$$\varepsilon_f^{/} = 0.0196 \cdot \varepsilon_f^{0.155} \cdot \left(\frac{R_m}{E} \right)^{-0.53} \tag{4.11c}$$

$$c = -0.56 \tag{4.11d}$$

4.2.6 Uniform material law

The uniform material law, UML, was developed in Germany by Bäumel and Seeger (1990) as a means of approximating the material variables used in the local strain approach without the relatively expensive material tests. Bäumel and Seeger were the first to recognize the importance of using alternate material estimates for different alloy families. It is generally observed that measured exponents b and c are lower for aluminium and titanium alloys than for steels. They proposed different estimates for low-alloy steels and for aluminium and titanium alloys.

Table 4.1 Coefficients of uniform material law (Bäumel and Seeger 1990)

	Unalloyed and low-alloy steels	Aluminium and titanium alloys
σ'_f [MPa]	$1{,}5 \cdot R_m$	$1{,}67 \cdot R_m$
b	-0,087	-0,095
ε'_f	$0{,}59 \cdot \psi$	0,35
c	-0,58	-0,69
σ_D [MPa]	$0{,}45 \cdot R_m$	$0{,}42 \cdot R_m$
ε_D	$0{,}45 \cdot \frac{R_m}{E} + 1{,}95 \cdot 10^{-4} \cdot \psi$	$0{,}42 \cdot \frac{R_m}{E}$
N_D	$5 \cdot 10^5$	$1 \cdot 10^6$
K' [MPa]	$1{,}65 \cdot R_m$	$1{,}61 \cdot R_m$
n'	0,15	0,11

According to UML the dimensionless value ψ is related to the ultimate strength and elastic modulus.

$$\begin{aligned} \psi &= 1{,}0 && \text{if } \frac{R_m}{E} \le 3 \cdot 10^{-3} \\ \psi &= \left(1{,}375 - 125 \cdot \frac{R_m}{E}\right) && \text{if } \frac{R_m}{E} > 3 \cdot 10^{-3} \end{aligned} \tag{4.12a}$$

4.2.7 Hardness method

The so-called hardness method has been proposed by Roessle and Fatemi (2000) and represents a simple method for estimating low cycle fatigue material properties from Brinell hardness and the elastic modulus. The method is considered valid for steel with hardness in the range 150 – 700 HB. The exponents b and c are same as those of the modified universal slopes method, i.e., -0.09 and -0.56, respectively.

$$\sigma'_f = 4.25 \cdot (HB) + 225 \tag{4.13a}$$

$$b = -0.09 \tag{4.13b}$$

$$\varepsilon'_f = \frac{1}{E} \cdot \left[0.32 \cdot (HB)^2 - 487 \cdot (HB) + 191000\right] \tag{4.13c}$$

$$c = -0.56 \quad (4.13d)$$

The hardness method has a significant advantage over other methods in that it only requires hardness and modulus of elasticity. Other methods use tensile properties. Hardness of steel can be determined from non-destructive tests and the modulus of elasticity is normally considered to be constant within a class of materials.

4.2.8 Statistical evaluation

Meggiolaro and Castro (2006) have hypothesized that the coefficients and exponents needed for the local strain analysis method can be approximated based on statistics. In study of Meggiolaro and Castro, strain-controlled constant amplitude fatigue and monotonic tests were performed on eight steels and one aluminium alloy. A minimum of ten specimens of each material were tested at strain amplitudes from 0,2 to 1,2 %. All tests were made using completely reversed strain control. These nine series were combined with the material properties obtained from the literature.

Meggiolaro and Castro concluded that the best life predictions could be obtained from constant estimates of parameters. Median values of the coefficients and exponents for steels computed as: $\sigma_f^{/} = 1{,}5 \cdot R_m$, $\varepsilon_f^{/} = 0{,}45$, b = -0,09 and c = -0,59. It is proposed by Meggiolaro and Castro that these can be used for fatigue assessment.

The predicted and observed fatigue lives using the statistical method are presented in Fig. 4.3. This figure also shows the distribution of fatigue lives for material parameters also estimated using the uniform material law, Mitchell's method and Muralihadran-Manson's modified universal slopes method. The median values proposed by Meggiolaro and Castro and the uniform material law proposed by Bäumel and Seeger gave the most appropriate prediction of fatigue life. Observed fatigue life was obtained for strain controlled tests with strain amplitude $\varepsilon_a = 1{,}0\%$.

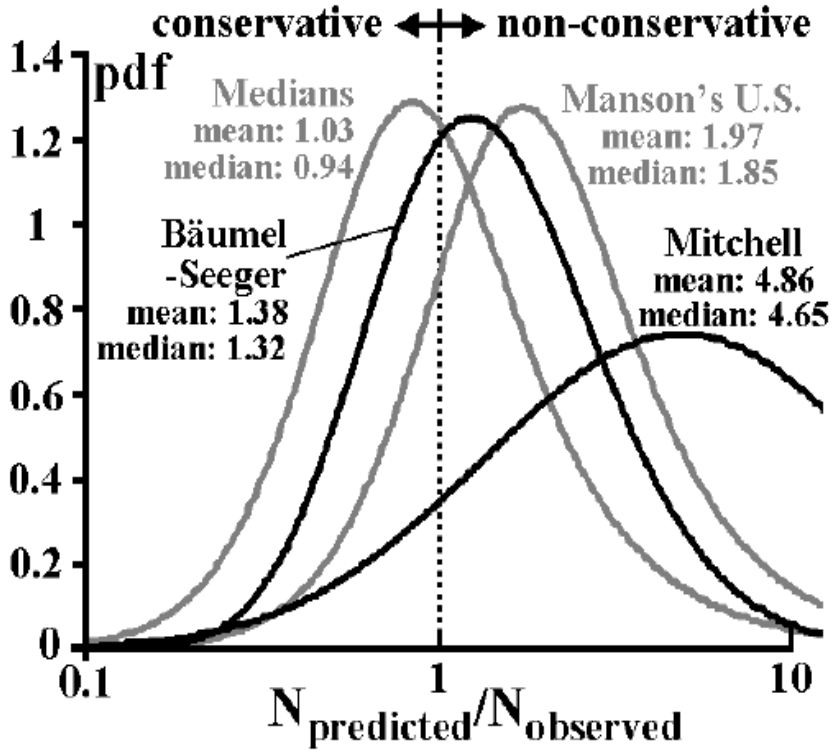

Figure 4.3 Probability density functions of four estimation methods for steels (Meggiolaro and Castro, 2006).

4.2.9 Summary of the approximation methods

Eight alternative methods for estimating the material parameters needed in the Coffin-Manson-Basquin equation have been presented. All methods except UML and the hardness method require that ε_f is measured experimentally. The comparative work of Meggiolaro and Castro showed that UML gave promising results for the materials tested. UML still requires that R_m for the material is known. In the case of UIT treated welds, this value can not be determined directly and is therefore estimated based on hardness similar to the hardness method of Roessle and Fatemi. A synthesized method, involving the main features of UML, but also including hardness of the material in the UIT zone is used in Chapter 6 of this thesis to estimate the crack initiation life using the Coffin-Manson-Basquin equation.

5 EXPERIMENTAL METHODS

5.1 Test specimens: geometry, fabrication and UIT treatment

5.1.1 One-sided longitudinal attachment

Longitudinal attachment test specimens were fabricated from hot-rolled (EN 10025-2) S355J0 general structural steel, which is currently marketed under the trade name Multisteel. Both 5 mm and 8 mm thick plates were used for the main plate while the attachment thickness was 8 mm. Overall specimen length was 600 mm and the width was 40 mm at gripping section and 34 mm in the narrowed portion of the specimen. The attachments of 100 by 40 mm were welded to along one side of base plate. The test specimen geometry and dimensions are shown in Fig. 5.1.

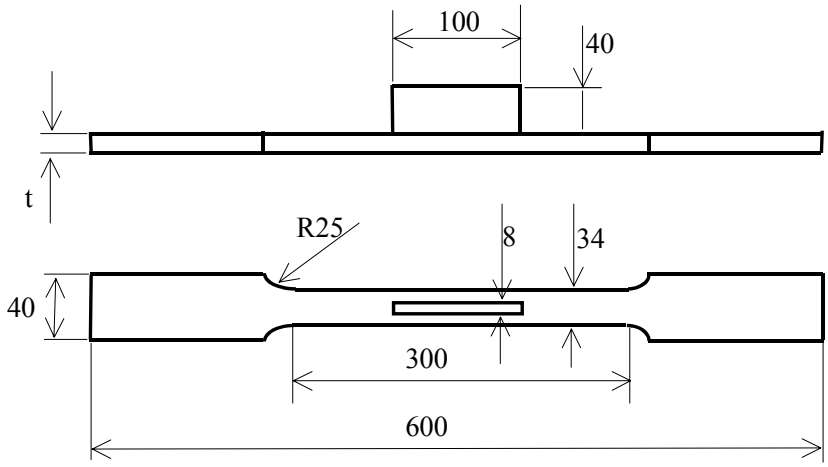

Figure 5.1 Test specimen of structural steel S355 longitudinal attachment. Specimen thickness t = 5 mm or t = 8 mm

This longitudinal attachment specimen type is used extensively in laboratory fatigue experiments. The relatively small specimens are known to have high tensile residual stresses similar to those found in larger and more complex structures. Additionally, the specimen has a relatively small region of high stress concentration so the location of expected fatigue crack initiation is more predictable than for many other weld geometries. The longitudinal welded attachment specimen has been used in many investigations and a large database is available. For example, the fatigue strength of ultrasonic impact treated longitudinal attachments has earlier been presented by Haagensen (1998).

Chemical analysis and mechanical properties of material S355J0 are shown in Tables 5.1 and 5.2 (Rautaruukki 1996). The gas metal arc (MAG, GMAW) welding and UIT treatment parameters for the one-sided longitudinal attachment specimen are given in Table 5.3.

Table 5.1 Chemical analysis of material S355J0 [%].

C	Si	Mn	Al	Nb	S	P
<0,18	<0,50	<1,60	>0,02	<0,05	<0,02	<0,025

Table 5.2 Mechanical properties of material S355J0.

Yield strength R_e [MPa] minimum	Ultimate strength R_m [MPa]	Elongation A_5 [%] minimum	Impact ductility KV [J] 0°C
355	490-630	20	27

Table 5.3 Welding and UI -treatment parameters.

Welding parameters	
Welding process	MAG
Current [A]	280
Voltage [V]	29
Shielding gas: Argon/CO_2 [%]	90 / 10
Filler material	OK 12.51
Travel speed [cm/min]	34
UI -treatment parameters	
Depth of treated groove [approximate,mm]	0,5
Diameter of UIT intender end [mm]	3
Carrier frequency of transducer vibrations [nominal, kHz]	27
Ultrasonic vibration amplitude/power [μm/W]	30 / 1100*
Ultrasonic impact frequency [kHz]	350 - 400*
Amplitude of ultrasonic impacts, rebounds [mm]	1,5 - 1,8*
Press force on the tool without its weight [kgf]	Up to 2,5*
Groove roughness	< 2,5 μm*
Treatment speed [cm/min]	42
Number of passes	3

*Data provided by the Northern Scientific and Technology Company, Severodvinsk, Russian Federation.

The two plates needed to fabricate the specimen, i.e., the base plate and the attachment, were removed from large steel plates using laser cutting. The quality of the plate edges was high and no specimens failed from the base material. The MAG welding process was used with the filler material OK 12.51, see Table 5.4.

Table 5.4 Composition of filler material OK 12.51 [%] (ESAB 2000).

C	Si	Mn
0,1	0,85	1,5

The leg length of the fillet welds was from 8 to 10 mm. Start and stop positions of welds were not located at the corners of attachment. UIT was applied in the weld toe region at the attachment ends. This area is the most sensitive to the fatigue cracks for non-load carrying longitudinal attachment specimens.

In the IIW recommendations on post weld improvement methods (Haagensen and Maddox 2006), burr grinding to the end of longitudinal attachment should extend around end of attachment and continuously along both sides of the attachment. The length of treatment along the attachment sides should reach approximately four times of plate thickness, see Fig. 5.2. In this research, the extent of treatment recommended for burr grinding was used as a guideline for determining the extent of ultrasonic impact treatment. Start and stop position of treatment along the weld line was 50 mm from the original weld toe at the attachment end. Treatment around the end of attachment was repeated 3 times and the treatment speed was about 42 cm/min. Visual inspection were executed after treatment and the specimens were accepted if the original weld toe was completely removed and if the material in the UIT grooves had a smooth appearance.

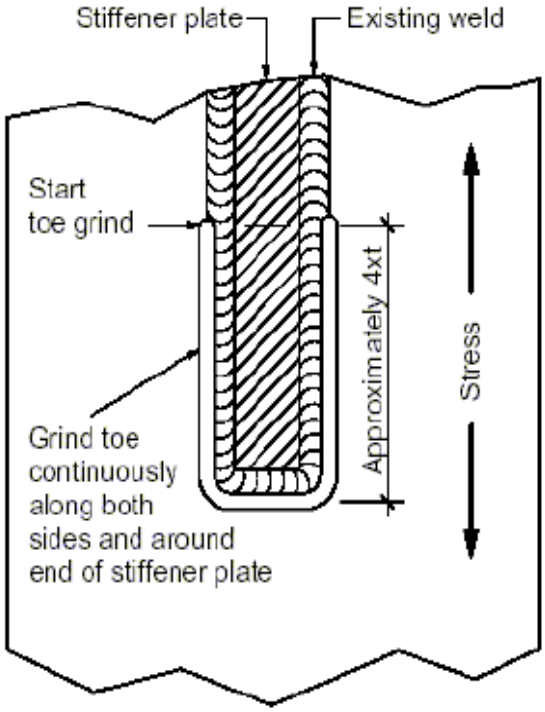

Figure 5.2 Recommendation for burr grinding weld toe technique (Haagensen and Maddox 2006).

In total 33 specimens were fabricated. Of these, 13 remained in the as-welded condition and 20 were treated using UI -treatment.

5.1.2 Two-sided longitudinal attachment

Six additional test specimens with longitudinal attachments were fabricated specifically with the intent of trying to measure the fatigue crack initiation period observed in ultrasonic impact treated specimens. Material for specimens, S355J0, was the same as that used in the original series. Material thickness and overall specimen length were 8 and 650 mm, respectively. Base plate width in the gripping region was 60 mm and 48 mm in the narrowed part of specimen where the gusset was attached. Dimensions of the welded attachments for both sides of the specimen were 100 x 40 x 8 mm. A specimen drawing is shown in Fig 5.3. Welding and treatment parameters of these specimens are presented in Table 5.5.

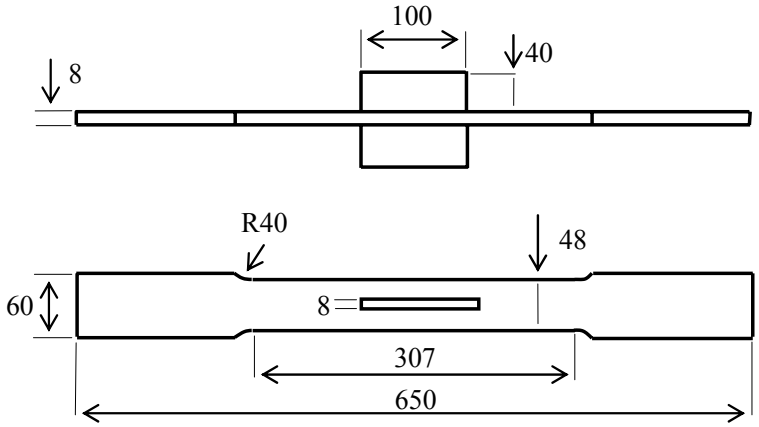

Figure 5.3 Geometry of specimens of two-sided longitudinal attachment.

All six specimens were UI -treated. Welding and treatment of additional specimen were prepared based on same principles and recommendation as in original series. Composition of filler material OK 12.50 is same as that of filler material OK 12.51 used in original specimens.

Table 5.5 Welding and UI - treatment parameters

Welding parameters	
Welding process	MAG
Current [A]	245
Voltage [V]	28,4
Shielding gas: Argon/CO_2 [%]	92 / 8
Filler material	OK 12.50
Wire feed rate [m/min]	11,7
Travel speed [cm/min]	37
UI -treatment parameters	
Depth of treated groove [approximate,mm]	0,5
Diameter of UIT intender end [mm]	3
Carrier frequency of transducer vibrations [nominal, kHz]	27
Treatment speed [cm/min]	40
Number of passes	3

5.2 Testing procedures

Fatigue testing was carried out to experimentally define the as-welded fatigue strength and the UIT improved fatigue strength for the welded non-load carrying longitudinal attachments. Fatigue testing was performed using a 100 and 150 kN servo-hydraulic test frames with axial tension loading in laboratory environment. Test frequency was 5-15 Hz. The ratio between minimum and maximum stress was $R=\sigma_{min}/\sigma_{max}=0,1$ in most cases. However, some tests were carried out using a constant maximum stress ($\sigma_{max} = f_y$) based on the test method presented by Ohta (1994). In this paper, this test procedure is referred as the Ohta –method. The goal of the Ohta -method is to simulate the effect of yield magnitude residual stresses that are normally present in large structures but are lacking in most small-scale specimens. Figure 5.4 shows the test arrangement used.

The primary aim of the testing was to compare the fatigue strength of specimens in the as-welded condition and those improved using UIT. The thickness effect, with specimen thicknesses 5 mm and 8 mm, was also investigated. The additional tests were executed specifically try to observe the crack initiation period in UIT treated welds. Tests were performed using constant amplitude loading.

Data for the constant amplitude loading are reported numerically in Appendices 1.1-1.3. In order to avoid bias in the experimental result due to specimen lack-of-straightness, stress values of one-sided attachment specimen are reported as structural stress values in Appendix 1.1. Nominal stress values of one-sided attachment specimen are presented in Appendix 1.2 and test results for the two-sided attachment specimens in Appendix 1.3. Fatigue data is presented graphically in Chapter 7 of this thesis.

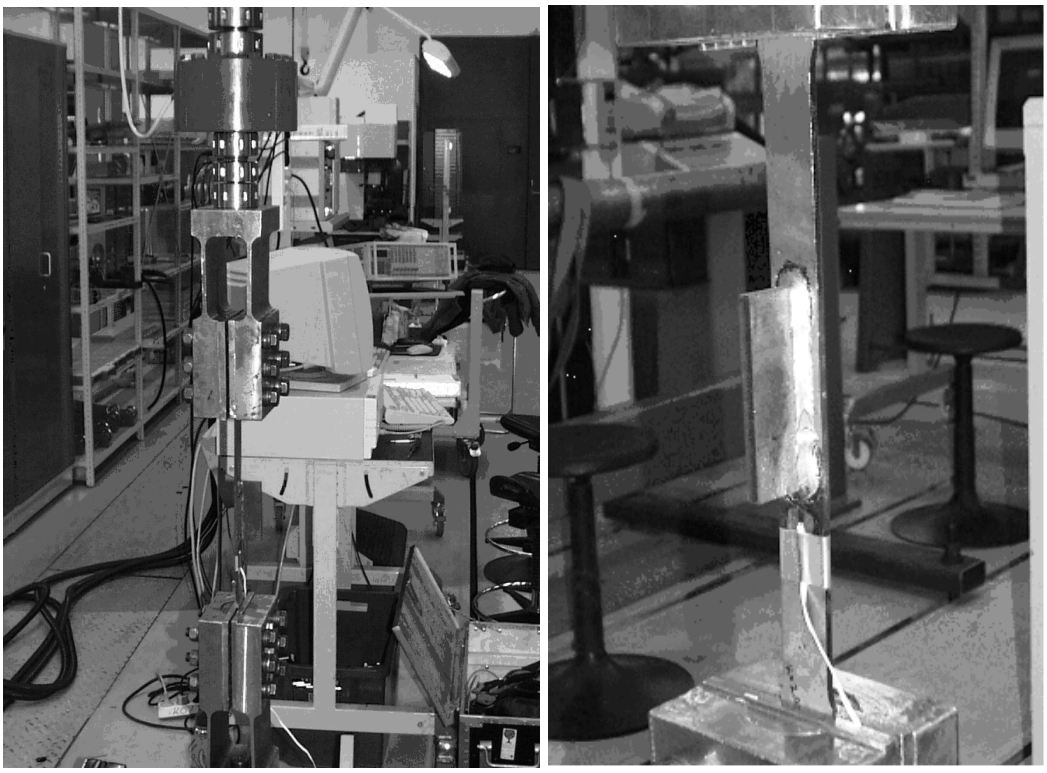

Figure 5.4 Axial tension fatigue test of one-sided longitudinal attachment specimen.

The structural stress, which is often called hot spot stress, includes the stress concentration effects of the detail, but not the local non-linear stress peak caused by the notch at the weld toe. This notch effect is included in the hot spot S-N curve determined experimentally (Niemi 2001). In most hot spots, the structural stress increases almost linearly when approaching the weld toe. Then, the structural stress can be determined using linear extrapolation. The linear structural hot spot stress extrapolation procedure is shown graphically in Fig. 5.5.

The advantage of using the structural stress compared to nominal stress is that secondary bending stresses are considered and, thus, specimens with different geometries are more easily compared. The structural stress range can be calculated as the nominal stress range multiplied by a structural concentration factor, K_s.

In this study, one strain gauge per test specimen has been used to evaluate the secondary bending and the concentration of membrane stress. Strain gage data was also used for determining the structural stress. The structural stress has been defined for the specimens of one-sided longitudinal attachments. The single strain gauge attached to one side of the attachment is seen in Fig. 5.4.

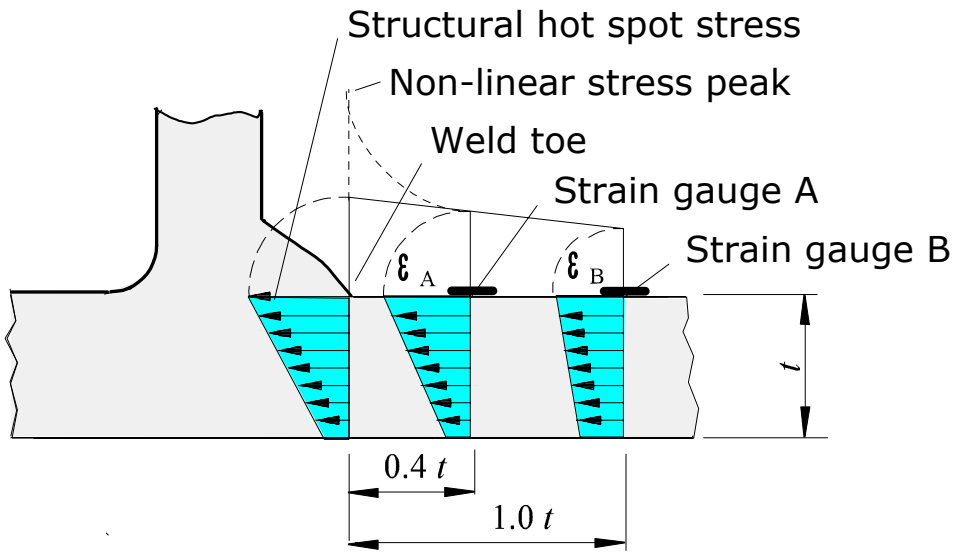

Figure 5.5 Linear extrapolation to the weld toe (Niemi 2001).

In the case of welded structures, the linear extrapolation presented in Fig. 5.5 represents a practical means of determining the structural stress for fatigue analysis. However, in the case of UIT treated welds, the stress gradient in the region of the attachment end is not as clear as that shown in Fig. 5.5. The reason for this is that UIT produces a semi-circular groove in the region of the weld toe. The groove has a radius of several millimetres depending on the type of indenters used. The groove produces a discontinuous stress gradient that alters the structural stress. In this study, the structural stresses presented in Appendix 1.1 are values of one strain gauge.

The strain gauge was positioned such that the gauge centre 5 mm from the original weld toe. The same distance was used for both base plate thicknesses, t = 5 mm and 8 mm, and for specimens in the as-welded and UIT condition. Graphical presentation of the measured K_s factors of one-sided longitudinal attachment specimen is shown in Fig. 5.6. Ks –factors of non-failed specimens are also included in this figure. Specimen to specimen variation is primarily caused by small variations in initial specimen curvature and small differences in the weld leg lengths. Mean values are given in Table 5.6.

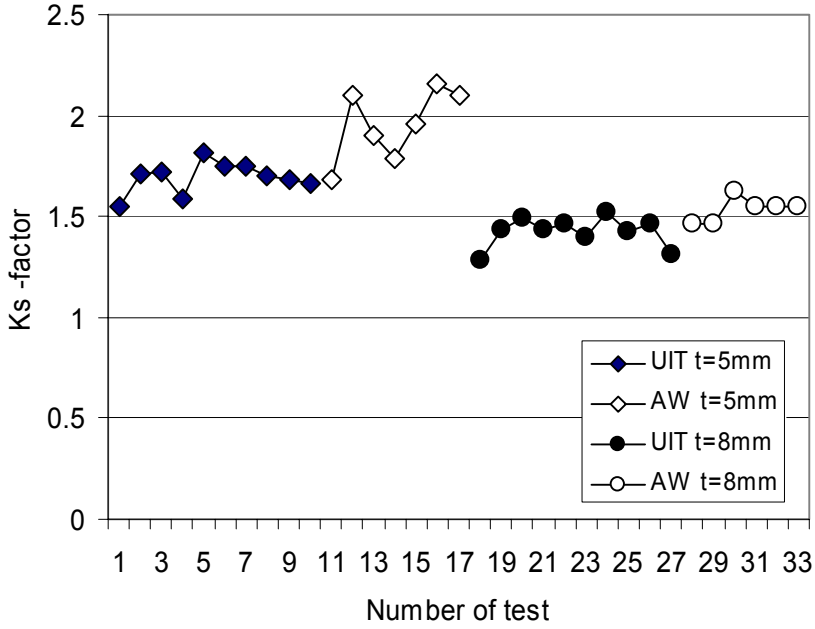

Figure 5.6 Measured structural stress concentration factors for the one-sided longitudinal attachment specimens

Table 5.6 Mean values of structural stress factors.

	t=5 mm	t=8 mm
UIT	1,69	1,42
AW	1,96	1,53

As shown in Table 5.6, mean values of as-welded condition are 1,16 (t=5 mm) and 1,08 (t=8 mm) per cent higher than these of UI –treated condition. The groove caused by the ultrasonic impact treatment slightly reduces the structural stress concentration factor. As previously mentioned, the strain gauges were located 5 mm from original weld toe. In the case of specimens with a base plate thickness of 8 mm, the strain gauge was, therefore, relatively closer to the original weld toe with respect to plate thickness (in comparison to the 5 mm thick specimens).

One major emphasis in the this thesis has been to define the so-called fatigue crack initiation period that exists for UIT treated welds but which is negligible for as-welded structures. Some of the experiments were designed to observe this empirically. Following UIT, no initial crack-like flaws were present and specification of initiation and propagation periods was quite difficult. In this research, beach marking –technique has been adapted for clarifying the

initiation part of fatigue life. A surface replication technique was also tried, but the resolution available was found to be insufficient.

The principle of the beach marking technique can be understood by the simple load history shown in Fig. 5.7. The concept is based on fatigue cycling which varies between two stress levels. The larger stress range, $\Delta\sigma_1$, produces the majority of fatigue damage both in terms of crack initiation and propagation. The lower stress range, $\Delta\sigma_2$, is applied at intervals to produce a region of slower crack growth. The period of slower crack growth is easily observed from the specimen fracture surfaces as beach marks. Results of these experiments, including an example of the beach marks, are given in Chapter 7.2 of this thesis.

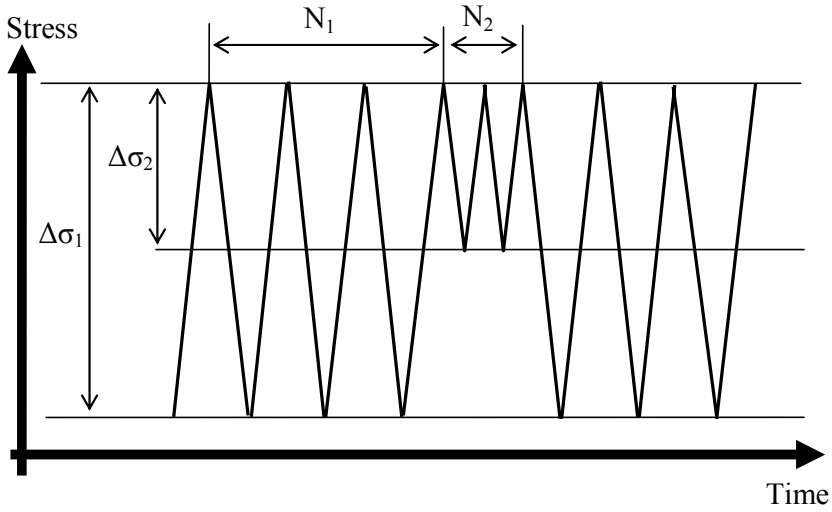

Figure 5.7 Schematic principle of beach marking -technique.

In this study, one load block consisted of 50000 cycles. The number of cycles of higher and lower stress ranges was 40000 and 10000, respectively. The magnitude of the lower stress range was half of higher stress range.

Table 5.7 Details of one block used in this study.

$\Delta\sigma_1$	$\Delta\sigma_2 = \Delta\sigma_1 / 2$
$N_1 = 40000$	$N_2 = 10000$

Because of two stress levels, the equivalent stress range, $\Delta\sigma_{eq}$, could be calculated with equation:

$$\Delta\sigma_{eq} = \sqrt[3]{\frac{\sum\left(\Delta\sigma_i^3 \cdot N_i\right)}{N_{tot}}} \tag{5.1}$$

Based on this equation, it can be computed that the small cycles in the loading block have practically no influence on the overall fatigue damage of the spectrum. The effect of small cycles is less than 7 per cent. The beach marking technique has been applied to three of the two-sided longitudinal attachment specimens. Data for these tests are presented in Appendix 1.3.

6 FATIGUE LIFE CALCULATION

6.1 Two-stage method

The total fatigue life of a structure can be considered to be the sum of three fatigue stages: crack initiation (nucleation), crack propagation (crack growth) and the final fracture. In many practical design situations, the propagation life may be insignificant as compared to the initiation life. In other cases, however, the propagation life may comprise the most significant part of the total fatigue life. Especially in welded structures, the propagation life is normally assumed to have a dominant role. Sometimes both stages, initiation and propagation, must be taken account into fatigue life estimations (Stephens 2001). This is sometimes termed the two-stage method. In this thesis initiation and propagation have both been included in the fatigue life calculations. In the research of Haagensen et al. (1987), a similar idea of two-stages has been applied to grinding, TIG –dressing, shot peening and profile improvement. The final fracture stage is rarely significant in engineering design, but it may be important in some special cases, e.g., pressure vessel design.

6.2 Fatigue crack initiation life

As mentioned in Chapter 3, the fatigue strength improvement produced by UIT is considered to be due to a number of factors including:

1) local geometric improvement at the weld toe region
2) inducement of compressive residual stresses in the weld
3) cold working and hardening of the material

The first of these factors includes the removal of cold laps, undercuts or other defect types that are normally present in welds and act as initial cracks for as-welded joints. In this thesis it is considered that the fatigue strength improvement from UIT is due primarily to the introduction of a significant crack initiation period that can be modelled using a local model of the weld toe.

The analytical calculation of crack initiation period after ultrasonic impact treatment is based on local strain approach. The local strain approach to fatigue analysis was developed largely within the Society of Automotive Engineers Committee on Fatigue Design and Evaluation in the 1970-1980's (Wetzel 1977, SAE 1988). The original purpose of the local strain approach was the fatigue life assessment of structures without welds. The local strain method was chosen because the ultrasonic impact treatment demolishes the initial crack caused by welding and a common analytical method of fracture mechanics is not applicable.

In the case of UIT treated welds, only a very small volume of material must be treated to accomplish the desired improvement and experimental determination of the needed material parameters for local strain analysis is not possible or, at least, extremely difficult. Calculation of material parameters used in the local strain method based on UML has been discussed in Chapter 4 and is shown in Table 4.1.

Several parameters from this table are based on the ultimate tensile strength R_m. This is not specifically known for the UIT treated material but has been estimated based on Brinell -hardness. The flow chart for calculating the fatigue crack initiation life of ultrasonic impact treated details is presented in Fig. 6.1.

The Brinell hardness (HB) has been measured approximately 0,1 mm below the surface of the UI -treated groove. Hardness measurements from the UI -treated and the as-welded state are presented in Chapter 6.2.3. The ultimate strength of low- and medium-strength carbon and alloy steel can be estimated as follows (Dowling 1999):

$$R_m = 3{,}45 \cdot HB \tag{6.1}$$

In Fig 6.1, possible mean stresses due to loading and residual stresses is taken into consideration by modifying the applied nominal stress amplitude as presented in Equation (6.2) (Dowling 1999, Stephens 2001). In using this equation, it is assumed that residual stresses caused by ultrasonic impact treatment have the same effect as applied mean stresses. The compressive residual stress S_{res} evaluated by X-ray analysis has been added to the mean stress due to loading. Determination of residual stresses is discussed in Chapter 6.2.2.

$$S_{ar} = \frac{S_a}{1 - \frac{S_m + S_{res}}{R_m}} \tag{6.2}$$

The local strain amplitude is equal to the nominal stress amplitude multiplied by the elastic stress concentration factor, K_t, see Equation (6.3). The magnitude of the stress concentration factor K_t alternates significantly based on the exact shape of the UIT groove. Sensitivity analysis of the relationship between K_t factor and the radius of the groove is presented in Chapter 6.2.1.

$$\sigma_a = K_t \cdot S_{ar} \tag{6.3}$$

The relationship between strain and stress amplitudes has been calculated with the Ramberg-Osgood relationship. In Equation (6.4), coefficient K' and exponent n' are taking account to cyclic hardening of material.

$$\varepsilon_a = \frac{\sigma_a}{E} + \left(\frac{\sigma_a}{K'} \right)^{\frac{1}{n'}} \tag{6.4}$$

The initiation fatigue lives have been defined based on strain amplitudes with the Basquin-Coffin-Manson relationship presented in Equation (6.5). Fatigue strength and ductility coefficients and exponents of UI –treated material have been determined using Uniform Material Law presented in Chapter 4.

$$\varepsilon_a = \left(\frac{\sigma_f'}{E}\right) \cdot \left(2 \cdot N_f\right)^b + \varepsilon_f' \cdot \left(2 \cdot N_f\right)^c \qquad (6.5)$$

Details of the calculation procedure for crack initiation are shown in Appendix 2.1 and the results are discussed in Chapter 7.

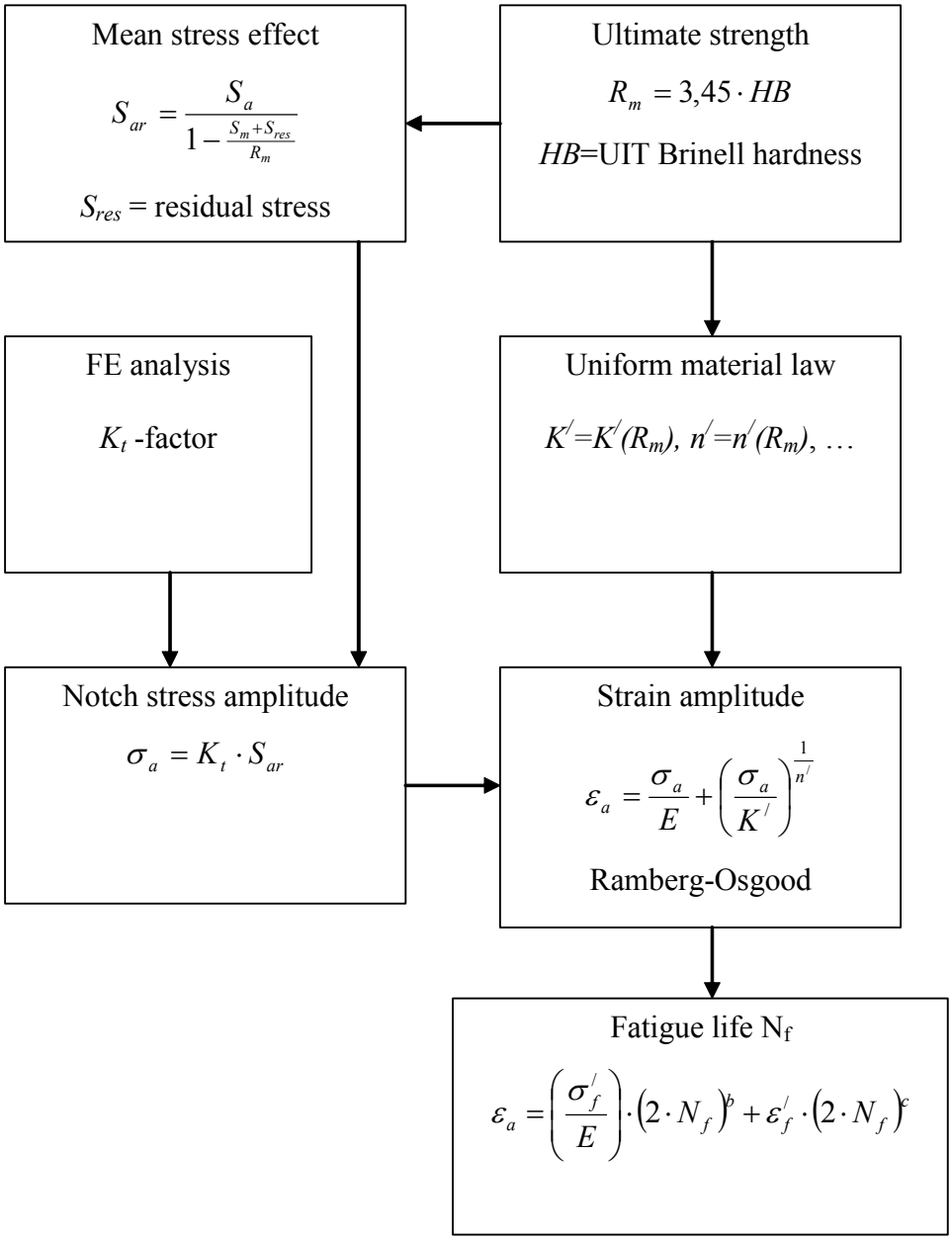

Figure 6.1 Flow chart of fatigue crack initiation life assessment.

6.2.1 Finite element analysis

With respect to fatigue strength improvement, UIT has the benefit of producing a smooth weld metal to base metal transition. Finite element analysis was used to calculate the local stress and the stress concentration factor, K_t, in the UIT region near the end of the longitudinal attachment. In this study, specimens of one-sided longitudinal attachment have been analysed using finite element method. The theoretical stress concentration factor is assumed to be the notch stress divided by the nominal stress. The notch and nominal stresses in the X-direction, see Fig. 6.2, were used for determining the K_t –factor.

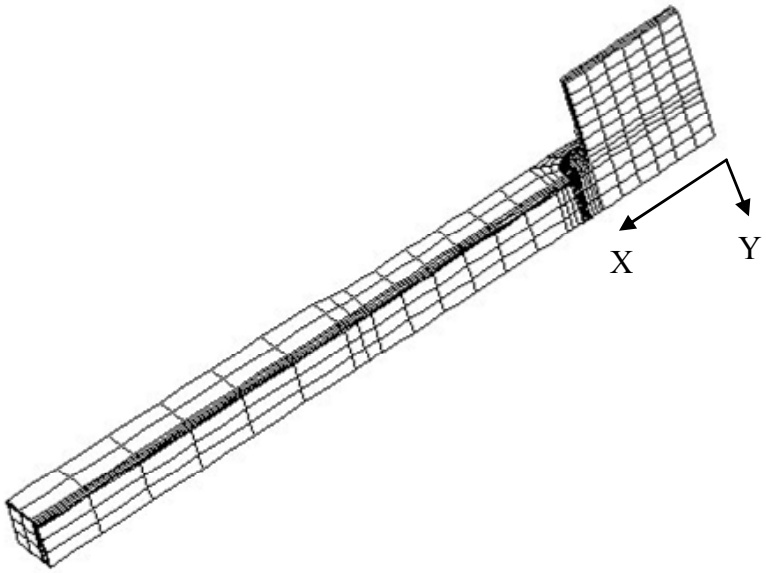

Figure 6.2 The finite element model of longitudinal attachment test specimen.

Due to symmetry, it was possibility to use a finite element model of ¼ of the original structure. Parabolic solid brick elements were used. The total number of elements was 1962. Modelling and solving of the FE models were performed with I-DEAS 9.0 software. An example of the model of ¼ size is shown in Fig. 6.2.

The stress concentration factor, K_t, has a dominant influence on the magnitude of the local notch stress amplitude. For this reason, K_t is one of the most important factors when assessing the expected fatigue crack initiation life. The radius of the treated groove, R, and the thickness of the base plate, t, are the two dimensions that most significantly influence K_t. The sensitivity of R and t on K_t has been studied using finite element analysis. A total of 18 finite element models were prepared and analysed. Three radii (R = 1.7, 2.4 and 3) and six thicknesses (t = 3, 5, 8, 10, 15 and 20) were calculated.

The local notch for one model is shown in greater detail in Fig. 6.3. To ensure that proper local stresses were computed and all results would be comparable, the area close to the surface of treated groove was similar in all 18 models. This area consisted of ten elements within the arc of the UIT groove and three layers of elements in the direction of base plate thickness. The area of constant size elements can be seen in Fig. 6.3.

The height and length of the smallest elements on the surface of groove were 0,35 and 0,34 mm, respectively. The element size in the direction of specimen width was approximately 1,33 mm. The location from which the local stress was taken in order to compute K_t was, in all models, the highest stress value in the arc of the UIT groove in the XY-symmetry plane of the specimen. The highest X -stress was usually between the fourth and fifth element, assuming that the first element was at the border of base material and groove.

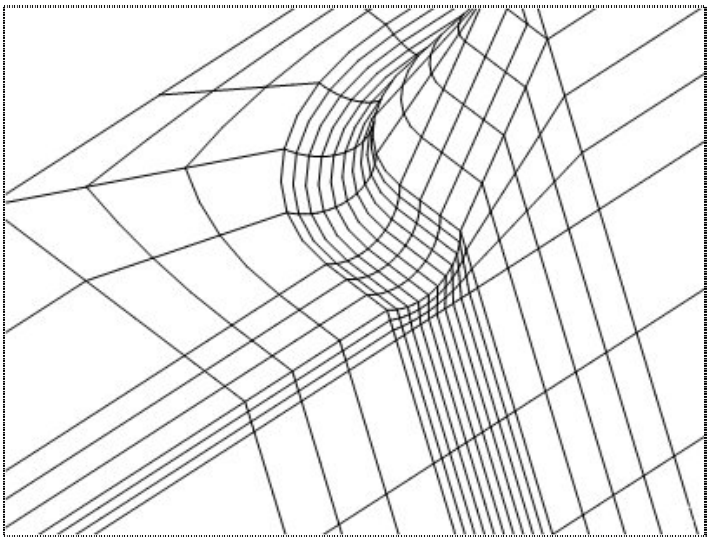

Figure 6.3 Local geometry of longitudinal attachment element mesh.

The sensitivity analysis was prepared based on the assumptions that the depth of treated groove was 0,5 mm and all other dimensions of specimens remain unchanged. Dimensions are shown in Fig 6.4. The weld throat thickness was constant for all models. Results of the sensitivity analysis are shown in Figs. 6.5 and 6.6. Figure 6.5 shows K_t defined based on gross area and Fig. 6.6 is based on net area. Gross and net thicknesses are defined in Fig 6.4.

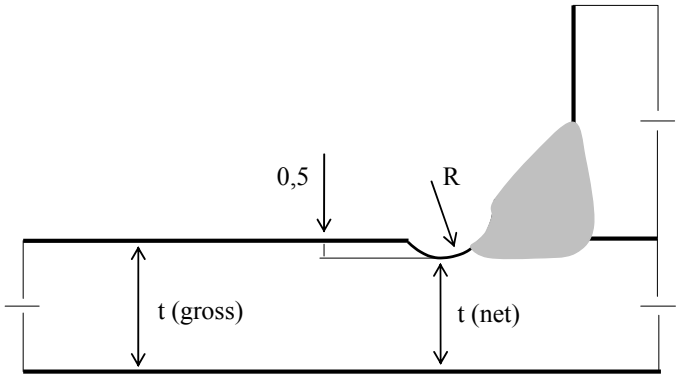

Figure 6.4 Gross and net section of test specimen.

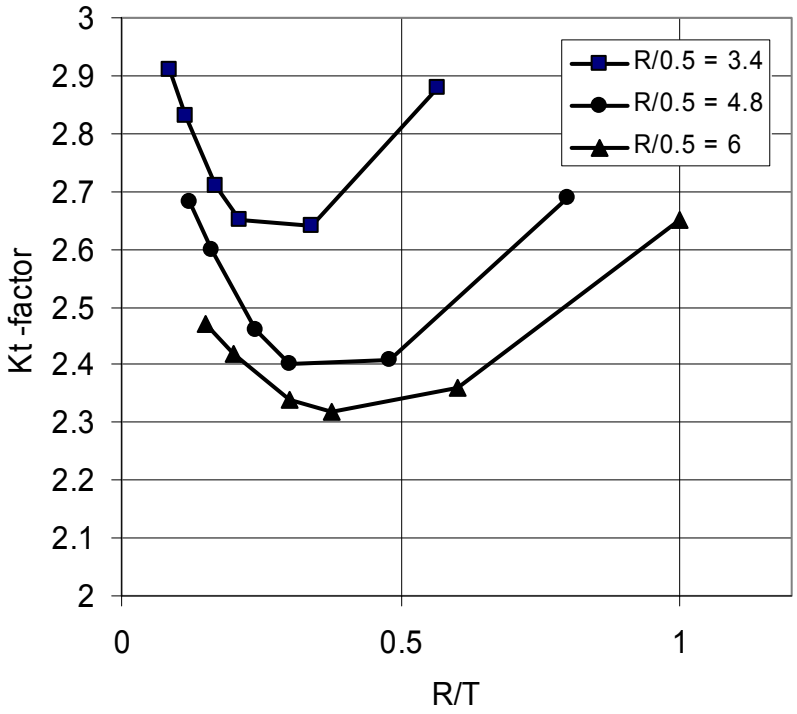

Figure 6.5 Kt –factor calculated according to gross area.

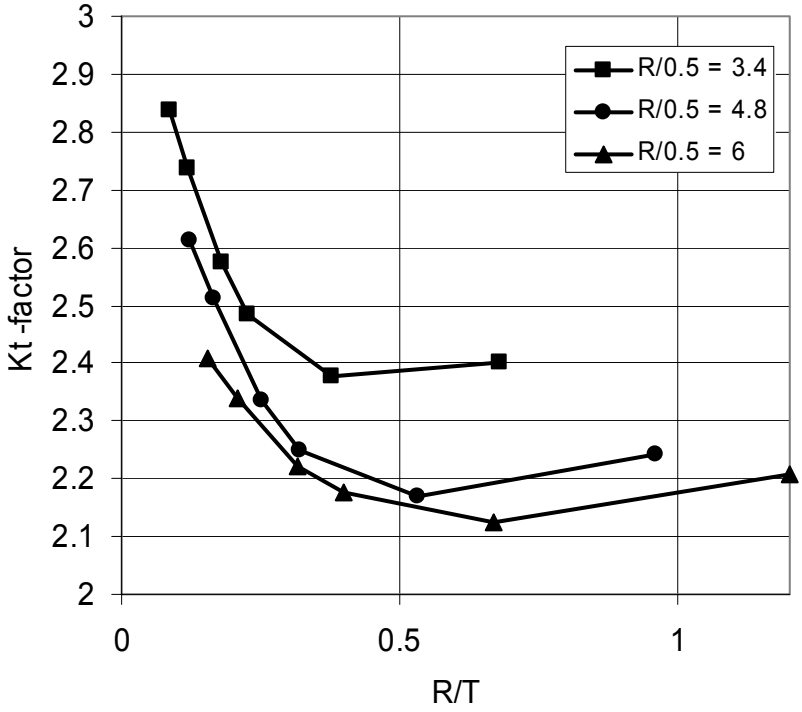

Figure 6.6 Kt –factor calculated according to net area.

6.2.2 Residual stresses

One of the main advantages of the UIT method is its ability to induce high compressive residual stress in the region of the weld and induce plastic deformation at depths up to 1500 μm. The magnitude of the compressive residual stress has an important influence on the effective stress amplitude value, see Equation (6.2), used in calculating the fatigue crack initiation life. In this research, the surface residual stresses developed as a result of UIT have been measured using X-ray diffraction. The X-ray measurements have been made in Stresstech Oy, Finland (Suoknuuti 2002).

The purpose of X-ray measurement was to find the interaction between residual stresses and the state of treatment. The state of treatment was quantified as the total treatment time over area of the weld. By knowing the impact frequency it would also be possible to calculate the approximate number of impacts per millimetre applied. The welded plate specimens used for residual stress analysis was an 8 mm thick thermo mechanically rolled structural steel plate, QSTE 460 TM (EN 10149-2). A rectangular 12 x 12 mm rod was welded on the sheet plate as shown in Fig. 6.7. After welding the plate was sectioned to seven specimens with width of 40 mm. The weld toe region of six of the seven specimens was treated using UIT with needles of diameter of 3 mm. One specimen was left in the as-welded condition (AW).

Table 6.1 Chemical analysis of material QSTE 460 TM [%].

C	Mn	Si	P	S	Al
0,06	0,91	0,17	0,011	0,001	0,036

Table 6.2 Mechanical properties of material QSTE 460 TM.

R_e [MPa]	R_m [MPa]	A_5 [%]
460	550	26

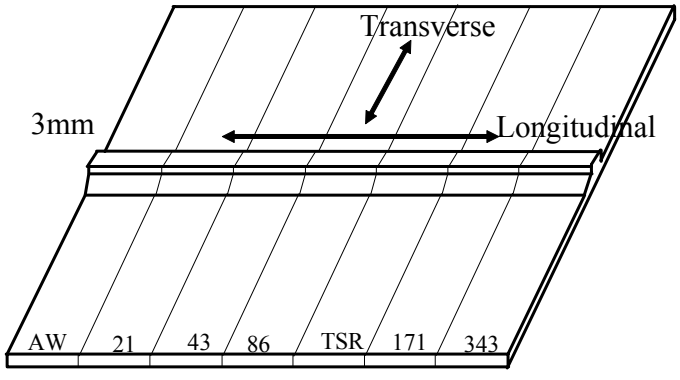

Figure 6.7 Test plate used to study the development of UIT residual stresses.

The manual treatment speed using UIT was approximately 42 cm/min. The transverse and longitudinal residual stresses were measured from the bottom of the treated groove. The measurement location was in the middle of 40 mm width specimen. The frequency of intender impacts to the weld toe was approximately 150 impacts/second. For each of the seven specimens the UIT tool was passed over the weld toe a varying number of times. The numbers of UIT passes applied to the various specimens were 0 (as-welded), 1, 2, 4, 4 (+TSR = thermal stress relief after UIT), 8 and 16. Based on the average impact frequency and travel speed, the number of impacts per millimetre for the seven specimens was 0, 21, 43, 86, 86 (+TSR = thermal stress relief after UIT), 171 and 343. As noted, one of the specimens was also thermally stress relieved following UIT treatment.

The results of X-ray measurements are presented graphically in Fig. 6.8. The longitudinal compressive residual stresses for UIT treated specimens were clearly higher than the transverse residual stresses (note the definition of longitudinal and transverse in Fig. 6.7). Residual stresses of the specimen in the as-welded condition were only slightly tensile. Higher tensile residual stresses could have been expected, but the residual stresses in relatively small transverse welded specimens are frequently not large. Also, the measurement point for the X-ray diffraction could not be positioned precisely at the very small weld toe region. The measurement point was about 1 mm from the weld toe.

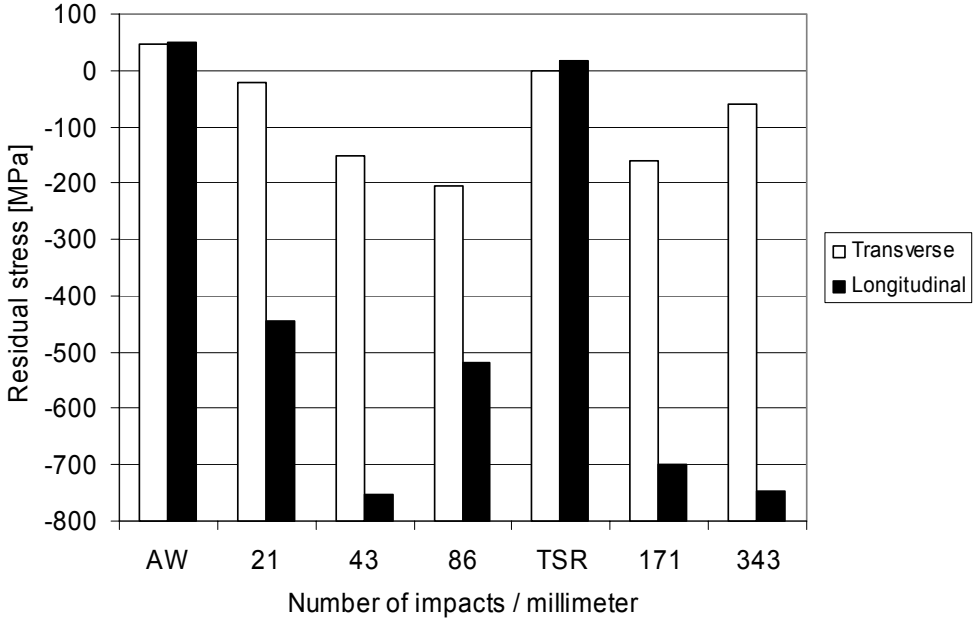

Figure 6.8 Residual stresses as a result of treatment state.

The X-ray method is based on measurement of the elastic distortion of the metal's crystallographic structure. The measured values are strain-based which are then transformed to stresses by simply multiplying by the elastic modulus. The measured residual strains correspond to very high stresses values and indicate significant work hardening of the material. One specimen was heat-treated following UIT treatment. This was done primarily as a test of the X-ray method. As expected that specimen had very small residual stress values. From Fig. 6.8 it can be seen that large compressive residual stresses were present after 4

passes (about 86 impacts/mm) and more impacts did not necessarily produce higher compressive residual stresses.

When computing the fatigue crack initiation life using UML the beneficial effect of compressive mean stress have been considered. The measured transverse residual stress S_{res} in the UML calculation was assumed to be -178,5 MPa which is the average of the residual stresses measured for 86 and 43 impacts/mm, i.e., 2 and 4 passes. For the longitudinal attachment specimens in this study, it was estimated that UIT treatment produced about 65 impacts/mm.

6.2.3 Hardness measurement

Brinell hardness of both UIT treated and as-welded one-sided longitudinal attachment specimens was measured through the thickness of specimen base plate. Specimens were cut into two pieces following the symmetry plane in X-Y direction presented in Fig. 6.2. The polished micro sections were prepared from the region of the weld toes. In the case of as-welded specimens, Brinell hardness was determined in the through-thickness direction beginning from the original weld toe as shown in Fig. 6.9. In UI –treated specimens, hardness measurements started from the boundary layer of base and weld material. The first measurements were 0,1 mm below the surface and the last hardness measurement was taken at a depth of two millimetres. Hardness measurements of as welded and UI –treated specimens are shown in Fig. 6.9.

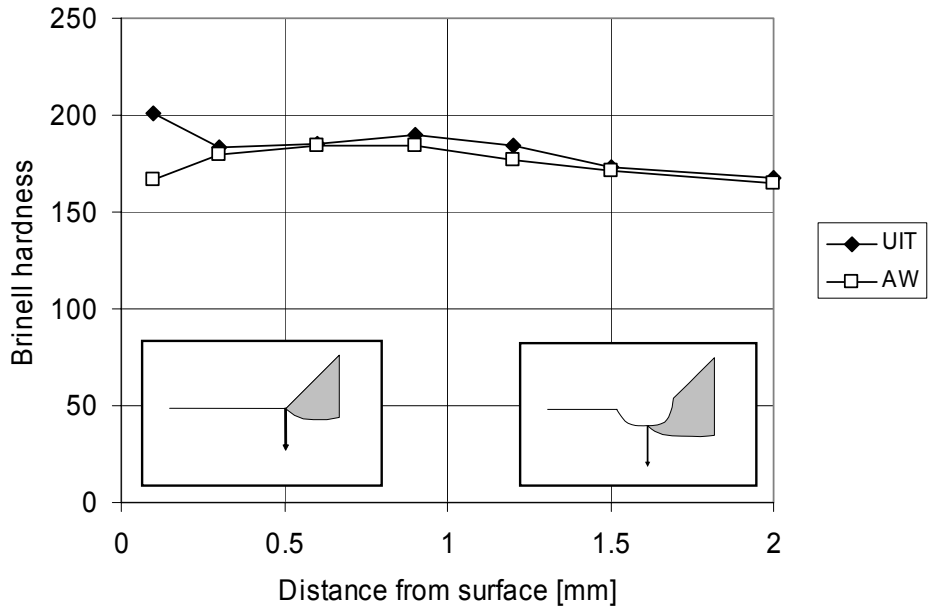

Figure 6.9 Hardness distributions beginning from surface of treated groove.

Based on the measurements, a Brinell hardness value of HB 201 was used as approximating the ultimate strength of the material at the bottom of the UIT groove. The corresponding value for specimens in the as-welded condition was HB 167.

6.3 Fatigue crack propagation life

Stephens (2001) divided the fatigue life of a structure into two stages:
Stage 1: Life to the formation of a crack on the order of 1 mm: “crack initiation, nucleation”
Stage 2: Life from this existing crack to fracture: “crack growth”

In this thesis, the same categories regarding stages 1 and 2 have been used. Stage 1 has been computed according to the local strain analysis method presented in Chapter 6.2. As previously presented in Fig. 3.5, the volume of material plastically deformed during the UIT process extends to a depth of 1,0-1,5 mm from the surface of the treated groove. In this thesis, a limiting value of 1 mm between the two stages has been assumed to be an appropriate boundary value.

Linear elastic fracture mechanics has been used for evaluating the period of crack growth. Predicting the stage 2 fatigue lives requires that the stress intensity factor range, ΔK, is calculated for the given loading, geometry and crack size. This is combined with material parameters in the form of the crack growth rate curve, da/dN versus ΔK, the initial crack size and knowledge of fracture toughness (Stephens 2001). Crack growth was calculated assuming that there is a valid connection between the crack growth relationship and the stress intensity factor range (Newman and Raju 1981). The Paris law equation as presented in Equation (6.6) has been used. Mean values of the material constants for steel in this equation were m=3 and C_{fm}=0,1832*10^{-12} (units ΔK in MPa mm$^{1/2}$ and da/dN in mm/cy) following the recommendations of Gurney (1991).

$$\frac{da}{dN} = C_{fm} \cdot (\Delta K)^m \tag{6.6}$$

The range of stress intensity factor ΔK is a function of nominal stress range, $\Delta\sigma_{nom}$, crack depth a, stress gradient through the thickness as given by the magnification function, $M_k(a)$ and the crack shape function Q(a,c) (Gurney 1991).

$$\Delta K = \Delta\sigma_{nom} \cdot \sqrt{\pi \cdot a} \cdot M_k(a) \cdot Q(a,c) \tag{6.7}$$

An approximation for the crack shape function Q(a,c) has been given as:

$$Q(a,c) = \frac{1}{\sqrt{1 + 1{,}464 \cdot \left(\frac{a}{c(a)}\right)^{1{,}65}}} \tag{6.8}$$

Where, a, is crack depth and c(a) is the half width of the semi-elliptical surface crack.

In all specimens, the fatigue cracks initiated at the weld toe or at the bottom of the ultrasonic impact treated groove. The fracture surface from one specimen showing a typical crack shape is presented in Fig. 6.10. This figure from a 5 mm thick specimen shows that the crack initiated at approximately the centreline of the specimen and crack grew through the thickness of the base plate.

In this research it was assumed that final depth of crack, a_f, was the same as the base plate thickness. It was also assumed the crack aspect ratio, a/c(a), remained constant at a/c(a) = 1/ 2,15. This aspect ratio was an average value observed from the fracture surfaces of several specimens, see Fig. 6.10.

Figure 6.10 Cross section and crack shape of specimen (UIT-5) broken from UI –treated groove.

Several existing $M_k(a)$ functions can be found from the literature. For example, Niu and Glinka (1990) have provided a useful survey of weight functions for edge and surface cracks.

In this study, $M_k(a)$ was defined using finite element analysis and Equation (6.9). The sensitivity analysis concerning the stress concentration factors as defined by FE analysis was presented previously in Chapter 6.2.1. The same FE volumes were used for calculating the stress gradient in the direction of crack growth. In the FE model used for fracture mechanics analysis, there were 20 elements in the direction of crack growth and 10 elements in the arc of the treated groove. The smallest element in the surface of groove had a dimension of 0,075 mm in the through thickness direction. A total of 9832 solid parabolic brick elements were used in these analyses. A typical mesh for crack propagation analysis is given in Fig. 6.11.

$$M_k(a) = \frac{2}{\pi \cdot a} \cdot \int_0^a \frac{\sigma_x(y)}{\sqrt{1-\left(\frac{y}{a}\right)^2}} dy \qquad (6.9)$$

The $M_k(a)$ function presented in Equation (6.9) gives the weighted stress values at the crack tip (Albrecht and Yamada 1977, Hobbacher 1992). When the stress through the plate is known as a function of thickness, the $M_k(a)$ function can be integrated. The stress distribution, $\sigma_x(y)$, through the thickness of base plate and the value of weight function are shown in Fig. 6.12. The vertical axis represents values of $\sigma_x(y)$ and M_k normalized based on the nominal stress in the base plate. As is expected, the magnitude of M_k is slightly higher than $\sigma_x(y)$.

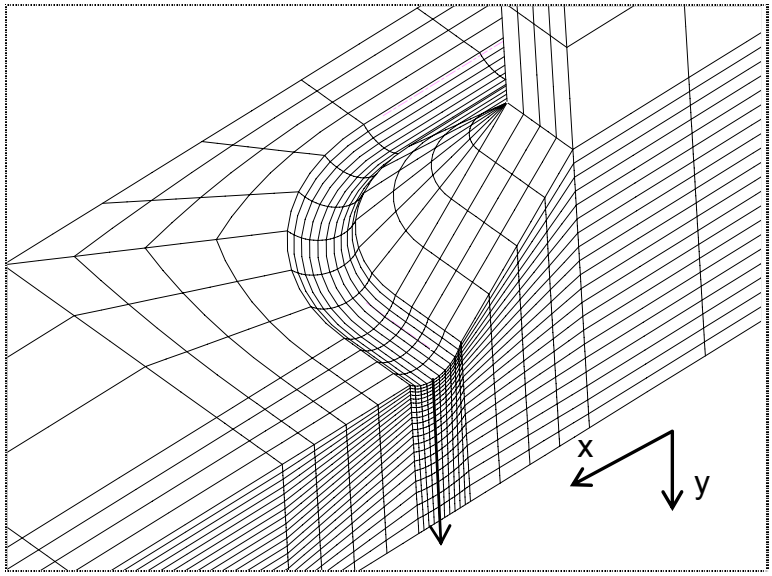

Figure 6.11 A dense FE -mesh for fracture mechanics analysis. The direction of crack growth is indicated.

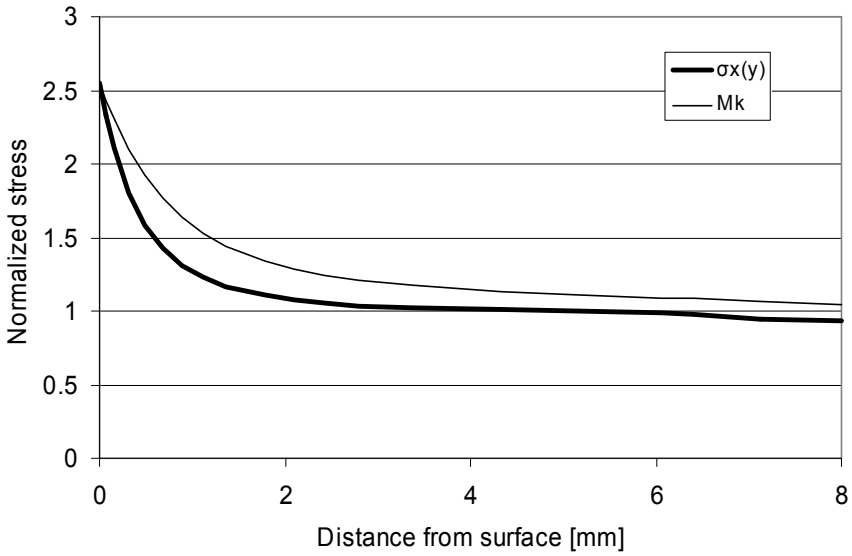

Figure 6.12 M_k and $\sigma_x(y)$ normalized by the nominal stress.

A closed form solution for computing the fatigue crack propagation life of the welded structure is given in Equation (6.10). This equation is easily solved numerically. Details of the calculation procedure for crack propagation are given in Appendix 2.2 and final results are presented and further discussed in Chapter 7.

$$N = \frac{1}{C_{fm} \cdot \Delta\sigma_{nom}^{3} \cdot \pi^{\frac{3}{2}}} \cdot \int_{a_0}^{a_f} \frac{1}{\left(Q(a,c) \cdot M_k(a) \cdot \sqrt{a}\right)^3} da \qquad (6.10)$$

7 RESULTS AND DISCUSSION

7.1 Fatigue test results

Fatigue test results are presented both in terms of structural stress and nominal stress. Chapter 7.1.1 covers structural stress while 7.1.2 presents the same data in terms of nominal stress. The structural stress values have slightly less scatter, because the secondary bending stresses are included in the reported stress range.

7.1.1 Structural stress approach

The fatigue strength of welded joints can be represented graphically by a fatigue life vs. stress range curve, i.e., the so-called S-N curve, which is usually presented on a log-log scale. The fatigue data based on structural –stress range are presented graphically in Figures 7.1–7.2. It should be noted that the vertical axis in Figures 7.1 and 7.2 is the structural stress range at the point of strain gauge and the horizontal axis is number of cycles.

In Figure 7.1, the fatigue strength of UIT treated welds are shown in comparison to welds in the as-welded condition. This figure clearly shows the significantly higher fatigue strength values obtained using UIT. No significant differences in fatigue strength between the 5 mm and 8 mm specimens were observed.

Figure 7.2 shows only the data obtained from the UIT treated specimens. In this case the comparison is based on the two different R ratios applied during testing. It can be seen in the figure that specimens tested at a low stress ratio (R=0,1) and at a high stress ratio (Ohta) had approximately equal fatigue strength. Additionally, no significant differences in fatigue strength as a function of specimen base plate thicknesses were observed.

Results of statistical analysis of constant amplitude loading for the six sets of data are presented in Tables 7.1-7.4. Statistical analysis of the data is based on the methods outlined in Chapter 4 of this thesis. The mean fatigue class, standard deviation and characteristic fatigue class of the various test series are shown in Table 7.1. The number of fatigue tests per series, n, was five for each case. These values were calculated with an assumed S-N slope m = 3. For this reason, the standard deviations of the as-welded series appear lower than those of the UIT treated series. The data in Figure 7.2 shows significant scatter in UIT data in terms of fatigue life, but this is a function of the relatively large S-N slope that would be obtained based on a free-slope linear regression of the data for specimens treated with UIT.

Table 7.1 Results of statistical analysis based on structural stress range, (m = 3).

	t	R	m	n	$FAT_{50\%}$	s	$FAT_{95\%}$
UIT	5	0,1	3	5	211	0,167	160
UIT	5	Ohta	3	5	207	0,260	135
AW	5	0,1	3	5	125	0,076	110
UIT	8	0,1	3	5	254	0,236	172
UIT	8	Ohta	3	5	187	0,151	145
AW	8	0,1	3	5	136	0,101	115

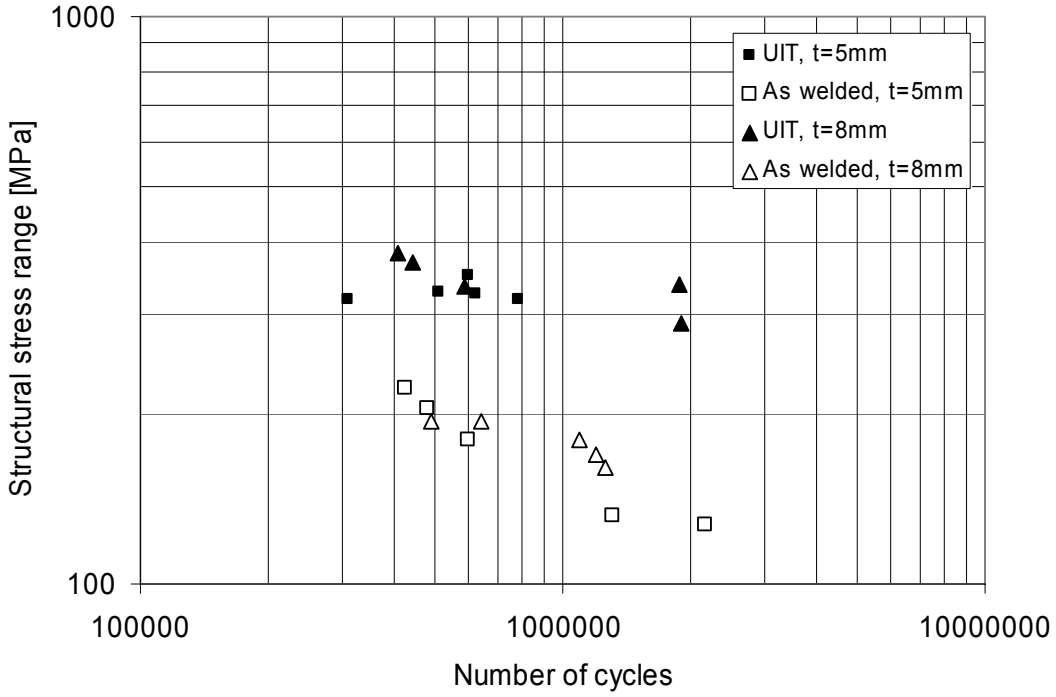

Figure 7.1 The comparison between as-welded and UIT treated series, R=0,1.

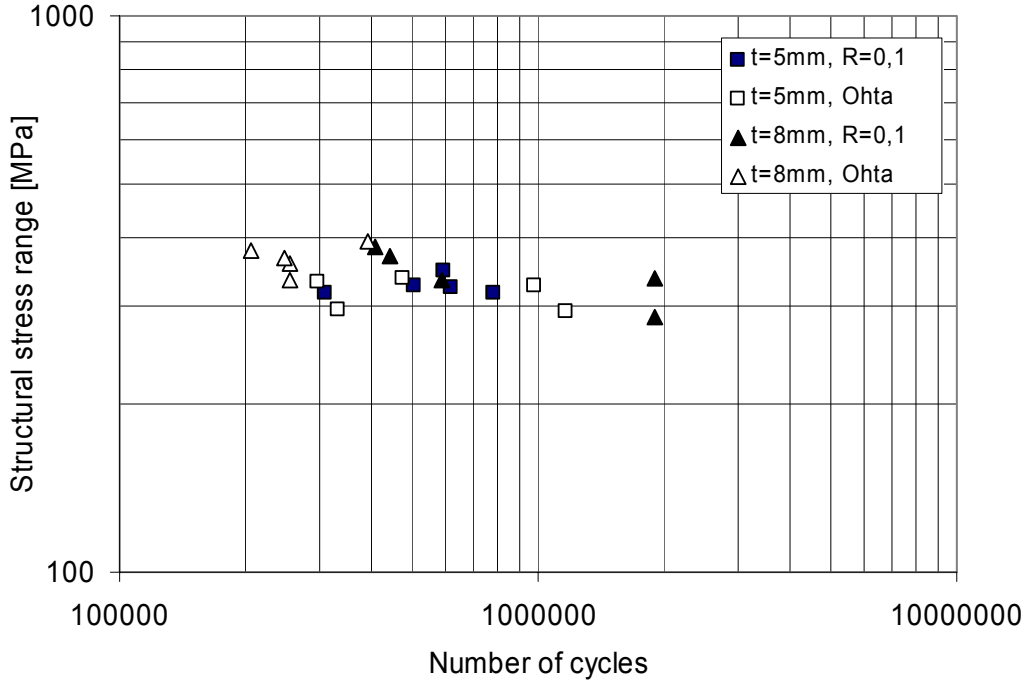

Figure 7.2 The comparison between R=0,1 and Ohta -test series, UIT.

In Table 7.2, the characteristic structural fatigue strengths of ultrasonic impact treated specimens tested at R=0,1 are compared to the structural fatigue strengths from the as-welded test series. From this table it can be seen that the as-welded fatigue strength for both material thicknesses was slightly higher than the structural hot spot design value of 100 MPa (Hobbacher 2006). This indicates that the welds were of slightly higher quality than average welds. As seen in the last column of Table 7.2, the fatigue strength of ultrasonic impact treated test specimens was 45-50 per cent greater than the fatigue strength of the as-welded test specimens. If the S-N slope of 3 is assumed, the fatigue life improvement due to UIT is approximately a factor of $1{,}45^3 = 3$. In reality, the fatigue life improvement at a given stress range is probably greater, but the slope of the S-N curve is difficult to determine reliably with the limited number of data available. The fatigue strength of the 8 mm thick test series was computed to be only 5-8 % higher than that of test series of material thickness 5 mm.

Table 7.2 The comparison between thickness and treatment (m = 3), R = 0,1.

	UIT	AW	UIT / AW
8 mm	172	115	1,50
5 mm	160	110	1,45
8 mm / 5 mm	1,08	1,05	

Traditional post weld treatment methods that rely on modifying the residual stress state near the weld toe, i.e., hammer peening and needle peening, have been included in recommendations of the International Institute of Welding (Haagensen and Maddox 2006). It is recommended that, for steel structures with main plate thickness exceeding 4 mm, the structural hot spot - fatigue class for hammer and needle peening is FAT 160. This characteristic hot spot fatigue class is based on structures with non-load carrying fillet welds and with base material yield strengths greater than the minimum specified level of 350 MPa. Characteristic hot spot -design values obtained in this study for 8 and 5 mm thick plates with R=0,1 are 172 and 160, respectively. Fatigue strengths are consistent with IIW recommendations.

Table 7.3 provides a comparison of UIT treated welds tested at both R=0,1 and according to the Ohta -method. As seen in the table, the characteristic fatigue class for specimens tested at R=0,1 are 19% higher than fatigue class for specimens tested using the Ohta -method. This difference is consistent with design recommendations summarized by Hobbacher (2006):

"*In case of S-N data, proper account should be taken of the fact that residual stresses are usually low in small-scale specimens. The results should be corrected to allow for the greater effects of residual stresses in real components and structures. This may be achieved either by testing at high R –ratios, e.g. R=0,5 or by testing at R=0 and lowering the fatigue strength at 2 million cycles by 20%.*"

Table 7.3 Comparison between thickness and R –ratio (m = 3), UIT.

	R = 0,1	Ohta	R = 0,1 / Ohta
8 mm	172	145	1,19
5 mm	160	135	1,19
8 mm / 5 mm	1,08	1,07	

It is significant to note that the high stress ratio fatigue testing did not fully erase the degree of fatigue improvement obtained in the UIT treated welds. The UIT –method, therefore, should be useful, also for improvement of large-scale structures with high residual stresses.

From these tables it is seen that the 8 mm thick specimens had consistently greater fatigue strength than did the 5 mm thick specimens. This difference is not large but this result is somewhat contrary to what is expected. Normally thin specimens tend to have, especially when the thickness is higher than 25 mm, higher fatigue strength, at least in terms of nominal stress. However, it can be noted that the stress values in this section are based on structural stress. The structural stress concentration factor used for the 5 mm thick specimens was approximately 1.7 as compared to only 1.4 for the 8 mm thick specimens. The difference in hot spot -strength is small and has not been further investigated here.

It should be noted that statistical analysis of the UIT treated specimens was done with using an assumed slope of 3. This is a conservative estimate. At long lives the fatigue strength improvement tends to be much greater. The slope of the S-N curve can, of course, also be calculated via linear regression analysis. The effect of free slope analysis is presented in Table 7.4. Because there was only a small difference in the measured fatigue strength of 5 and 8 mm thick specimens, these data have been integrated in to single data set to produce the values in Table 7.4. The number of specimens in both series, AW and UIT, is then 10.

Table 7.4 Fatigue strength based on free and fixed (m = 3) slope regression analysis.

Condition	R	m	$FAT_{50\%}$	$FAT_{95\%}$
AW	0,1	2,8 (free slope)	127	108
		3,0 (fixed slope)	130	111
UIT	0,1	3,7 (free slope)	248	187
		3,0 (fixed slope)	231	162

In the as-welded condition, the free slope m=2.8 is close to the assumed slope of S-N -curve for welded structures m=3. Characteristic fatigue classes of as-welded condition with free and fixed slopes are 108 and 111. The corresponding values are 187 and 162 in ultrasonic impact treated condition. Table 7.5 includes a comparison of the measured characteristic fatigue strengths based on both a fixed slope S-N curve and based on linear regression analysis of the slope. The bottom row in this table also includes the strength ratio UIT treated specimens to as-welded specimens. The degree of enhancement due to UIT treatment is 1,73, if free slopes are used to calculate the characteristic hot spot -fatigue classes. This value is somewhat greater than the value of 1,46 which is computed the if fixed slope of m = 3 is used.

Table 7.5 Comparison characteristic fatigue strengths assuming free and fixed (m = 3) slopes.

	Free slope	Fixed slope
UIT	187	162
AW	108	111
Improvement UIT / AW	1,73	1,46

7.1.2 Nominal stress approach

Results of nominal stress based fatigue classes are shown in Tables 7.6, 7.7 and 7.8. Data are presented graphically in Figures 7.5 and 7.6. The comparisons between UIT treated and as-welded is given in Table 7.7. The influence of mean stress is summarized in Table 7.8. Influence of thickness effect can be seen in both Table 7.7 and 7.8.

Table 7.6 Results of statistical analysis based on nominal stress range, (m = 3).

	t	R	m	n	$FAT_{50\%}$	s	$FAT_{95\%}$
UIT	5	0,1	3	5	126	0,191	92
UIT	5	Ohta	3	5	121	0,269	78
AW	5	0,1	3	5	66	0,072	59
UIT	8	0,1	3	5	179	0,271	114
UIT	8	Ohta	3	5	131	0,101	111
AW	8	0,1	3	5	89	0,076	78

Table 7.7 The comparison between thickness and treatment (m = 3), R = 0,1.

	UIT	AW	UIT / AW
8 mm	114	78	1,46
5 mm	92	59	1,56
8 mm / 5 mm	1,24	1,32	

Characteristic nominal stress fatigue classes for specimens in the as-welded condition were 78 MPa and 59 MPa for in series with base plate thicknesses 8 and 5 mm, respectively. The length of the longitudinal attachment was 100 mm in all cases. According to Hobbacher (2006), the nominal design fatigue class of as-welded series should be 71, see Fig. 7.3. Characteristic values of those specimens with base plate thickness of 5 mm were less than this design value. The thickness of the longitudinal attachment was 8 mm in all series, also in the series with base plate thickness of 5 mm. Reason for low fatigue strength of the 5 mm thick specimens was that the total width of base plate in the test region was only 34 mm. As mentioned in the previous section, the structural stress concentration of the 5 mm thick specimens was significantly greater than that of the 8 mm thick specimens.

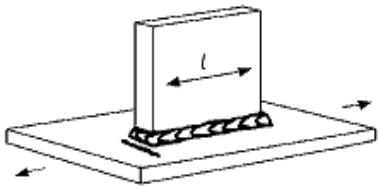

Longitudinal fillet welded gusset at length l	
l < 50 mm	80
l < 150 mm	71
l < 300 mm	63
l > 300 mm	50

Figure 7.3 Characteristic fatigue classes based on attachment length (Hobbacher 2006).

Because of the similarity of methods, the enhancement of ultrasonic impact treatment can be compared to enhancement of hammer peening. The nominal stress improvement of hammer peening has been detailed presented in the IIW recommendation of Haagensen and Maddox (2006):

"For steels with specified yield stress higher than 350 MPa the benefit consists of an upgrade by a factor of 1,6 applied to the stress range, with a change in slope to m = 5 at $2 \cdot 10^6$ cycles. The highest class that can be claimed is FAT 125."

The minimum specified yield strength of material S355J0 used in specimens with one-sided longitudinal attachments was 355 MPa. As shown in Table 7.7, the enhancement of ultrasonic impact treatment is 1,46 and 1,56 with the specimen thicknesses of 8 and 5 mm. These results did not fully achieved the assumed enhancement factor of 1,6. A reason for this is that slightly alternate definitions of stress range were used. This is understood with the help of Fig. 7.4. Haagensen and Maddox (2006) have defined the stress range as function of maximum stress.

"Due to the sensitivity of hammer peened welded joints to applied mean stress, the higher S-N curves can only be used under the following circumstances: When the applied stress ratio R>0 (all stress in tension) the S-N curve is used in conjunction with the maximum stress instead of full stress range."

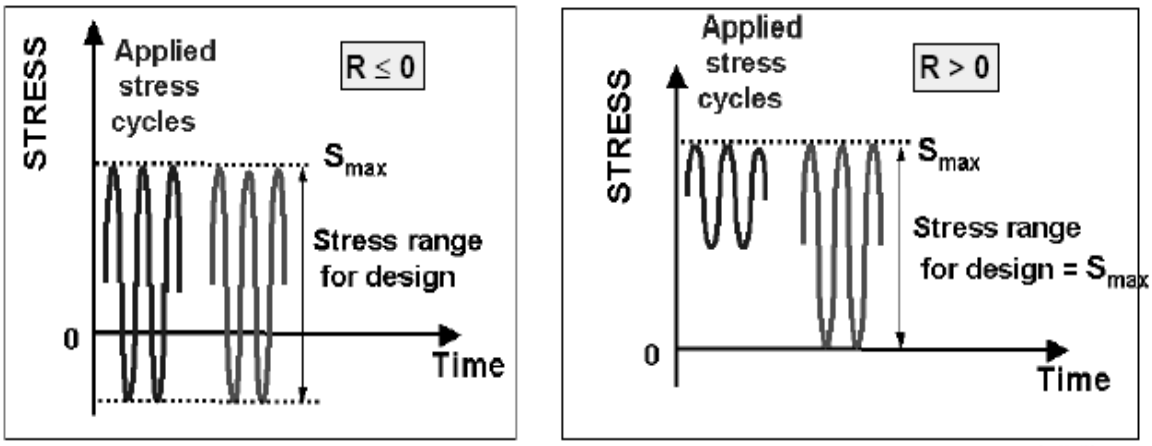

Figure 7.4 Limitations in allowable stress range for hammer peened welds in steel and aluminium alloys (Haagensen and Maddox 2006).

If this effect is taken into account, the improvement due to UIT would be close to the expected improvement due to hammer and needle peening defined by Haagensen and Maddox. Test data are shown graphically in Fig. 7.5. Table 7.8 and Fig. 7.6 provides a comparison of UIT treated welds tested at both R=0,1 and according to the Ohta -method. The characteristic fatigue class for specimens tested at R=0,1 are 3–18 % higher than fatigue class for specimens tested using the Ohta –method, depending on specimen thickness. This difference is less than that expected by Hobbacher (2006):

Table 7.8 The comparison between thickness and R –ratio (m=3), UIT.

	R = 0,1	Ohta	R=0,1 / Ohta
8 mm	114	111	1,03
5 mm	92	78	1,18
8 mm / 5 mm	1,24	1,42	

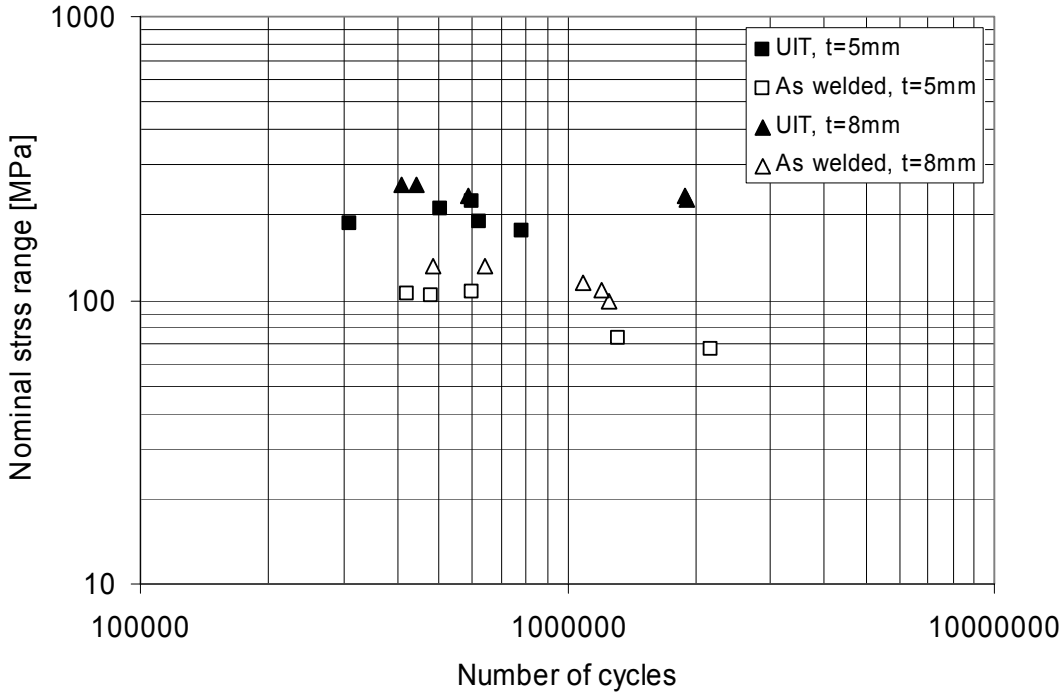

Figure 7.5 The comparison between as-welded and UI -treated series, R=0,1

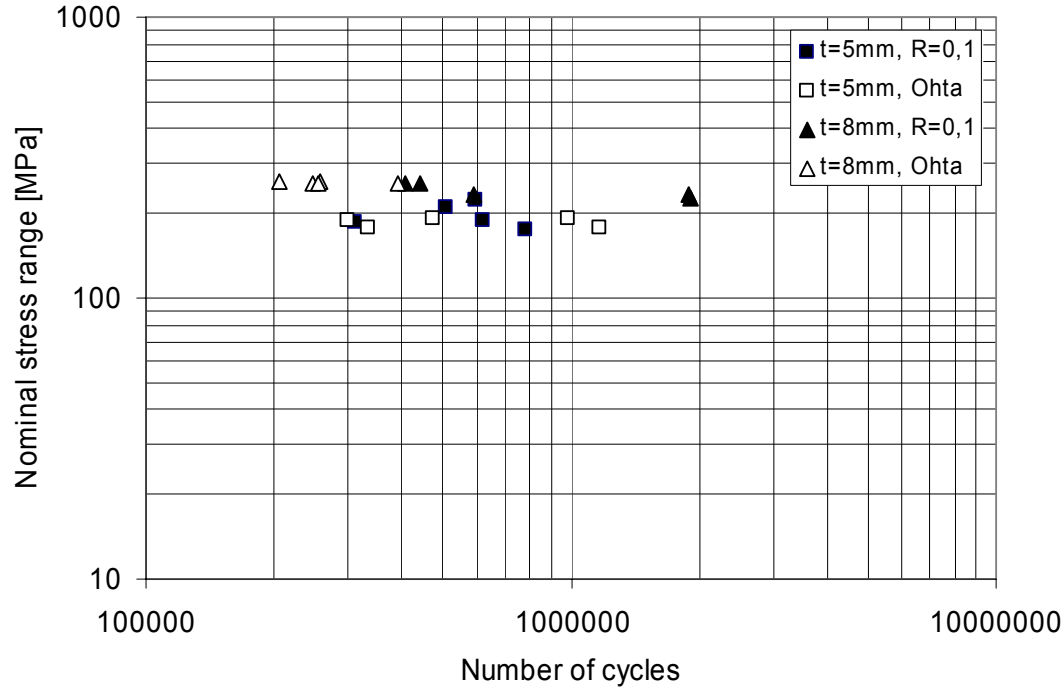

Figure 7.6 The comparison between R=0,1 and Ohta -test series, UIT

In the case of structural stress presented in Chapter 7.1.1, the influence of base plate thickness in terms of structural stress was only 1,05-1,08. The differences between series based on nominal stress of 8 and 5 mm thick base plate are 1,32 in as-welded condition and 1,24-1,42 in ultrasonic impact treated state. Thickness effect is more clearly seen, if nominal stress is used as the basis for comparison.

7.2 Experimental evaluation of initiation period

The crack initiation period for UIT treated specimens has been determined experimentally using the beach marking procedure presented in Chapter 5.2. The beach mark –procedure is based on two –levels of nominal stress. The higher stress range, $\Delta\sigma_1$, is the primary driving force for small crack initiation and crack growth while the lower stress range, $\Delta\sigma_2$, causes a small period of reduced crack growth with less tortuousity. This forms the so-called beach marks on the specimens' surfaces which can be observed even without magnification and can be evaluated using a low power magnification. The maximum stress for both stress ranges is held constant, however, so that extra crack closure effects are not introduced. As mentioned previous, a surface replication technique using an elastic mass was also tried, but the crack resolution was not sufficient for any meaningful measurements of crack initiation.

Constant amplitude loading was applied for three tests UIT-41, UIT-42 and UIT-43. The operation of beach marking was adapted for tests UIT-44, UIT-45 and UIT-46. Data are reported more in Appendix 1.3. Figure 7.7 shows the fracture surface from beach mark specimen UIT-45. The surface poorly shows a band representing one repetition of $\Delta\sigma_2$ of the load spectrum. During testing, more than six repetitions of the spectrum were applied, but the crack propagation portion required less than two repetitions. These observations are rather qualitative and more testing with a slightly altered load spectrum would be needed.

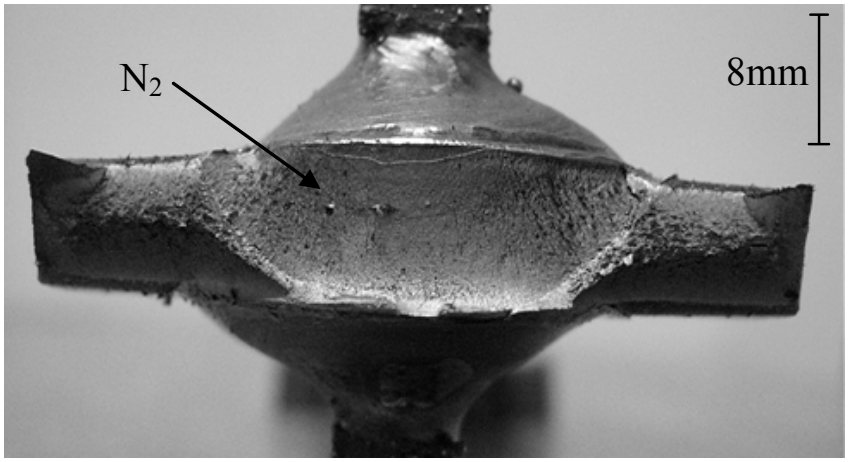

Figure 7.7 Beach marks observable on a fractured two-sided attachment specimen, UIT-45

The location of final rupture of specimen UIT-46 was in the base material outside the UIT treated zone. In specimens UIT-44 and UIT-45, the fatigue cracks initiated at the UIT groove. The number of beach marks was not large in each specimen, UIT-44 and UIT-45. The main difficulty with this technique was that a large cyclic nominal stress range needed to produce any type of fatigue failure in the specimens. The UIT treatment was so effective that high

nominal stresses were needed to get crack initiation. At this high stress level, however, the crack, once initiated advanced relatively rapidly so that the entire propagation period consisted of only a couple blocks of loading.

The final rupture of four specimens, UIT-42, UIT-43, UIT-44 and UIT-45, initiated from the bottom of UI -treated groove. Results of statistical analysis based on nominal stress approach are presented in Table 7.9. The ratio, R, between minimum and maximum stress is 0,1 in tests with constant amplitude loading and for the larger cycles in the beach mark tests. The stress ratio for the smaller cycles in the beach mark tests was 0,53.

Table 7.9 Results of statistical analysis of two-sided longitudinal attachment.

	t	R	m	n	$FAT_{50\%}$	s	$FAT_{95\%}$
UIT	8	0,1-0,53	3	4	149	0,107	125

The characteristic fatigue class of UIT treated specimens with double-sided longitudinal attachments was 125 MPa. This value is higher than the nominal stress fatigue classes of UIT treated one-sided longitudinal attachments presented in Chapter 7.1.2. In the IIW recommendations (Haagensen and Maddox 2006), the highest fatigue class that can be claimed for needle or hammer peening is FAT 125. Based on this, the effectiveness of UIT treatment of specimens with two-sided attachment was considered to be adequate.

7.3 Theoretical calculation of fatigue life

In this thesis, the analytical fatigue life calculations have been made for UIT treated specimens with base plate thickness of 8 mm and subject to constant amplitude loading. Both mean stress states, R=0,1 and Ohta, have been included in the theoretical analyses.

The fatigue life of ultrasonic impact treated specimens has been calculated in two stages. The detailed calculations of initiation life (stage 1) are presented in Appendix 2.1 and propagation life (stage 2) in Appendix 2.2. The fatigue initiation life, estimated according to uniform material law and local strain approach, is presented in Appendix 2.1 using symbols S_{ar} and N_{ini}. The crack propagation life is presented as symbol N_{pro}. The total theoretical fatigue life estimation N_{tot} of two-stage is initiation life N_{ini} + propagation life N_{pro}.

The predicted initiation lives, propagation lives and total fatigue lives are summarized in Table 7.10. The applied stress ranges and mean stresses for the 10 specimens in this table were different. The predicted fatigue lives ranged from 486 000 cycles to 2 838 000 cycles. The percentage of the total life predicted to be involved in crack initiation ranged from 87 – 97 %. In this Table specimens 18 - 22 were tested at R = 0,1 and 23 - 27 were tested using the Ohta method. However, it can be noted that for UIT treated specimens, the applied stress ranges needed to produce any failures were so large that even the Ohta method had R ratios only slightly greater than 0,1.

Table 7.10 Theoretical initiation, propagation and total fatigue life.

Test	18	19	20	21	22	23	24	25	26	27
N_{ini} $[10^6]$	2,744	0,424	0,424	1,804	1,804	0,424	0,464	0,464	0,424	0,464
N_{pro} $[10^6]$	0,094	0,063	0,063	0,086	0,086	0,062	0,063	0,063	0,062	0,063
N_{tot} $[10^6]$	2,838	0,487	0,487	1,890	1,890	0,486	0,527	0,527	0,486	0,527
N_{ini}/N_{tot}	0,97	0,87	0,87	0,96	0,96	0,87	0,88	0,88	0,87	0,88

Experimental evaluation of the initiation period based on beaching marking presented in Chapter 7.2 did not produce sufficient data to give a reliable S-N curve based on life to crack initiation for UIT treated welds. The beach marking traces were clearly observed only on one specimen. The applied stress range was high enough that crack growth through the base plate was very rapid with respect to the block size of the variable amplitude spectrum. In the future a larger number of blocks with a significantly smaller number of cycles would be needed. In any case, the beach marking exercise did confirm that the great majority of life is spent in initiating cracks up to 1,0 mm in depth. The choice of 1,0 mm as the point of differentiation between crack initiation and propagation is somewhat arbitrary. Other crack depths could be justified, but the conclusions would not change.

A comparison between test results and life predictions based on the two-stage approach is presented graphically in Fig. 7.8. Analytical predictions fall within the +/-2s scatter band of the experimental data. Data for specimens UIT-18 - UIT-27 have been included in statistical analysis. Slope of the S-N curve were defined with linear regression analysis of all ten specimens. Value of linear regression analysis gave a very high slope, m=13, and high mean fatigue strength 222 MPa. The computed characteristic fatigue strength is 210 MPa. The slope of the scatter lines represented in Fig. 7.8 is m=13.

Table 7.11 Results of statistical analysis of UI - treated 8 mm thick specimen.

	t	R	m (free)	n	$FAT_{50\%}$	s	$FAT_{95\%}$
UIT	8	0,1-Ohta	13	10	222	0,157	210

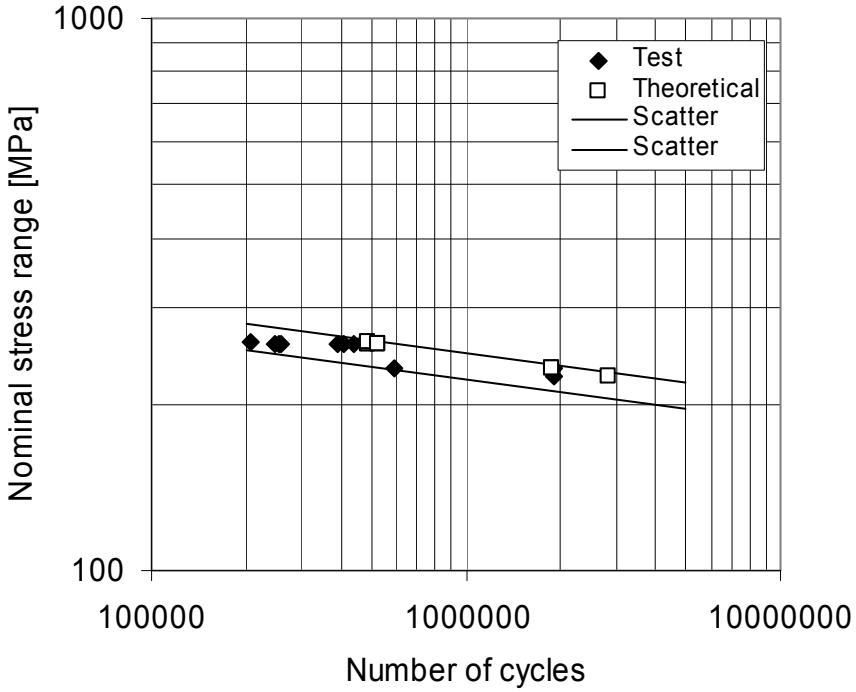

Figure 7.8 Theoretical and experimental results, scatter of experimental tests

Figure 7.8 shows clearly that the analytical predictions fall within the +/-2 standard deviation scatter band of the experimental data. For this reason it is considered that the two-stage fatigue life prediction method provided a fairly good estimation of the fatigue life of UI treated welds.

The theoretical calculation of total fatigue life, presented in this thesis, has included a number of assumptions. The assessment method is sensitive to a number of initial values. For example, the hardness and compressive residual stress of the UI treated surface have a great effect on final predicted total fatigue life. These values are measured only over very small areas and differ significantly in the depth direction. Quantifying this gradient and the sensitivity of the predictions this gradient on is an area for further study. The radius of the UIT groove is largely dependent on the UIT indenter geometry. However, there will be some variation depending on the position of the tool during treatment. The magnitude of the resulting stress concentration factor, K_t, has also to be clarified properly. As seen in Chapter 6.2.1, the thickness of base plate and radius of the UI treated groove have an effect on the stress concentration.

7.4 Potential application for complex structures

This section is intended to provide an outline as to how the analysis procedure developed in this thesis could be applied to complex engineering structures. One fundamental assumption in this thesis has been that the total fatigue life can be computed with a two-stage approach as the sum of initiation life plus propagation life. For the simple UIT improved specimens tested in this research project, it was observed that the initiation life was 87% or more of the total fatigue life. If the structural stresses in a complex structure are of the same order as those in the small laboratory specimens and if the post-weld treatment procedures are similar, then it can be assumed that the part of initiation life is approximately same from total fatigue life also in complex structures.

Precise calculations of propagation period in complex structures are normally considered to be time-consuming and complicated. If fracture mechanics is used, then crack propagation in complex structures is normally relegated to a small group of experts. For these reasons, it is initially recommended that the propagation life can be assumed to be zero in thin complex UI -treated structures and the entire fatigue life is assumed to be fatigue crack initiation. This provides a conservative estimate which can later be refined if desired. Many large structures can have significant residual fatigue life even with fairly large cracks. In such cases fractures mechanics is the only suitable life assessment method available.

In general, the procedure of fatigue initiation life computation outlined in Fig. 6.1 in Chapter 6.2 can be applied for any UIT treated structure. The procedure is not limited to ultrasonic impact treatment, but could also probably be adapted to other peening methods including shot, hammer, needle and ultrasonic peening.

The main issues that must be clarified for analysing structures using the proposed method are: notch stress concentration, residual stress and the ultimate strength of the cold-worked material in the bottom of the treated groove. Of these three issues, defining the notch stress concentration is probably the most difficult task. Complex structures contain three-dimensional stress states and the location and direction of crack initiation is not always clear. In addition, the finite element model of a large and complex structure that also has sufficiently small elements from which to be able to derive notch stresses would require a significant amount of modelling effort and a model with many degrees of freedom.

Working group 3 of Commission XIII of IIW is currently drafting a document giving guidelines for FE modelling of complex structures when the effective notch stress fatigue assessment method is used. This fatigue assessment method requires accurate modelling of notches with 1 mm radii (Fricke 2006A). For UIT improved structures, the radii will typically range from 2-6 mm. In this respect, computing the notch stress at a groove created by post weld treatment is not beyond reason and is easier than assessing effective notch stress. After evaluating the results of a recent round robin exercise on the effective notch method, it was concluded that the use of quadratic elements in the notch region with element sizes up to r/4 can be used (Fricke 2006b). With this as a guideline, it can be recommended that a typical UIT groove with a 3 mm radius should be modelled with quadratic elements 0.75mm on a side. The FE mesh shown in Fig. 6.3 is sufficiently refined for deriving the notch stress concentration factors.

The second concern is that of defining the residual stress at a notch in a real structure. Hole drilling or sectioning are destructive which limit their use. For cost reasons, neutron diffraction is not a realistic alternative for routine measurements. X-ray techniques can be used on many types of structures, but such devices are not widely available. For simplicity, however, it would probably be more efficient to derive simple relationships between the post weld treatment process, the material strength and the resulting residual stress state obtained. The relationships may be expressed as tables, graphically or using empirical or analytic equations. Examples of residual stresses at the bottom of UIT grooves obtained by LUT are presented in Table 7.12 and in Fig. 7.9.

An industrial company which regularly uses 2-3 grades of material in its fabrication processes could measure the resulting residual stress state that reliably occurs due to a specific and well controlled peening process. Such results could be used regularly in analysis.

Table 7.12 Residual stresses measured using X –ray diffraction.

Material	Type of attachment	f_y [MPa]	S_{res} [MPa]
QSTE 460 TM	Transverse	460	-178,5
S355 – current study	Longitudinal	355	-168
Domex700*	Longitudinal	700	-382

*Venkateshwaran 2005

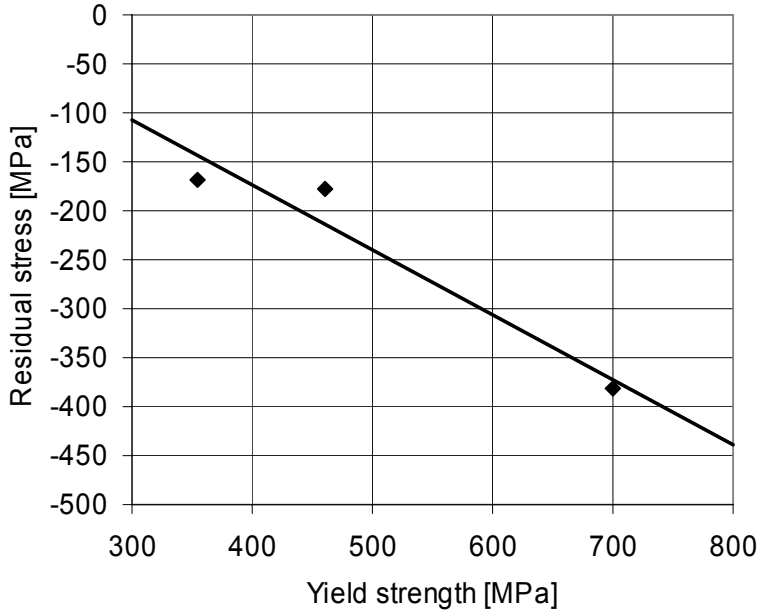

Figure 7.9 Relationship between yield strength and compressive residual stress.

The three points presented in Table 7.12 are shown graphically in Fig. 7.9. The mean line through these points was computed using linear regression analysis. This mean line is also shown in Fig. 7.9. Figure 7.9 shows a clear trend, but there is not sufficient data to derive an empirical relationship between residual stress and yield strength of base material.

Residual stress stability is currently a topic of research at numerous laboratories. It is known that high tensile or high compressive residual stresses will relax during fatigue loading. Predicting the rate of relaxation and more importantly the steady-state residual stress state for different initial stress states, materials, load histories and component geometries is beyond our current engineering science. The simple assumptions made in this thesis will need to be revised as more knowledge is gained.

The final initial input value, which is as important as residual stress, is the hardness of the material at the bottom of the treated groove. Hardness measurement is destructive. For this reason hardness measurement can not be applied for real structures which will be later put into service. The calculation method presented in this thesis requires that the local hardness of the surface will be measured after treatment. It can be assumed that hardness attained during the treatment of a complex structure is the same as that of a simple specimen fabricated from the same steel, with the same welding process and post treated using a similar procedure. Some examples of these relationships are presented in Table 7.13. The hardness was found to increase from 6% to 20% during treatment. Note that the value of Huo et al. (2001) was based on the hardness ratio between ultrasonic peening versus hardness in the as-welded state. Other values are comparisons between the UIT treated vs. the as-welded state.

Table 7.13 Hardness of treatment versus as welded –condition.

Source	Material	Method	Ratio
This study	S355	UIT / AW	1,20
Statnikov (2004A)	AlMg5	UIT / AW	1,20
Statnikov (2004B)	AISI4150	UIT / AW	1,06
Huo et al. (2001)	Q235B	UP / AW	1,07

As with the case of the residual stresses, an industrial company which regularly uses a limited number of material grades could measure the resulting hardness increase due to a well controlled post-treatment process. These constant values could be tabulated and used in fatigue life assessment.

8 CONCLUSIONS

8.1 General conclusions

The literature survey has shown that a variety of post weld improvement methods have been developed for welded structures. Many of these methods have been verified to be reliable and are frequency applied in industry. Methods are generally categorized as either geometry improvement or residual stress improvement methods. Many methods, however, improve both the residual stress state and the local geometry of the weld toe. Ultrasonic impact treatment, UIT, is classified as a residual stress method. The benefit of UIT is based on three mechanisms: initial crack-like flaws are removed, the local stress concentration is decreased and compressive residual stresses are introduced in place of the as-welded tensile residual stresses.

This thesis adds to the ever growing body of experimental evidence that demonstrates the benefits of ultrasonic impact treatment as a means of improving the fatigue strength of welded specimens. Fatigue tests on 5 mm and 8 mm longitudinal non-load carrying joints in both the as-welded and UIT treated condition have been performed. A total 33 specimens with one-sided and 6 with two-sided longitudinal attachments are specifically reported in this thesis. The material tested were structural steel S355J0.

The fatigue life of a UI –treated welded joint can be assessed with a theoretical two-stage analysis method. The analysis consists of computing an initiation life which is then added to the crack propagation life. In the current tests, the majority (87–97 %) of total life consist of initiation period. For this reason, ignoring the crack propagation period would not greatly reduce the accuracy of the fatigue life prediction of UI –treated thin specimens.

The fatigue crack initiation period was evaluated based on a local strain approach. The coefficients and exponents of the material in the UI –treated zone required for local strain analysis are not available from literature. Eight common methods for calculating these coefficients were found in literature and assessed as to their usefulness for post weld treated structures. A modified version of the uniform material law, UML, was chosen for defining the material coefficients in the local strain approach. UML requires only that the ultimate strength of the treated material is known. The treated material is highly local formed and ultimate strength is correlated to the hardness of the material at the bottom of the UIT notch. The residual stresses caused by UI –treatment were measured using X–ray diffraction measurement. Residual stress was treated as a mean stress for fatigue analysis. FE analysis was used to define the stress concentration factors due to the UIT notch

The fatigue propagation life was calculated using linear-elastic fracture mechanics. This approach is based on detailed finite element model. Weight functions through the thickness of the base plate were integrated and the shape of crack was taken account in the propagation life analysis.

A beach marking method was used to estimate the experimental crack initiation life of UIT treated welds. The data was insufficient for statistical analysis because the propagation life was relatively short with respect to the block size used. These observations did confirm,

however, that the majority of fatigue life was consumed in forming cracks up to 1,0 mm depth.

The analytical model for estimating the degree of improvement observed in UIT treated welds was verified based on the experimental fatigue tests. The sum of initiation and propagation lives gave a good prediction of the total specimen life observed in experiments. The predicted values fall within the +/-2 standard deviation scatter band of the experimental data. Also, the experimentally observed proportion of fatigue life spent initiating a fatigue crack agreed well with the analytical predictions.

From a mechanistic point of view, the two-stage approach presented in this thesis should also be valid for other peening methods including shot, hammer, needle and ultrasonic peening.

8.2 Summary of results

8.2.1 Specimens with one-sided longitudinal attachment

Structural stress range

Stress values are recorded as structural stress ranges, which has the advantage in that potential secondary bending stresses are also taken into consideration and specimens with different geometries can be compared more easily.

Statistical evaluation indicates that the structural fatigue class of UIT treated welds was 45 – 50 % higher than the fatigue class for as-welded specimens based on the recommended fixed S-N curve slope, m = 3. This is consistent with IIW recommendations for other improvement techniques.

Based on free slope regression analysis the increase of fatigue strength is clearly higher. Free slope regression analysis of UIT treated welds produced m=3.7 and as-welded condition m=2.8. In that case the fatigue strength improvement at $2x10^6$ cycles is 73 %.

The effect of specimen thickness on fatigue strength was only slight. The structural fatigue class of specimens t=8 mm is 5-8 per cent higher than fatigue class of specimens t=5 mm. The cause of this difference has not been investigated.

Structural fatigue strength based on low mean stress testing (R=0,1) is about 19 % higher than the measured fatigue strength at a high mean stress obtained using the Ohta-method ($\sigma_{max} = f_y$). This value is similar to that expected for as-welded structures and indicates that UIT will retain its effectiveness for large fabricated structures that have yield magnitude reactive residual stress states.

Nominal stress range

Fatigue strengths have also been calculated based on the nominal stress ranges. In the case of nominal stresses, statistical analyses indicated that fatigue classes of ultrasonic impact treated welds were 46–56 % higher than corresponded welds in the as-welded condition.

The effect of base plate thickness on nominal fatigue strength was higher than compared to the thickness effect observed when comparison is based on the structural stresses. The fatigue classes of 8 mm thick plates were 24–42 % higher than these of 5 mm thick plates.

Nominal fatigue strengths at high mean stresses ($\sigma_{max} = f_y$) were 3–18 % lower than at low mean stresses (R=0,1). That is less than the expected value of 20% reduction suggested by the IIW recommendations.

In the case of nominal stresses, some fatigue results were lower than expected. The characteristic fatigue strength of specimens fabricated from 5 mm thick plates in the as-welded condition was only 59. The reason for this poor weld quality is not fully understood. The recommendation of IIW gives the fatigue class of 71 for the same detail.

8.2.2 Specimens with two-sided longitudinal attachment

One series of specimens with attachments welded on both sides of base plate were manufactured for confirming the nominal fatigue classes of UIT treated welds. Specimens with two-sided attachments were additionally used for the experimental evaluation of the fatigue crack initiation period. The nominal characteristic fatigue class of this series was 125 MPa, which is same as the highest class for hammer peened welds in the IIW recommendations.

8.2.3 Theoretical calculation of fatigue life

An analytical method for estimating the degree of improvement observed in UIT treated welds has been developed and verified based on experimental measurements. Test results of UIT treated welds with 8 mm thick base plate were compared to analytical predictions made using a two-stage approach. The sum of initiation and propagation life gave a good prediction of the total specimen life observed in experiments. The predicted values fall within the +/-2 standard deviation scatter band of the experimental data.

8.3 Recommendations for future work

The thesis has specifically focused on fatigue life of simple specimens fabricated from conventional structural steel. Post weld improvement by UIT at LUT has also been observed for high strength steels (Venkateshwaran 2005) and welded stainless steels (Maddox 2005). Future work remains to verify the proposed two-stage method for these materials. The uniform material law used in this thesis for structural steels is not valid for stainless steels and some alternate rules would need to be developed.

The presented method can be adapted for complex UI –treated structures. Initial stages of a proposal have been given in Chapter 7.4. It is difficult or even possible to measure the residual stress and local hardness of complex structures. In order to define these values, some approximations found from literature and previous research of simple structures would need to be adapted. Recommendations and rules will need to be developed based on these assessments. Hardness and residual stresses are functions of material properties. Parametric

equations relating local stresses to structural stresses based on joint dimensions are currently being developed.

The presented approach is not limited to ultrasonic impact treatment. It is expected that the method can be expanded to the other peening methods.

Studies on residual stresses due to welding and due to post weld treatment methods is an area of active research. Better understanding of residual stresses and how these change due to constant amplitude and spectrum loading remains as a major challenge to welded structures researchers. The current assumption of simply treating of residual stress as a component of mean stress will need to be further verified.

REFERENCES

Albrecht P., Yamada K., Rapid calculation of stress intensity factors, J. Struct. Div., ASCE 103, No. ST2, pp. 377-389, 1977.

Bannantine J, Comer, J., and Handrock, J., Fundamentals of metal fatigue analysis, Prentice Hall, New Jersey, 1990.

Boller, C., Seeger T., Materials data for cyclic loading, Elsevier Science Publishers, Amsterdam, 1987.

Bäumel A., Seeger T., Materials data for cyclic loading, Supplement 1, Elsevier Science Publishers, Amsterdam, 1990.

Dowling N.E., Mechanical behaviour of materials, Second edition, Prentice Hall, New Jersey, 1999.

ESAB hitsauslisäaineet [filler materials for welding], ESAB Oy, Finland, 2000.

Fisher J.W., Statnikov E., Tehini L., Fatigue improvement of the bridge girders by ultrasonic impact treatment (UIT), Proceedings of the IIW fatigue seminar, 2nd April 2002, Tokyo Institute of Technology, Japan 2002.

Gurney, T.R., Fatigue of welded structures, Second edition, Cambridge University Press, Cambridge, 456 p., 1979.

Gurney T.R., The fatigue strength of transverse fillet welded joints, A study of the influence of joint geometry, An Abington publishing special report, 1991.

Fricke, W., Annual Report of Working Groups XIII-3 and XV-10 on Stress analysis, International Institute of Welding, IIW-document XIII-2111-06/XV1217-06, August 2006

Fricke, W., Round-robin study on stress analysis for the effective notch stress approach, International Institute of Welding, IIW-document XIII-2129-06/XV1223-06, August 2006

Haagensen P.J., Chapter 6: Improving the fatigue strength of welded joints, Fatigue handbook, Edited by A. Almar-Naess, Trondheim, 1985.

Haagensen P.J., Drågen A., Slind T., Örjesäter O., Predictions of the improvement in fatigue life of welded joints due to grinding, TIG dressing, weld shape control and shot peening, SIMS 87, Proceedings of the 3rd International ECSC Offshore Conference on Steel in Marine Structures, Delft, The Netherlands, June 15-18 1987.

Haagensen P.J., IIW's Round Robin and Design Recommendations for Improvement Methods, International conference on performance of dynamically loaded welded structures, IIW 50th Annual Assembly Conference, Proceedings of the Conference held in San Francisco, Editors: S.J.Maddox and M.Prager, 1997.

Haagensen P.J., Statnikov E., Lopez-Martinez L., Introductory fatigue tests on welded joints in high strength steel and aluminium treated by various improvement methods including ultrasonic impact treatment (UIT), International Institute of Welding, IIW-document XIII-1748-98, 1998.

Haagensen P.J. and Maddox S.M., IIW recommendations on post weld improvement of steel and aluminium structures, International Institute of Welding, IIW-document XIII-1815-00, version March 2006.

Harris I.D., Abrasive water jet cutting and its applications at TWI (UK), Welding in the World, Vol.33, No.4, 1994.

Hill, M., DeWald, A., Denna, A., Hackel, L., Chen, H. Dane, C., Specht, R., and Harris F., Laser peening technology, Advanced Materials and Processes, 161, No. 5, 2003.

Hobbacher A. Stress intensity factors of plates under tensile load with welded on flat side gussets, Engineering Fracture Mechanics, Vol. 41, No. 6, pp.897-905, Printed in Great Britain, 1992.

Hobbacher A., IIW Recommendation for fatigue design of welded joints and components, International Institute of Welding, IIW –document JWG-XIII-XV-122-94.

Hobbacher A., Recommendations for fatigue design of welded joints and components, International Institute of Welding, IIW-document XIII-1965-03/XV-1127-03, version April 2006.

Huo, L., Wang, D. and Zhang, Y., Chen J., Investigation on improving fatigue properties of welded joints by ultrasonic peening method, Welding in the World, Vol. 45, No. 3-4, 2001.

Huo, L., Wang, D. and Zhang, Y., Investigation of the fatigue behaviour of the welded joints treated by TIG dressing and ultrasonic peening under variable amplitude load, International Institute of Welding, IIW-document XIII-1915-02, 2002.

Huther I., Lieurade H.P., Janosch J.J., Chabrolin B., Ryan I., The influence improvement, techniques on welded joint fatigue strength, International Institute of Welding, IIW-document XIII-1562-94, 1994.

Huther M., IIW Guidance for statistics – Fatigue test results analysis, International Institute of Welding, Doc XIII-WG1-101-02.

James M.N., Peterson A.E., Sutcliffe N., Constant and variable amplitude loading of 6261 aluminium alloy I-beams with welded cover plates-Influence of weld quality and stress relief, International Journal of Fatigue, Vol. 19, No. 2, pp. 125-133, 1997.

Kado S., Influence of the conditions in TIG dressing on the fatigue strength in welded high tensile steels, International Institute of Welding, IIW-document XIII-771-75, 1975.

Keating P.B., Fisher J.B., Evaluation of fatigue tests and design criteria on welded details, National cooperative highway research program, Report 286, Lehigh University, 1986.

Kim K.S., Chen X., Han C., Lee H.W., Estimation methods for fatigue properties of steel under axial and torsional loading, International Journal of Fatigue 24 (2002) p. 783-793.

Kirkhope K.J., Bell R., Caron L., Basu R.I., Ma K-T., Weld detail fatigue life improvement techniques. Part 1: review, Marine Structures 12, p. 447-474, 1999.

Kosteas D., Quality consideration, TALAT lecture 2404, Comparison of techniques and cost, http://www.eaa.net/education/TALAT/lectures/2404.pdf, 21.4.2006.

Kudryavtsev Y., Kleiman J., Lugovskoy A., Lobanov L., Knysh V., Voytenko O. and Prokopenko G., Rehabilitation and repair of welded elements and structures by ultrasonic peening, International Institute of Welding, IIW-document XIII-2076-05

Kudryavtsev Y. and Kleiman J., Application of ultrasonic peening for fatigue life improvement of automotive welded wheels, International Institute of Welding, IIW-document XIII-2075-05

Lepistö J.S., Marquis G.B., MIG brazing as a means of fatigue life improvement, Welding in the World, Vol. 48, No. 48, ISSN 0043-2288, 9/10-2004.

Lihavainen V-M., Marquis G., and Statnikov E., Fatigue strength of a longitudinal attachment improved by ultrasonic impact treatment, International Institute of Welding, IIW-document XIII-1990-03, 2003.

Maddox S.J., Fatigue strength of welded structures, Second edition, Abington Publishing, Cambridge, 1991, 198 p.

Maddox S. J., Final report: Improving the fatigue performance of welded stainless steels, TWI Report No. 13631/7/05, June 2005.

Manson S., Fatigue-a complex subject-some simple approximations, Experimental Mechanics, Vol. 5., No. 7, 1965, p. 193.

Meggiolaro, M.A., Castro, J.T.P., Statistical evaluation of strain-life fatigue crack initiation predictions,http://www.tecgraf.puc-rio.br/vida/paper/R04_IJF_statistical_evaluation.pdf, 4.5.2006.

Mitchel M.R., Fatigue and microstructure, American Society for metals, Metals Pack (OH), 1979, p. 385.

Muralidharan U. and Manson S.S., Modified universal slopes equation for estimation of fatigue characteristic, ASME Trans. J. Engineering Mater. and Tech. 1988; 110.

Newman J.C., Raju S., An empirical stress-intensity factor equation for the surface crack, Engineering Fracture Mechanics Vol. 15, No 1-2, pp. 185-192, 1981.

Niemi E., Structural stress approach to fatigue analysis of welded structures, Designer's guide, International Institute of Welding, IIW-document XIII-1819-00, XV-1090-01, 2001.

Niu X., Glinka G., Weight functions for edge and surface semi-elliptical cracks in flat plates and plates with corners, Engineering Fracture Mechanics, Vol. 36, No. 3, 1990.

Ohta A., Matsuoka K., Suzuki N., Maeda Y., Fatigue strength of non-load-carrying cruciform welded joints by a test maintaining maximum stress at yield strength, Engineering Fracture Mechanics, Vol. 9, pp. 639-645, 1994.

Ohta A., Suzuki N., Maeda Y., Doubled fatigue strength of box welds by using low transformation temparature welding material, International Institute of Welding, IIW-document XIII-1825-2000.

Ohta A., Maeda Y., Suzuki N., Fatigue life extension by repairing fatigue cracks initiated around box welds with low transformation temperature welding wire, International Institute of Welding, IIW-document XIII-1835-2000.

Ong J.H., An improved technique for the prediction of the axial fatigue life from tensile data, International Journal of Fatigue 1993; 15: 213-9.

Park J-H., Song J-H., Detailed evaluation of methods for estimation of fatigue properties, International Journal of Fatigue, Vol. 17, No. 5, pp 365 – 373, 1995.

Rautaruukki, Designer's guide, Steel products, 1996.

Roessle M.L., Fatemi A., Strain-controlled fatigue properties of steel and some simple approximations, International Journal of Fatigue 22 (2000), p. 495-511.

SAE Fatigue Design Handbook, SAE Pub No. AE-10, Society of Automotive Engineers, Warrendale, PA, 2nd Ed. 1988.

Sougata R., Fisher J.W., Yen B.T., Fatigue resistance of welded details enhanced by ultrasonic impact treatment (UIT), International Journal of Fatigue 25, No.9-11, (2003).

Statnikov E., Trufyakov V.I., Mikheev P.P., Kudryavtsev Y.F., Specification for weld toe improvement by ultrasonic impact treatment, International Institute of Welding, IIW-document XIII-1617-96, 1996.

Statnikov E., Applications of operational ultrasonic impact treatment (UIT) technologies in production of welded joints, International Institute of Welding, IIW-document XIII-1667-97, 1997A.

Statnikov E., Comparison of efficiency and processibility of post-weld deformation methods for increase in fatigue strength of welded joints, Northern Scientific & Technological Fund, International Institute of Welding, IIW-document XIII-1668-97, 1997B.

Statnikov E., Guide for applications of ultrasonic impact treatment for improving fatigue life of welded structures, Applied Ultrasonics / Northern Scientific & Technology Company, International Institute of Welding, IIW –document XIII-1757-99.

Statnikov E., Muktepavel V.O., Trufyakov V.I., Mikheev P.P., Kuzmenko A.Z., Blomqvist A., Comparison of ultrasonic impact treatment (UIT) and other fatigue life improvement methods, International Institute of Welding, IIW-document XIII-1817-00, 2000.

Statnikov E., Physics and mechanism of ultrasonic impact treatment, International Institute of Welding, IIW –document XIII-2004-04, 2004A.

Statnikov E., Vitazev V., Korolkov O., Comparison of the efficiency of 27, 36 and 44 kHz UIT tools, International Institute of Welding, IIW –document XIII-2005-04, 2004B.

Statnikov E., Vitayazev V., Korolkov O., Ultrasonic impact treatment *Esonix* versus ultrasonic peening, International Institute of Welding, IIW –document XIII-2050-05, 2005.

Stephens R.I., Fatemi A., Stephens R.R., Fuchs H., Metal fatigue in engineering, Second edition, A Wiley-Interscience Publication, 2001.

Suoknuuti J., Lappeenrannan teknillinen yliopisto -Jännitysmittaus [Lappeenranta University of Technology -stress measurement], Stresstech Oy, Finland, 2002.

Suresh, S., Fatigue of Metals, Second edition, Cambridge University Press, 1998.

TO-13, Technology brokerage event in the field of industrial process and automation during the 58th International Technical Fair, 1-2 October 2002, Plovdiv, Bulgaria, http://www.bit.or.at/irca/events/Plovdiv.doc, 26.9.2003.

Venkateshwaran, P. Constant and variable amplitude fatigue strength of high strength steels welds treated with UIT, Master of Science Thesis, Lappeentanta University of Technology. 2005

Wetzel R.M. (ed.), Fatigue Under Complex Loading: Analysis and Experiments, V. 6, Society of Automotive Engineers, Warrendale, PA, 1977.

Fatigue test results **APPENDIX 1.1**

t Thickness of test specimen
R $R=\sigma_{min}/\sigma_{max}$, Ohta $\sigma_{max} = f_y$
$\Delta\sigma_{SG}$ Stress range at strain gauge [MPa]
N Number of cycles
RO Run-Out test, non-failed specimen
WT Crack initiated at weld toe
UITG Crack initiated at UIT groove

Data points of S355 one-sided longitudinal attachment, structural stress range.

	t	R	$\Delta\sigma_{SG}$	N	FAT(m=3)	Observation
UIT-1	5	0,1	349	596082	233	UITG
UIT-2	5	0,1	318	310170	171	UITG
UIT-3	5	0,1	324	620074	219	UITG
UIT-4	5	0,1	327	505913	207	UITG
UIT-5	5	0,1	318	781200	232	UITG
UIT-6	5	Ohta	333	298108	177	UITG
UIT-7	5	Ohta	338	473704	209	UITG
UIT-8	5	Ohta	327	980692	258	UITG
UIT-9	5	Ohta	297	333199	163	UITG
UIT-10	5	Ohta	295	1163070	246	UITG
AW-11	5	0,1	180	599377	120	WT
AW-12	5	0,1	221	422755	131	WT
AW-13	5	0,1	127	2173795	131	WT
AW-14	5	0,1	132	1313035	115	WT
AW-15	5	0,1	204	480284	127	WT
AW-16	5	0,1	173	6814655	-	RO
AW-17	5	0,1	134	3086407	-	RO
UIT-18	8	0,1	288	1902884	283	UITG
UIT-19	8	0,1	369	441958	223	UITG
UIT-20	8	0,1	383	407610	225	UITG
UIT-21	8	0,1	335	588203	223	UITG
UIT-22	8	0,1	338	1892369	332	UITG
UIT-23	8	Ohta	360	256226	181	UITG
UIT-24	8	Ohta	392	393186	230	UITG
UIT-25	8	Ohta	367	247240	183	UITG
UIT-26	8	Ohta	379	205424	177	UITG
UIT-27	8	Ohta	336	254817	169	UITG
AW-28	8	0,1	193	485897	120	WT
AW-29	8	0,1	193	640024	132	WT
AW-30	8	0,1	161	1257193	138	WT
AW-31	8	0,1	180	1091393	147	WT
AW-32	8	0,1	169	1199013	143	WT
AW-33	8	0,1	153	3453562	-	RO

Fatigue test results **APPENDIX 1.2**

$\Delta\sigma_{nom}$ Nominal stress range [MPa]

Data points of S355 one-sided longitudinal attachment, nominal –stress range.

	t	R	$\Delta\sigma_{nom}$	N	FAT(m=3)	Observation
UIT-1	5	0,1	224	596082	150	UITG
UIT-2	5	0,1	186	310170	100	UITG
UIT-3	5	0,1	188	620074	127	UITG
UIT-4	5	0,1	210	505913	133	UITG
UIT-5	5	0,1	175	781200	128	UITG
UIT-6	5	Ohta	190	298108	101	UITG
UIT-7	5	Ohta	193	473704	119	UITG
UIT-8	5	Ohta	192	980692	151	UITG
UIT-9	5	Ohta	177	333199	97	UITG
UIT-10	5	Ohta	177	1163070	148	UITG
AW-11	5	0,1	107	599377	72	WT
AW-12	5	0,1	105	422755	63	WT
AW-13	5	0,1	67	2173795	69	WT
AW-14	5	0,1	74	1313035	64	WT
AW-15	5	0,1	104	480284	65	WT
AW-16	5	0,1	80	6814655	-	RO
AW-17	5	0,1	64	3086407	-	RO
UIT-18	8	0,1	225	1902884	221	UITG
UIT-19	8	0,1	257	441958	155	UITG
UIT-20	8	0,1	257	407610	151	UITG
UIT-21	8	0,1	232	588203	154	UITG
UIT-22	8	0,1	232	1892369	228	UITG
UIT-23	8	Ohta	258	256226	130	UITG
UIT-24	8	Ohta	257	393186	149	UITG
UIT-25	8	Ohta	257	247240	128	UITG
UIT-26	8	Ohta	259	205424	121	UITG
UIT-27	8	Ohta	257	254817	129	UITG
AW-28	8	0,1	132	485897	82	WT
AW-29	8	0,1	132	640024	90	WT
AW-30	8	0,1	99	1257193	85	WT
AW-31	8	0,1	116	1091393	95	WT
AW-32	8	0,1	109	1199013	92	WT
AW-33	8	0,1	99	3453562	-	RO

Fatigue test results **APPENDIX 1.3**

$\Delta\sigma_{eq}$ Equivalent stress range
BM Crack initiated at base material
N_{tot} Total number of cycles

Data points of S355 two-sided longitudinal attachment, nominal –stress range.

	t	R	$\Delta\sigma_{nom}$	N	FAT(m=3)	Observation
UIT-41	8	0,1	233	2381012	-	RO
UIT-42	8	0,1	281	409068	166	UITG
UIT-43	8	0,1	281	314170	152	UITG

	t	R	$\Delta\sigma_{eq}$	N_{tot}	FAT(m=3)	Observation
UIT-44	8	0,1–0,53	264	334236	145	UITG
UIT-45	8	0,1–0,53	264	274219	136	UITG
UIT-46	8	0,1–0,52	219	2273000	-	BM

Stress ranges and number of cycles of beach marking loading.

	$\Delta\sigma_1$	N_1	$\Delta\sigma_2$	N_2
UIT-44	281	267400	148	66836
UIT-45	281	219400	149	54819
UIT-46	233	1818000	121	455000

APPENDIX 2.1-1

Fatigue crack initiation life (Stage 1). Experimental tests 18-27

$j := 0..9$

Nominal stress range ΔS | Test result N | Nominal mean stress S_m

$$\Delta S := \begin{pmatrix} 225 \\ 257 \\ 257 \\ 232 \\ 232 \\ 258 \\ 257 \\ 257 \\ 259 \\ 257 \end{pmatrix} \quad N := \begin{pmatrix} 1902884 \\ 441958 \\ 407610 \\ 588203 \\ 1892369 \\ 256226 \\ 393186 \\ 247240 \\ 205424 \\ 254817 \end{pmatrix} \quad S_m := \begin{pmatrix} 138 \\ 157 \\ 157 \\ 142 \\ 142 \\ 154 \\ 155 \\ 155 \\ 154 \\ 155 \end{pmatrix}$$

Nominal stress amplitude = nominal stress range / 2

$S_a := \frac{\Delta S}{2}$ Nominal stress amplitude

$HB := 201$ HB = Brinell hardness 0,1mm below the surface of treated groove

$R_m := 3.45 \cdot HB$

$R_m = 693.45$ R_m = Approximation for ultimate strength

APPENDIX 2.1-2

The effect of mean and residual stress

$S_{res} := -178.5$ X-ray measurement - 3 pass. transverse residual stress

$S_{mean} := S_m + S_{res}$ Mean stress = mean stress + residual stress

$$S_{ar_j} := \frac{(S_a)_j}{1 - \frac{(S_{mean})_j}{R_m}}$$ Corrected nominal stress amplitude

$$S_{ar} := \begin{pmatrix} 106.292 \\ 124.636 \\ 124.636 \\ 110.2 \\ 110.2 \\ 124.598 \\ 124.288 \\ 124.288 \\ 125.081 \\ 124.288 \end{pmatrix}$$

Uniform material law presented by Bäumel and Seeger. Chapter 4.2.6

$E := 2.1 \cdot 10^5$ Modulus of elasticity

$\sigma fp := 1.5 \cdot R_m \quad \sigma fp = 1.04 \times 10^3$ Fatigue strength coefficient

$b := -0.087$ Fatigue strength exponent

$\frac{R_m}{E} = 3.302 \times 10^{-3}$ $\psi := 1.375 - 125 \cdot \frac{R_m}{E}$ $\psi = 0.962$

$\varepsilon fp := 0.59 \cdot \psi$ $\varepsilon fp = 0.568$ Fatigue ductility coefficient

$c := -0.58$ Fatigue ductility exponent

$Kp := 1.65 \cdot R_m$ $Kp = 1.144 \times 10^3$ Strain hardening coefficient

$np := 0.15$ Strain hardening exponent

Strain amplitudes. Ramberg-Osgood

$K_t := 2.55$ Stress concentration -factor from FE -model of fracture mechanics

$S_{ar} := 106$ Corrected nominal stress amplitude. UIT-18

$\sigma_a := K_t \cdot S_{ar}$ Notch stress amplitude

$$\varepsilon_a := \frac{\sigma_a}{E} + \left(\frac{\sigma_a}{Kp}\right)^{\frac{1}{np}}$$

$\varepsilon_a = 1.354 \times 10^{-3}$ Strain amplitude. UIT-18

$$\varepsilon_a := \begin{pmatrix} 1.354 \cdot 10^{-3} \\ 1.717 \cdot 10^{-3} \\ 1.717 \cdot 10^{-3} \\ 1.421 \cdot 10^{-3} \\ 1.421 \cdot 10^{-3} \\ 1.717 \cdot 10^{-3} \\ 1.695 \cdot 10^{-3} \\ 1.695 \cdot 10^{-3} \\ 1.717 \cdot 10^{-3} \\ 1.695 \cdot 10^{-3} \end{pmatrix}$$

APPENDIX 2.1-4

Fatigue life

$N_{est} := 1000000$ Estimation for fatigue life

$\varepsilon_a := 1.354\,10^{-3}$ Strain amplitude of UIT-18

Given Calculation loop

$$\varepsilon_a = \frac{\sigma fp}{E}\cdot\left(2\cdot N_{est}\right)^b + \varepsilon fp\cdot\left(2\cdot N_{est}\right)^c$$

$N_{ini} := \mathrm{Find}\left(N_{est}\right)$

$N_{ini} = 2.744\times 10^6$ Initiation period of UIT-18

Initiation period

$$N_{ini} := \begin{pmatrix} 2744000 \\ 424600 \\ 424600 \\ 1804000 \\ 1804000 \\ 424600 \\ 464000 \\ 464000 \\ 424600 \\ 464000 \end{pmatrix}$$

Corrected nominal stress amplitude

$$S_{ar} := \begin{pmatrix} 106 \\ 125 \\ 125 \\ 110 \\ 110 \\ 125 \\ 124 \\ 124 \\ 125 \\ 124 \end{pmatrix}$$

APPENDIX 2.2-1

Fatigue crack propagation life (Stage 2). Experimental tests18-27

Stress gradient through thickness. Data points from FE -model of fracture mechanics presented in Chapter 6.3. 0-surface of UI -treated groove.

$$y := \begin{pmatrix} 0 \\ 0.075 \\ 0.149 \\ 0.312 \\ 0.488 \\ 0.681 \\ 0.890 \\ 1.118 \\ 1.366 \\ 1.783 \\ 2.090 \\ 2.424 \\ 2.788 \\ 3.390 \\ 4.327 \\ 5.149 \\ 6.068 \\ 6.411 \\ 7.127 \\ 8.000 \end{pmatrix} \qquad \sigma := \begin{pmatrix} 2.552 \\ 2.332 \\ 2.113 \\ 1.803 \\ 1.583 \\ 1.425 \\ 1.312 \\ 1.229 \\ 1.167 \\ 1.105 \\ 1.075 \\ 1.053 \\ 1.037 \\ 1.020 \\ 1.006 \\ 0.997 \\ 0.984 \\ 0.975 \\ 0.950 \\ 0.933 \end{pmatrix}$$

Stress gradient through thickness. FE -model of fracture mechanics

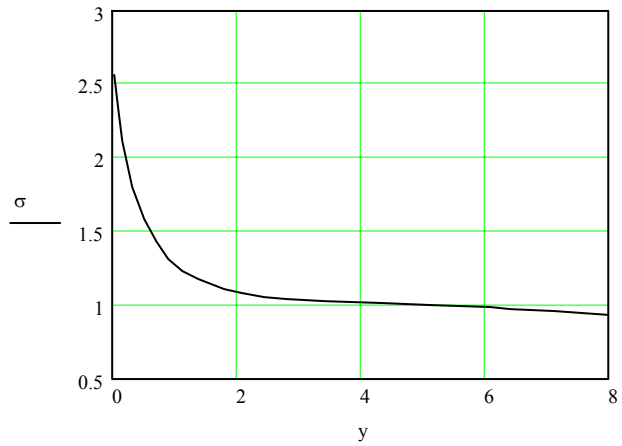

APPENDIX 2.2-2

Curve fitting. Cupic spline interpolation.

$A := 2 \quad B := 1 \quad C := 1$ Guess values

$D := 1 \quad E := 1 \quad F := 1$

Given Calculation loop

$A \cdot e^{B \cdot y_0} - C \cdot e^{D \cdot y_0} - E \cdot e^{F \cdot y_0} + 2.552 = 2.552$

$A \cdot e^{B \cdot y_3} - C \cdot e^{D \cdot y_3} - E \cdot e^{F \cdot y_3} + 2.552 = 1.803$

$A \cdot e^{B \cdot y_5} - C \cdot e^{D \cdot y_5} - E \cdot e^{F \cdot y_5} + 2.552 = 1.425$

$A \cdot e^{B \cdot y_9} - C \cdot e^{D \cdot y_9} - E \cdot e^{F \cdot y_9} + 2.552 = 1.105$

$A \cdot e^{B \cdot y_{14}} - C \cdot e^{D \cdot y_{14}} - E \cdot e^{F \cdot y_{14}} + 2.552 = 1.006$

$A \cdot e^{B \cdot y_{19}} - C \cdot e^{D \cdot y_{19}} - E \cdot e^{F \cdot y_{19}} + 2.552 = 0.933$

$R := \text{Minerr}(A, B, C, D, E, F)$ $R = \begin{pmatrix} 1.562 \\ -1.816 \\ 0.784 \\ 0.052 \\ 0.777 \\ -0.074 \end{pmatrix}$

$\sigma_x(y) := R_0 \cdot e^{y \cdot R_1} - R_2 \cdot e^{y \cdot R_3} - R_4 \cdot e^{y \cdot R_5} + 2.552$ Function through data points

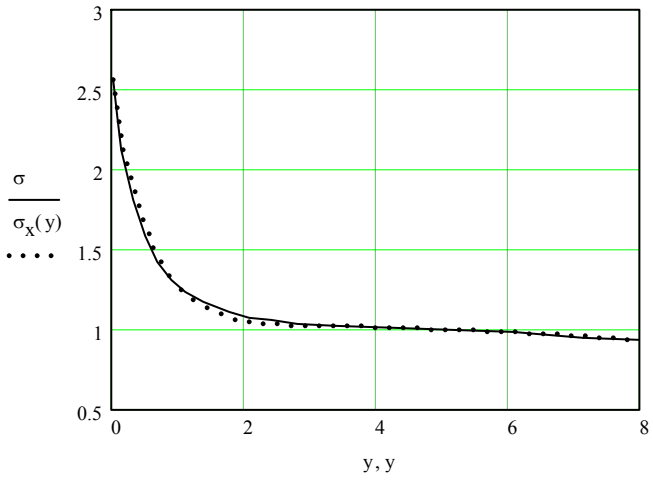

APPENDIX 2.2-3

Calculation of Mk -factor

$$M_k(a) := \left(\frac{2}{\pi \cdot a}\right) \cdot \int_0^a \frac{\sigma_x(y)}{\sqrt{1 - \left(\frac{y}{a}\right)^2}}\, dy$$

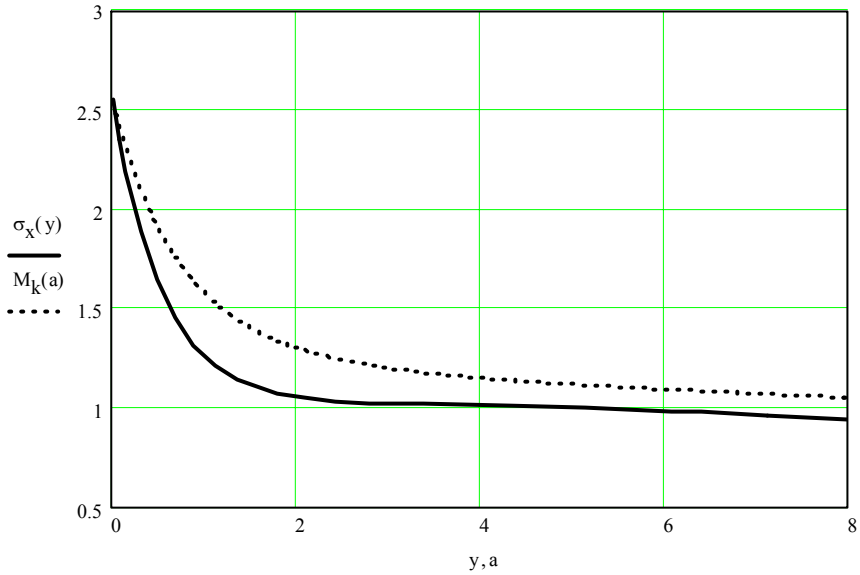

Propagation period

$C_{fm} := 0.183210^{-12}$ Crack growth speed

$a_0 := 1$ Initiatial depth of crack

$a_f := 8$ Final depth of crack.

$c(a) := 2.15 \cdot a$ Half width of crack

$$Q(a,c) := \frac{1}{\sqrt{1 + 1.464\left(\frac{a}{c(a)}\right)^{1.65}}}$$ Correction factor of crack shape

APPENDIX 2.2-4

$\Delta S := 225$ Nominal stress range of UIT-18

$$N_{pro} := \frac{1}{C_{fm} \cdot \Delta S^3 \cdot \pi^{\left(\frac{3}{2}\right)}} \cdot \int_{a_0}^{a_f} \frac{1}{\left(Q(a,c) \cdot M_k(a) \cdot \sqrt{a}\right)^3} da$$

$N_{pro} = 9.399 \times 10^4$ Propagation period of UIT-18

Nominal stress range

$$\Delta S := \begin{pmatrix} 225 \\ 257 \\ 257 \\ 232 \\ 232 \\ 258 \\ 257 \\ 257 \\ 259 \\ 257 \end{pmatrix}$$

Propagation period N_{pro}

$$N_{pro} := \begin{pmatrix} 93990 \\ 63070 \\ 63070 \\ 85740 \\ 85740 \\ 62340 \\ 63070 \\ 63070 \\ 61620 \\ 63070 \end{pmatrix}$$

ACTA UNIVERSITATIS LAPPEENRANTAENSIS

203. Säädöksiä, systematiikkaa vai ihmisoikeuksia? Oikeustieteen päivät 19. – 21.8.2003. Toim. Marjut Heikkilä. 2004. 350 s.

204. PANTSAR, HENRIKKI. Models for diode laser transformation hardening of steels. 2005. 134 s., liitt. Diss.

205. LOHJALA, JUHA. Haja-asutusalueiden sähkönjakelujärjestelmien kehittäminen – erityisesti 1000 V jakelujännitteen käyttömahdollisuudet. 2005. 201 s., liitt. Diss.

206. TARKIAINEN, ANTTI. Power quality improving with virtual flux-based voltage source line converter. 2005. U.s. Diss.

207. HEIKKINEN, KARI. Conceptualization of user-centric personalization management. 2005. 136 s. Diss.

208. PARVIAINEN, ASKO. Design of axial-flux permanent-magnet low-speed machines and performance comparison between radial-flux and axial-flux machines. 2005. 153 s. Diss.

209. FORSMAN, HELENA. Business development efforts and performance improvements in SMEs. Case study of business development projects implemented in SMEs. 2005. 209 s. Diss.

210. KOSONEN, LEENA. Vaarinpidosta virtuaaliaikaan. Sata vuotta suomalaista tilintarkastusta. 2005. 275 s. Diss.

211. 3rd Workshop on Applications of Wireless Communications. 2005. 62 s.

212. BERGMAN, JUKKA-PEKKA. Supporting knowledge creation and sharing in the early phases of the strategic innovation process. 2005. 180 s. Diss.

213. LAAKSONEN, PETTERI. Managing strategic change: new business models applying wireless technology as a source of competitive edge. 2005. 142 s. Diss.

214. OVASKA, PÄIVI. Studies on coordination of systems development process. 2005. U.s. Diss.

215. YANG, GUANGYU. Control and simulation of batch crystallization. 2005. U.s. Diss.

216. MUSTONEN–OLLILA, ERJA. Information system process innovation adoption, adaptation, learning, and unlearning: a longitudinal case study. 2005. U.s. Diss.

217. SAINIO, LIISA-MAIJA. The effects of potentially disruptive technology on business model – a case study of new technologies in ICT industry. 2005. 205 s. Diss.

218. SAINIO, TUOMO. Ion-exchange resins as stationary phase in reactive chromatography. 2005. 175 s. Diss.

219. CONN, STEFFEN. Software tools to support managers: development and application to new product development and strategic alliance management. 2005. 168 s. Diss.

220. TYNJÄLÄ, TERO. Theoretical and numerical study of thermomagnetic convection in magnetic fluids. 2005. U.s. Diss.

221. JANTUNEN, ARI. Dynamic capabilities and firm performance. 2005. 210 s. Diss.

222. KOLA-NYSTRÖM, SARI M. In search of corporate renewal: how to benefit from corporate venturing? 2005. 190 s. Diss.

223. SARÉN, HANNU. Analysis of the voltage source inverter with small DC-link capacitor. 2005. 143 s. Diss.

224. HUUHILO, TIINA. Fouling, prevention of fouling, and cleaning in filtration. 2005. U.s. Diss.

225. VILJAINEN, SATU. Regulation design in the electricity distribution sector – theory and practice. 2005. 132 s. Diss.

226. AVRAMENKO, YURY. Case-based design method for chemical product and process development. 2005. U.s. Diss.

227. JÄRVINEN, KIMMO. Development of filter media treatments for liquid filtration. 2005. U.s. Diss.

228. HURMELINNA-LAUKKANEN, PIA. Dynamics of appropriability – finding a balance between efficiency and strength in the appropriability regime. 2005. U.s. Diss.

229. LAARI, ARTO. Gas-liquid mass transfer in bubbly flow: Estimation of mass transfer, bubble size and reactor performance in various applications. 2005. U.s. Diss.

230. BORDBAR, MOHAMMAD HADI. Theoretical analysis and simulations of vertically vibrated granular materials. 2005. U.s. Diss.

231. LUUKKA, PASI. Similarity measure based classification. 2005. 129 s. Diss.

232. JUUTILAINEN, ANNELI. Pienen matkailuyrityksen yrittäjän taival. Oppiminen yrittäjyysprosessissa. 2005. 191 s. Diss.

233. BJÖRK, TIMO. Ductility and ultimate strength of cold-formed rectangular hollow section joints at subzero temperatures. 2005. 163 s. Diss.

234. BELYAEV, SERGEY. Knowledge discovery for product design. 2005. U.s. Diss.

235. LEINONEN, KARI. Fabrication and characterization of silicon position sensitive particle detectors. 2006. U.s. Diss.

236. DUFVA, KARI. Development of finite elements for large deformation analysis of multibody systems. 2006. U.s. Diss.

237. RITVANEN, JOUNI. Experimental insights into deformation dynamics and intermittency in rapid granular shear flows. 2006. U.s. Diss.

238. KERKKÄNEN, KIMMO. Dynamic analysis of belt-drives using the absolute nodal coordinate formulation. 2006. 121 s. Diss.

239. ELFVENGREN, KALLE. Group support system for managing the front end of innovation: case applications in business-to-business enterprises. 2006. 196 s. Diss.

240. IKONEN, LEENA. Distance transforms on gray-level surfaces. 2006. 132 s. Diss.

241. TENHUNEN, JARKKO. Johdon laskentatoimi kärkiyritysverkostoissa. Soveltamismahdollisuudet ja yritysten tarpeet. 2006. 270 s. Diss.

242. KEMPPINEN, JUKKA. Digitaaliongelma. Kirjoitus oikeudesta ja ympäristöstä. 2006. 492 s.

243. PÖLLÄNEN, KATI. Monitoring of crystallization processes by using infrared spectroscopy and multivariate methods. 2006. U.s. Diss.

244. AARNIO, TEIJA. Challenges in packaging waste management: A case study in the fast food industry. 2006. 260 s. Diss.

245. PANAPANAAN, VIRGILIO M. Exploration of the social dimension of corporate responsibility in a welfare state. 2006. 239 s. Diss.

246. HEINOLA, JANNE-MATTI. Relative permittivity and loss tangent measurements of PWB materials using ring resonator structures. 2006. U.s. Diss.